Miniemulsion Polymerization

F. Joseph Schork (✉)[1] · Yingwu Luo[2] · Wilfred Smulders[1] · James P. Russum[1] ·
Alessandro Butté[3] · Kevin Fontenot[4]

[1] School of Chemical and Biomolecular Engineering, Georgia Insitute of Technology,
  Atlanta Georgia30332–0100 USA
  joseph.schork@chbe.gatech.edu, wilfred.smulders@chbe.gatech.edu,
  james.russum@chbe.gatech.edu
[2] The State Key Laboratory of Polymer Reaction Engineering, College of Material
  and Chemical Engineering, Zhejiang University, Hangzhou, 310027 P. R. China
  yingwu.luo@cmsce.zju.edu.cn
[3] Prof. M. Morbidelli Group, ETH Zürich, Institute for Chemical- and Bioengineering,
  ETH Hönggerberg/HCI F 135, 8093 Zürich, Switzerland
  butte@tech.chem.ethz.ch
[4] Eastman Chemical Company, P.O. Box 1972, Kingsport TN 37662, USA
  fontenot@eastman.com

Abstract   The subject of miniemulsion polymerization is reviewed. The approach taken is
one that combines a review of the technology with historical and tutorial aspects. Rather
than developing an absolutely exhaustive review, a tutorial approach has been taken, em-
phasizing the critical features and advantages of miniemulsion polymerization. In keeping
with this tutorial approach, a discussion of conventional emulsion polymerization is included
in order to be able to compare and contrast miniemulsion polymerization and conventional
emulsion polymerization later in the review. Areas where miniemulsion polymerization has
been adopted commercially, or where it is likely to be adopted are highlighted.

Abbreviations and Symbols

AMBN	2,2′-azobis(2-methylbutyronitrile)
ATRP	atom transfer radical polymerization
CA	cetyl alcohol
CMC	critical micelle concentration
CSA	camphorsulfonic acid
CSTR	continuous stirred tank reactor
CTA	chain transfer agent
CTAB	cetyltrimethylammonium bromide
DDM	dodecyl mertcaptan
DLS	dynamic light scattering
DOM	dioctyl maleate
DPPH	diphenylpicrylhydrazol
EHA	2-ethylhexyl acrylate
F_i	copolymer composition, monomer i
f_i	monomer composition, monomer i
GPC	gel permeation chromatography
HD	hexadecane
K_{eq}	equilibrium constant
k_p	propagation rate constant
KPS	potassium persulfate
LPO	lauroly peroxide
MAETAC	2-(methacryloyoxy)ethyl]tri-methyl ammonium chloride
M_{aq}	molarity, aqueous phase
m_{ij}	ratio of molar size, i to j
mM	millimolar
MMA	methyl methacrylate
$[M_p]$	concentration of monomer in the particle
MWD	molecular weight distribution
$\bar{n}$	average number of radicals per particle
N	number of particles per liter
N_A	Avogadro's number

nm	nanometer
NMA	*n*-methylol acrylamide
NMCRP	nitroxide-mediated controlled radical polymerization
NMR	nuclear magnetic resonance spectroscopy
PFR	plug flow reactor
pMS	paramethyl styrene
PS	polystyrene
PSD	particle size distribution
PST	polystyrene
PVA	polyvinyl alcohol
PVAc	polyvinyl acetate
QSSA	quasi-steady state approximation
r	radius
r_i	reactivity ratio
R	gas constant
RAFT	reversible addition-fragmentation chain transfer
R_p	rate of polymerization
RX	organic halide
SE	Smith Ewart
SPS	sodium persulfate
T	temperature
T_g	glass transition temperature
$\bar{V}_i$	partial molar volume of i
VAc	vinyl acetate
VD	vinyl *n*-decanoate
VEH	vinyl 2-ethylhexanoate
VEOVA	vinyl neo-decanoate (vinyl versatate)
VH	vinyl hexanoate
VS	vinyl stearate
W	Fuchs stability ratio
X	halogen
χ_{ij}	Flory Huggins interaction parameter
$\Delta \bar{G}_i$	partial molar free energy or phase i
γ	interfacial tension
φ_i	volume fraction of component i
μ	viscosity
μ_i	chemical potential of component i
μm	micron
%wt	percent by weight

1
Introduction

Over the past 25 years, miniemulsion polymerization has grown from being the subject of a single paper to being the focus of a great deal of academic and industrial research. During that time, some products have been commercialized based on this technology, and in the next few years a number of new

commercializations of the technology are expected to take place. This text attempts to trace the development of miniemulsion polymerization, the physics and chemistry behind it, its unique features, and its potential for future applications. It is not an exhaustive bibliography of published work, but it does cite significant and/or representative papers. Previous reviews of this field can be found in [1–3].

1.1
Dispersed-Phase Polymerization

Free radical polymerization may be carried out in various media. Bulk polymerization is the simplest, but while the reactants (monomers) are most often liquid, the product (polymer) is solid. This leads to problems when removing the polymer from the reactor. In addition, since most free radical polymerizations are highly exothermic, the high viscosity of the monomer/polymer mix inhibits the removal of the heat of reaction. Solution polymerization will reduce, to some extent, the viscosity of the polymerizing mass, but it brings with it the environmental and health issues of organic solvents. In addition, the solvent reduces the monomer concentration, and hence the rate of polymerization. Finally, recovery and recycling of the solvent can add substantially to the cost of the process. Nevertheless, solution polymerization of vinylic monomers is used in a number of commercial processes.

An alternative to solution polymerization is the whole realm of *dispersed-phase polymerization*. In this class of processes, the liquid monomer is dispersed in a second, continuous phase, usually water. As the monomer polymerizes, the viscosity of the dispersion remains low, aiding the removal of the heat of polymerization. If the dispersed phase is water, the high thermal conductivity provides a very effective heat transfer medium. The high specific heat and large latent heat of vaporization provide a large safety margin in the event of a runaway polymerization. In addition, water is plentiful, nontoxic, environmentally friendly, and inexpensive.

If an oil-soluble monomer is dispersed in a continuous aqueous phase without the use of surfactants, *suspension polymerization* results. The viscosity of the resulting suspension will remain essentially constant over the course of the polymerization. Oil-soluble free radical initiators are used to effect polymerization. The monomer is dispersed into beads by the action of an agitator. Since little or no surfactant is used, no emulsification takes place, and, if the agitation is stopped, the monomer will form a separate bulk phase, usually above the aqueous phase. The monomer is polymerized by the initiator within the droplets, forming polymer beads of approximately the same size as the monomer droplets (0.1–10 mm diameter). The product can be readily separated from the aqueous phase (via filtration or decantation) in the form of macroscopic particles or beads, which can be easily packaged and/or transported. Heat transfer is facilitated by the presence of the continuous aqueous phase. Blocking agents such as clays or talcs are used to prevent particle ag-

glomeration. Small quantities of nonionic surfactants (such as polyvinyl alcohol) may be used to impart particle stability and to disperse the blocking agent. Viscosity enhancers such as carboxymethylcellulose may be used to inhibit particle settling. The loci of polymerization are the monomer/polymer beads. Due to the large sizes of the beads, such systems are suspensions rather than emulsions or stable dispersions. The particles are kept suspended by agitation throughout the course of the polymerization. The suspension polymerization process is described in detail by Trommsdorff and Schildknecht [4].

Kinetically, each bead acts as a small independent reactor; there is little exchange of material between the beads. Since there is no solvent present at the locus of polymerization, the kinetics are those of bulk polymerization, with the molecular weight distribution (MWD) characteristics similar to those of bulk or solution polymerizations. If water-soluble initiator is used in a suspension polymerization, very little polymerization will occur, since few free radicals will reach the locus of polymerization in the monomer beads.

If surfactant is added to a suspension polymerization system, a number of phenomena may occur. If the surfactant is added in small amounts (below the critical micelle concentration or CMC), the reduction in interfacial tension between the organic and aqueous phases will result in smaller monomer droplets, but it has hardly any other effect. If surfactant is added above the CMC, and an oil-soluble initiator is used, the process is commonly termed a *microsuspension polymerization*. Due to the reduced interfacial tension, the droplet diameter (and hence bead diameter) is reduced to approximately 10–40 μm. Little polymerization takes place in the aqueous phase or in particles generated from surfactant micelles because of the hydrophobic nature of the initiator. However, some smaller particles initiated from surfactant micelles may be found. The kinetics are still essentially those of a bulk free radical polymerization. Microsuspension polymerization is used to produce pressure-sensitive adhesives for repositionable notes.

If a water-soluble initiator is used, both droplet nucleation (to form large particles) and micellar nucleation (to form submicron particles) may occur. The balance between these two mechanisms is a function of surfactant type and amount and monomer water solubility. In general, small particles derived from micellar nucleation will dominate, giving what is know as a *conventional emulsion polymerization* system. The kinetics of conventional emulsion polymerization are no longer those of bulk free radical polymerization, since the small sizes of the loci of polymerization introduce segregation effects, in which bimolecular termination of the growing polymer chains is suppressed by the small likelihood of two growing chains existing in the same particle. This results in higher molecular weight at constant polymerization rate. The particle diameter will range from 50 to 500 nm.

If the monomer droplet size in a conventional emulsion polymerization can be reduced sufficiently (see below), the loci of polymerization become the monomer droplets. This system is referred to as a *miniemulsion* polymerization and will be discussed in detail below. The particle diameter will range from 50 to 500 nm.

If the surfactant concentration in a macroemulsion is greatly increased, or if the monomer concentration is greatly reduced, a *microemulsion* results. Microemulsions are thermodynamically stable systems in which all of the monomer resides within the micelles. At high surfactant concentration, the micelles may form a bicontinuous network, rather than discrete micelles. Polymerization (with water- or oil-soluble initiator) of the monomer within a microemulsion is referred to as *microemulsion polymerization*. The particles produced in this way are extremely small, ranging from 10 to 100 nm.

1.2
The Concept of Miniemulsion Polymerization

The mechanisms of conventional emulsion and miniemulsion polymerizations are, in some ways, significantly different. A conventional unseeded (no small particles added at the beginning) batch emulsion polymerization reaction can be divided into three intervals. Particle nucleation occurs during Interval I and is usually completed at low monomer conversion (2–10%) when most of the monomer is located in relatively large (1–10 μm) droplets. Particle nucleation takes place when radicals formed in the aqueous phase grow via propagation and then enter into micelles or become large enough in the continuous phase to precipitate and form primary particles which may undergo limited flocculation until a stable particle population is obtained. Significant nucleation of particles from monomer droplets is discounted because of the small total surface area of the large droplets. Interval II involves polymerization within the monomer-swollen polymer particles, with the monomer supplied by diffusion from the droplets. Interval III begins when the droplets disappear – or at least reach a polymer fraction similar to that of the particles – and continues to the end of the reaction. Because the nucleation of particles can be irreproducible, commercial emulsion polymerizations are often "seeded" with polymer particles of known size and concentration, manufactured specifically for use as seed particles. In this paper, for the purpose of clearly distinguishing between conventional emulsions and miniemulsions, the term *macroemulsion* will be used for the former. In addition, a *latex* will be defined as a polymerized monomeric emulsion, while the term *emulsion* will refer to an unpolymerized monomeric emulsion.

Miniemulsion polymerization involves the use of an effective surfactant/costabilizer system to produce very small (0.01–0.5 μm) monomer droplets. The droplet surface area in these systems is very large, and most of the surfactant is adsorbed at the droplet surface. Particle nucleation is primarily via radical (primary or oligomeric) entry into monomer droplets, since little surfactant is present in the form of micelles, or as free surfactant available to stabilize particles formed in the continuous phase. Both oil- and water-soluble initiators may be used; the important feature is that the reaction proceeds by polymerization of the monomer in these small droplets, so there is no true Interval II. The mechanisms of macro- and miniemulsion polymerization are shown schematically in Fig. 1.
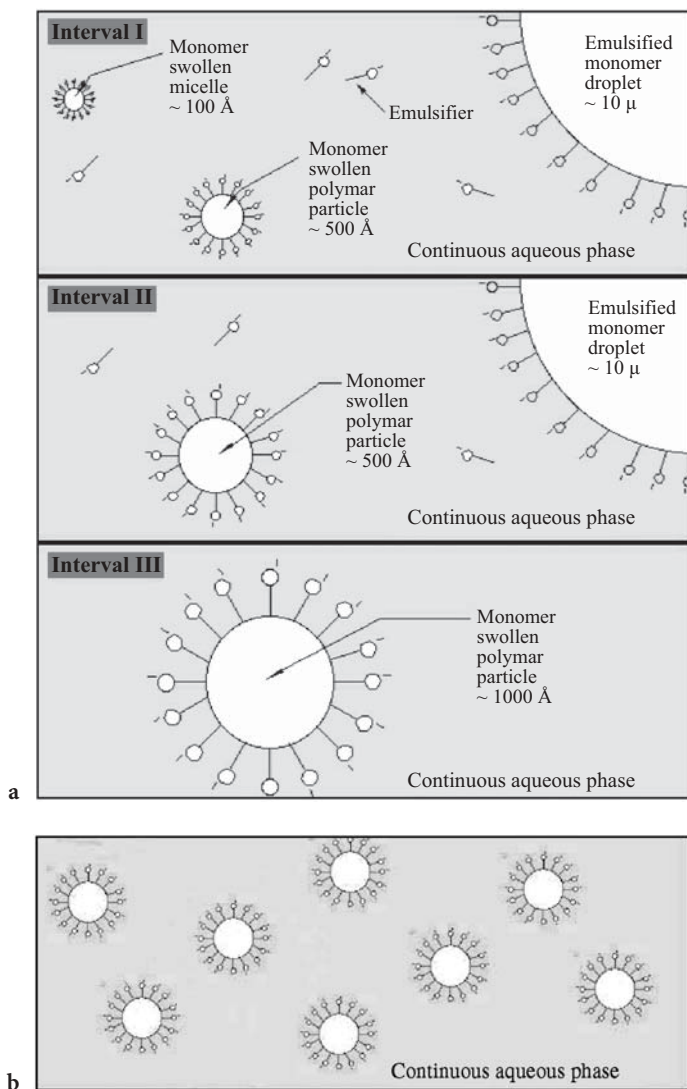
Fig. 1 Macroemulsion polymerization (**a**) versus miniemulsion polymerization (**b**)

1.3
Publication History

Miniemulsion polymerization began with a single paper [5]. Professor John Ugelstad of Norway was visiting John Vanderhoff in the Department of Chemistry at Lehigh University. Their discussions lead to speculation about the possibility of nucleation and polymerization in very fine monomer droplets during emulsion polymerization. Micellar nucleation is considered to be the
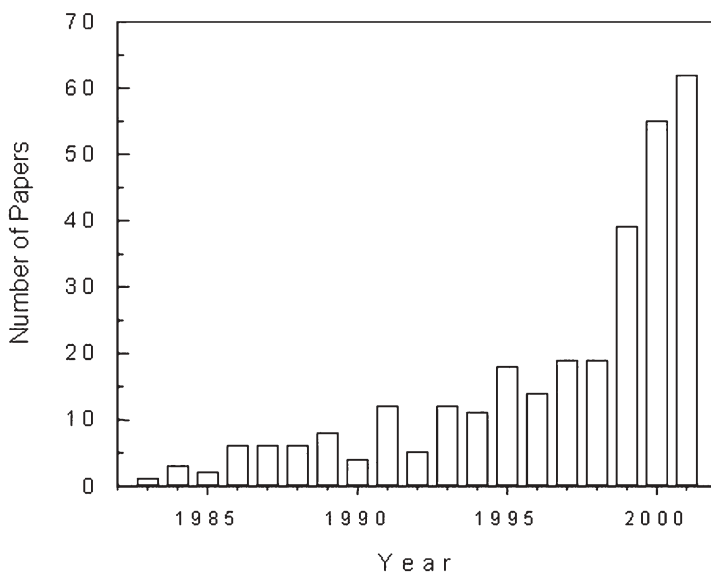
Fig. 2 Growth in the number of publications on miniemulsion polymerization. (Courtesy of Prof. M. S. El-Aasser)

dominant mechanism of particle nucleation in emulsion polymerization, but might nucleation in droplets occur if the droplets were sufficiently small? The task of investigating these ideas was given to a new postdoctoral fellow in Vanderhoff's lab, Dr. (now Provost) Mohamed S. El-Aasser. From this point, the field grew slowly. Figure 2 shows the total number of papers per year published on miniemulsion polymerization. It may be seen that, after a slow start, the number of contributions in the field has risen rapidly, as the scientific community made use of the basic research of the early years, and began to see the commercial utility of the process.

2
Miniemulsion Polymerization

In order to adequately discuss miniemulsion polymerization, it will be necessary to review the mechanism of macroemulsion polymerization.

2.1
The Mechanism of Macroemulsion Polymerization

Macroemulsion polymerization is a complex process. The literature contains extensive reviews of emulsion polymerization theory [6–11]. Only a brief review of the current state of the literature is given here. The theory of emul-

sion polymerization revolves around one equation (neglecting the aqueous phase),

$$R_p = k_p[M]_p N_p \bar{n}/N_A$$

where each of these terms is explained below.

The earliest qualitative theory of emulsion polymerization was developed by Harkins [12] and was quickly quantified by Smith and Ewart (SE) [13]. Although this theory only holds for the special case of water-insoluble monomers, it is the typical starting point for most other theories. This theory is based on the batch emulsion polymerization of styrene. It includes three intervals, as depicted in the left half of Fig. 1. The first interval begins with the initiation of the reaction and continues until all micelles become nucleated or are used up as surface stabilizing agents. At this point particle formation ceases. During Interval II, the particles grow at a constant rate in the presence of monomer droplets. Once the monomer droplets disappear, Interval III begins. The monomer concentration in the particle decreases and the reaction within the particles becomes diffusion-limited throughout the remainder of the polymerization.

Micellar nucleation may not be the only, or even primary process of nucleation and growth. Other mechanisms are discussed later. To provide a comprehensive model for emulsion polymerization, the applicability of each mechanism must be considered.

Equation 1 illustrates the concept of *radical segregation*, that is significant in macroemulsion, miniemulsion and microemulsion polymerization. In a bulk or solution free radical polymerization, the radical flux can be increased in order to increase the rate of polymerization, but only at the cost of reducing molecular weight. Equation 1 indicates that one might increase the rate of polymerization by increasing the surfactant level. This does not adversely impact the molecular weight of the product. The ability to decouple reaction rate and molecular weight come about because of the segregation of the free radicals in segregated disperse-phase polymerization. Since each radical is confined to a particle, bimolecular termination is suppressed, resulting in higher rates of polymerization and molecular weight. Segregation occurs only when $\bar{n}$ is reasonably close to unity, or lower than unity.

2.1.1
Interval I – Particle Nucleation

Nucleation mechanisms are generally divided into three types: micellar, homogeneous, and droplet. Statistically, all three types can occur simultaneously in every reaction. However it is the preponderance of one mechanism above the others in a given system that causes authors to consider only one in their studies. Numerous extensions have been made to the SE micellar nucleation theory in an effort to furnish explanations for experimental results observed

for monomers with slight water solubilities. Detailed reviews of these extensions are readily available [10, 11, 14, 15]. Monomer droplet nucleation is normally neglected, except when considering mini- and microemulsions, due to its insignificant contribution to the particle number and the size distribution.

2.1.1.1
Micellar Nucleation

All quantitative theories based on micellar nucleation can be developed from balances of the number concentrations of particles, and of the concentrations of aqueous radicals. Smith and Ewart solved these balances for two limiting cases: (i) all free radials generated in the aqueous phase assumed to be absorbed by surfactant micelles, and (ii) micelles and existing particles competing for aqueous phase radicals. In both cases, the number of particles at the end of Interval I in a batch macroemulsion polymerization is predicted to be proportional to the aqueous phase radical flux to the power of 0.4, and to the initial surfactant concentration to the power of 0.6. The Smith Ewart model predicts particle numbers accurately for styrene and other water-insoluble monomers. Deviations from the SE theory occur when there are substantial amounts of radical desorption, aqueous phase termination, or when the calculation of absorbance efficiency is in error.

Deviations with respect to order from the SE theory increase as the monomer water solubility increases.

2.1.1.2
Homogeneous Nucleation

Although the SE micellar nucleation theory explains data for certain systems, it fails for others. This has led some authors to propose a different mechanism for nucleation. In the homogeneous nucleation theory, aqueous phase radicals polymerize to form oligomers. These continue to grow until they reach a critical chain length, the size of a primary particle, and then precipitate. Throughout the growth process, the oligomers may also flocculate or coagulate. This theory is typically employed for relatively water-soluble monomers. Slight variations of this theory have also been postulated.

Prior to 1952, little evidence for homogeneous nucleation existed [16, 17]. In 1952, Priest [18] studied the polymerization of vinyl acetate and presented a qualitative theory for homogeneous nucleation. He concluded from experimental work that aqueous phase nucleation is important in systems with monomers that have a relatively high water solubility. Primary particle formation occurs throughout the course of the reaction. During later periods of the reaction, large monomer-swollen polymer particles act as sinks for these primary particles, encouraging coagulation.

In 1968, Roe [19] developed the SE limiting case equations for particle number from the homogeneous nucleation theory. He showed that the SE equation

for particle nucleation is not unique to micellar nucleation, but results from the SE assumptions. By assuming that (i) the nucleation stops upon depletion of micelles, (ii) the volumetric growth rate is constant, and (iii) the radical absorption is strictly a function of radical generation, he showed that the SE dependency on radical flux and surfactant concentration could be generated from homogeneous nucleation theory.

Fitch and Tsai [20, 21] developed a quantitative theory for homogeneous nucleation. By using the collision theory for radical capture, Fitch [22] has shown that the rate of radical capture is a function of radical production, particle number, particle size, and diffusion distance. Primary particles may coagulate with each other because of their small size and lower surface charge. As particles coagulate, the surface to volume ratio decreases, which causes an increase in surface potential. When particles become sufficiently large, coagulation ceases due to insufficient kinetic energy to overcome the biparticle surface repulsion. Fitch and Tsai have provided experimental support for this theory by polymerizing MMA with different initiators.

Ugelstad and Hansen [11] proposed that free radicals in the aqueous phase propagate with dissolved monomer. Primary particles form by precipitation when a critical chain length is reached. During growth from a monomer radical to a primary particle, each oligomer can (i) terminate with other radicals, (ii) precipitate if its length exceeds the critical chain length, or (iii) be captured by particle.

A fundamental extension to the homogeneous nucleation theory was proposed by Lichti et al. [23] and Feeney et al. [24]. Their theory is based on the positive skewness of the particle size distribution (PSD) as a function of volume during Interval II. This implies that the rate of nucleation during Interval I increases with time until it eventually drops off at the cessation of nucleation. Lichti and Feeney claim that micellar nucleation or one step homogeneous nucleation incorrectly predict either decreasing or constant nucleation rates.

This theory has been given the name coagulative nucleation. According to Lichti and Feeney's mechanism, precipitated "precursor particles" undergo coagulation to form "true" or "mature" latex particles. A precursor particle is unstable and said to be formed in either a micelle or the aqueous phase. Due to their small size and hydrophilic nature, the precursors have low swelling capacity and high radical desorption rates. Consequently, the propagation rate is low and these precursors tend to coagulate with other precursors or mature latex particles. These conclusions then rule out micellar nucleation as a possible mechanism for precursor formation.

More recently, Maxwell et al. [25] suggested that the values to be used for the critical chain length are much smaller than originally thought. They also suggested that oligomeric radical capture is independent of particle size and limited by the rate of propagation of the radical in the aqueous phase. However, this theory does not consider variations in other parameters with particle size.

2.1.1.3
Droplet Nucleation

Nucleation of monomer droplets has typically been neglected in emulsion polymerization. The large diameter (1–10 µm) and small number (~10^{13} versus 10^{21} micelles) of droplets in macroemulsions usually makes their consideration of no importance. Regardless of this, all droplets do get nucleated, because of their large size. These droplets show up in TEM photographs as abnormally large particles in very low concentrations. In 1973, Ugelstad et al. [5] showed how submicron styrene monomer drops can be made stable enough to become numerically significant in nucleation when a cosurfactant is used to enhance the stability of the smaller droplets. Table 1 shows how the micelle number varies with monomer droplet size at constant surfactant levels. Chamberlain et al. [26] have presented experimental evidence that the efficiency of radical capture by droplets is much lower than that for micelles or particles. This would affect the results in Table 1. Ugelstad et al. [27, 28] have shown how nucleation of monomer droplets can lead to latexes with large monodisperse particles. However, if insufficient shear or cosurfactant is used, the potential for production of bimodal PSD's exists [29, 130]. This could be desirable in certain instances.

The distinguishing feature of droplet nucleation as opposed to micellar or homogeneous nucleation is the nature of the particle at "birth". Droplets, which are nucleated into particles, begin as nearly 100% monomer. Micellar or homogeneous nucleated particles start out with much lower monomer concentrations and eventually swell to around 60% (for MMA) in the presence of monomer droplets. This fundamental difference may lead to large differences between miniemulsion and macroemulsion polymerizations in radical desorption and/or intraparticle termination during Intervals I and II.

Table 1 Variation of number of micelles with droplet size for MMA droplets and SLS surfactant in a basic emulsion recipe

Monomer droplet diameter (µm)	10.0	1.0	0.5	0.1
Volume of monomer droplet (liter)	5.2×10^{-13}	5.2×10^{-16}	6.5×10^{-17}	5.2×10^{-19}
Number of monomer droplets (#/1)	7.8×10^{11}	7.8×10^{14}	6.3×10^{15}	7.8×10^{17}
Total area of droplets (m^2/1)	247	2470	4930	24700
Surface area micelles (m^2/1)	5246	3027	562	0
Number of micelles (#/1)	1.5×10^{20}	8.6×10^{19}	1.6×10^{19}	0.0
Total number of preparticles (#/1)	1.5×10^{20}	8.6×10^{19}	1.6×10^{19}	7.8×10^{17}
Droplet percent area	4.5	45	90	100
Droplet percent number	5.3×10^{-7}	9.2×10^{-4}	0.040	100

Base case parameters: temperature=50 °C; monomer/water ratio=0.4 g/g; surfactant CMC= 0.004 mol/L(aq); surfactant concentration=0.020 mol/L; surfactant surface area=0.57 nm^2/ molecule; molecules per micelle=62; monomer watersaturation=0.137 mol/L(aq)

2.1.1.4
Competition for Radicals

As pointed out above, particle nucleation includes all three mechanisms – micellar, homogeneous, and droplet, since these mechanisms may compete and coexist in the same system. Often one will dominate. Therefore, any general model of emulsion polymerization should include all three mechanisms. Hansen and Ugelstad [31] and Song [10] have presented probabilities for each of these mechanisms in the presence of all three.

The competition for oligomeric radicals also includes particles that have been created. In miniemulsion polymerizations, the nucleation of one droplet results in the formation of one particle of equal surface area. Therefore, nucleation therein has little effect on competition for radicals. This is not so with macroemulsions, since both micellar and homogeneous nucleation result in a large shift in the surface area from micelles to particles as the particles are created and grow.

2.1.2
Interval II – Particle Growth

SE Interval II begins at the cessation of nucleation, or in light of the nucleation theory just reviewed, when the particle number becomes relatively constant. Most theories developed for this interval assume a constant particle number and use the quasi-steady-state approximation (QSSA) for average number of radicals per particle. The kinetics and mechanisms of Interval II have been some of the most studied aspects of macroemulsion polymerization. SE Interval II ends when the monomer droplets disappear and the monomer concentration in the particles begins to decrease.

The rate of polymerization during Interval II is usually considered constant for two reasons. The monomer concentration within the particle, as defined by equilibrium thermodynamics, is approximately constant in the presence of excess monomer. Mass transfer is assumed to be fast and particle size has little effect on this concentration. Secondly, emulsion polymerization kinetics tend to give a constant radical concentration within the particles during Interval II. Therefore, the rate of polymerization given by Eq. 1 is approximately constant until the end of Interval II, where $[M]_p$, $\bar{n}$, and k_p begin to change. These two assumptions have been substantiated by experimental observations and are considered reasonable. The challenge for Interval II is to determine the average number of radicals per particle. Particle monomer concentration can be determined as a function of particle radius by an equilibrium relationship such as the Morton [32] equation that considers both surface energy and mixing energy. Propagation rate coefficients have been widely studied and are readily available [33]. The particle number concentration is assumed constant.

Smith and Ewart developed three limiting cases for Interval II. Each of these cases can be generated through a balance of N_{pi} (the number of particles con-

taining i radicals), where the number of particles is considered constant (no nucleation). For Case 1, Smith and Ewart assume $N_{p0} \gg N_{p1} \gg N_{p2} \gg \dots$. For this case $\bar{n}$ will be significantly less than 0.5. This case occurs when significant monomeric radical desorption occurs, and is more common with monomers of significant water solubility.

Case 2, assumes instantaneous termination of the existing radical with an entering radical. In this case, each particle will contain either zero or one radical, and $\bar{n}$ becomes 0.5. Styrene generally follows Case 2 kinetics. Smith and Ewart Case 3 assumes that both desorption from particles and aqueous phase termination may be neglected, and so $\bar{n} \geqslant 1.0$. This occurs with large particles, and in the limit results in bulk kinetics.

Coagulation of latex particles during Interval II is often neglected. If surfactant is available in great enough proportion, the particles will remain stable throughout the reaction.

2.1.3
Interval III – Gel and Glass Effects

Interval III begins when all monomer droplets have vanished and/or the aqueous phase becomes unsaturated. Since each droplet in a macroemulsion actually absorbs radicals, they cannot disappear but rather shrink to a point where they have no excess monomer. The monomer in the aqueous phase decreases corresponding to the decrease in the particles. The conversion at which Interval III begins varies for different monomers and systems, but is typically around 40 to 50%. However, it may not be as distinguishable in miniemulsions due to early initiation of the gel effect.

As the monomer within the particles is consumed by polymerization, the viscosity rises within the particles and the diffusion rate of the polymeric radicals decreases. This causes a reduction in the rate of termination, which corresponds to a dramatic increase in the radical concentration. A higher radical number within the particle results in an "auto acceleration" in the rate of polymerization. Common practice is to model this auto acceleration or gel effect by decreasing the termination rate constant byseveral orders of magnitude as a function of percent monomer in the particle. A free volume approach has been used by Sundberg et al. [34]. Gilbert and coworkers [35] suggest a completely empirical approach from precise experimental data. Empirical correlations used in modeling the gel effect in bulk or solution polymerization have also been modified for use in emulsion processes [36–38].

The problem with applying correlations derived from other systems to emulsion polymerization is twofold. First, normal macroemulsion particles are said to be created with 30 to 40% monomer in them and so the unbiased (zero conversion) termination rate is unknown. Secondly, the diffusional limitations in particles might be quite different from those observed in bulk or suspension polymerizations. It is for these reasons that an empirical approach is suggested.

If the reaction temperature is below the polymer glass transition temperature and the amount of monomer in the particle decreases far enough, the glass effect may become important. The polymerization rate virtually goes to zero because the particle becomes so internally viscous, essentially glasslike, that the diffusion of monomer to the radicals is limited. The glass transition point varies for different polymers. This effect has also been studied by several authors [34, 39, 40].

2.2
The Mechanism of Miniemulsion Polymerization

In the previous discussion of macroemulsion polymerization, all three forms of particle nucleation were discussed. In macroemulsion polymerization, micellar and homogenous nucleation dominate. This is because the large sizes of the monomer droplets, and their consequent low interfacial area, makes them ineffective in competing for water-borne free radicals. Droplet nucleation undoubtedly takes place in macroemulsion polymerization, but it is generally considered to be insignificant. If the monomer droplet size can be reduced to below 0.5 μm, two phenomena will occur. First, the droplets will be able to compete successfully for water-borne free radicals with any remaining micelles. Second, the huge increase in interfacial area caused by the reduction in droplet size will result in a huge increase in interfacial area. This new interface will require a monolayer of surfactant to remain stable. The surfactant necessary to support this large interfacial area will come from the break-up of surfactant micelles. In a properly formulated miniemulsion, all micelles will be sacrificed to support the droplet interfacial area. Therefore, not only do the small droplets compete effectively for micelles, their presence causes the destruction of the micelles, leaving droplet nucleation as the dominant particle nucleation process.

Miniemulsions are produced by the combination of a high shear to break up the emulsion into submicron monomer droplets, and a surfactant/costabilizer system to retard monomer diffusion from the submicron monomer droplets. Both are necessary to effect predominant droplet nucleation (nucleation in which a preponderance of the particles originate from droplets rather than from micelles or from homogeneous nucleation). High shear is provided by a sonicator or a mechanical homogenizer. The surfactant is necessary to retard droplet coalescence caused by Brownian motion, settling or Stokes law creaming or settling. The costabilizer (also referred to in earlier works as a *cosurfactant*) prevents Ostwald ripening [41]. When a liquid emulsion is subjected to high shear, small droplets will result. There will still be a statistical distribution of droplet sizes. If the monomer is even slightly soluble in the continuous aqueous phase (and most are, as evidenced by the fact that Interval II of macroemulsion polymerization takes place), the monomer will, over time, diffuse from the smaller monomer droplets into the larger ones. This results in a lower interfacial area (and interfacial energy), since the loss in interfacial area of the

smaller droplets is larger than the gain in interfacial area of the larger ones. The reduction in interfacial energy is the driving force for degradation of the small droplets.

If Ostwald ripening is allowed to continue unchecked, creaming of the monomer will occur as the droplet sizes become large enough for Stokes law creaming to occur. This will occur in a matter of seconds to minutes. If the system is initiated, bulk polymerization of the monomer layer will occur. If the emulsion is stirred, an emulsion of large monomer droplets (of the order of those of a macroemulsion) will result, and if the stirred emulsion is initiated, macroemulsion polymerization will take place. A costabilizer functions to prevent Ostwald ripening by retarding monomer diffusion from the smaller droplets to the larger. Costabilizers should be highly insoluble in the aqueous phase (so that they will not diffuse out of the droplets), and highly soluble in the monomer droplets. Under these conditions, diffusion of the monomer out of the smaller droplets results in an increase in the concentration of the co-stabilizer in those particles (since, by definition costabilizers are too insoluble in the aqueous phase to leave the droplet). The increase in free energy associated with the concentration of the costabilizer balances the decease from reduced interfacial area caused by Ostwald ripening, and, at some point, ripening stops. Since all costabilizers are somewhat water-soluble, Ostwald ripening will proceed, but on a timescale of months, which is unimportant since the timescale of polymerization is minutes to hours. This phenomenon is shown in Fig. 3 [42]. Here a macroemulsion and a miniemulsion of methyl methacrylate (same recipe, but with no costabilizer, and no high shear for the macroemulsion) are shown after three hours without mixing. The macroemulsion is completely creamed, since Stokes law creaming has taken place on the large monomer droplets. The miniemulsion has not creamed, since Brownian motion is sufficient to prevent creaming of the submicron monomer droplets. Similar miniemulsions have remained stable for six months or more.
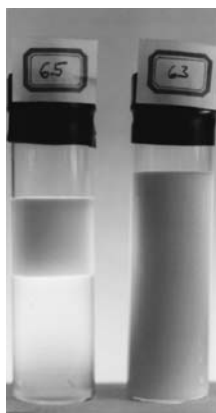
Fig. 3 Macroemulsion and miniemulsion after three hours

In their original discovery of miniemulsion polymerization, Ugelstad and co-workers [5] used either cetyl alcohol (CA: water solubility estimated at 6×10^{-8} [43]) or hexadecane (HD: water solubility estimated at 1×10^{-9} [43]) to retard monomer diffusion from submicron monomer droplets. Both CA and HD, referred to here as costabilizers, are volatile organic components and are therefore not entirely desirable in the final product. Other researchers have used polymers, chain transfer agents, and comonomers as stabilizers, as will be discussed later.

Monomer droplet stability can be understood in terms of free energy. The partial molar free energy of adding a second component to a droplet is made up of two terms, the partial molar free energy of mixing and the interfacial partial molar free energy. The partial molar free energy of mixing (the Flory Huggins expression [44]) can be combined with the interfacial partial molar free energy to give

$$\frac{\Delta \bar{G}_i}{RT} = \ln\varphi_i = (1 + m_{ij})\varphi_j + \chi_{ij}\varphi_j^2 + \frac{2\bar{V}_i\gamma}{RTr} \tag{2}$$

Ugelstad et al. [45] have applied this equation to various monomers and surfactants. It is clear from this equation that the free energy increases as the phase diameter decreases. The smaller the monomer droplet, the less stable it is. Therefore, a driving force exists for the monomer to diffuse from a small droplet to a larger one. Over time, non-monodisperse systems of droplets of pure monomer will decrease in number as the smaller droplets swell the larger ones and then disappear. Jannson [46] has shown that this occurs in unagitated systems, and that the timescale for diffusional instability can be on the order of seconds.

Prior to 1962, droplets below 1 μm were considered too unstable to participate in the nucleation process. In 1962, Higuchi and Misra [47] proposed that the addition of a water insoluble compound to the monomer will enhance the stability of small droplets by prohibiting diffusion. In 1973, Ugelstad et al. [48] showed how submicron styrene droplets could be made stable enough to participate in the nucleation processes by adding small amounts of cetyl alcohol. Later, Ugelstad [48] used Eq. 2 to explain these experimental observations.

It can be shown [49] for two phases in equilibrium that the partial molar free energies must be equal. In an emulsion (or miniemulsion) there are three phases: monomer droplets, the aqueous phase and polymer particles. Since monomer is soluble in all of these phases, the equilibrium condition requires that the three phases have equal partial molar free energies. In the presence of monomer droplets, emulsion polymer particles contain 30–80% monomer in them. Therefore, they are said to be "swollen" with monomer. Ugelstad et al. [48] and Azad and Fitch [50] have shown that addition of a third water-insoluble component to a swollen polymer particle can increase the monomer to polymer ratio. They have shown that an optimum chain size for the additive exists since the solubility of the additive increases as the chain size decreases. They found

that the optimum hydrocarbon stabilizer is hexadecane. Others have found that if a fatty alcohol is used as the stabilizer, the minimum chain length required is 12 carbon atoms [51].

Ugelstad et al. [52] have shown how this theory may be used to devise a method to prepare large monodisperse particles of predetermined size. By using the appropriate amount of cosurfactant, polymer particles can be swollen with monomer to the desired size. Polymerization in conditions that prevent additional nucleation results in large monodisperse polymer particles of size 1–100 μm. This method has been criticized by other groups as being in error due to measurement selectivity.

If Ostwald ripening is retarded by using a costabilizer, predominant droplet nucleation can be achieved. This is the basis of miniemulsion polymerization. One of the first comprehesive studies of miniemulsion polymerization was done on styrene by Choi et al. [53].

2.3
Mathematical Modeling of Miniemulsion Polymerization

Various mathematical treatments of specific mechanisms within the miniemulsion polymerization reaction abound. This section will be limited to those papers that attempted to model the overall miniemulsion polymerization reaction. Perhaps the earliest (1981) serious attempt to model this system was that by Chamberlain, Napper and Gilbert [54]. Balances of the number of droplets, number of polymer particles and monomer conversion were constructed for batch miniemulsion polymerization. Droplets and particles were considered to be monodisperse. Comparison of the model with experimental data led to the conclusion that free radical entry into monomer droplets is substantially less than for ordinary macroemulsion particles. Chen, Gothjelpsen and Schork [55] published a model of approximately the same complexity for continuous stirred tank miniemulsion polymerization with an oil-soluble initiator. El-Aasser and coworkers [56–60] published a series of papers focusing on the modeling of miniemulsion copolymerization, particularly in relation to monomer transport. They described monomer transport in terms of a mass transfer coefficient and a driving force derived from an equilibrium concentration calculated from equating the partial molar free energies. This same group [61] modeled seeded miniemulsion polymerization (containing both polymeric seed particles and miniemulsion droplets) with oil-soluble initiator. Monomer transfer by collision of droplets with particles was found to be important. Fontenot and Schork [62, 63] published a very detailed model of batch macro- and miniemulsion polymerization, indicating the differences between the two mechanisms, and including both micellar and droplet nucleation mechanisms. Significant droplet coalescence was predicted. The model was in good agreement with data. Samer and Schork [64] published a mathematical model of continuous stirred tank (CSTR) and plug flow (PFR) miniemulsion polymerization reactors. They were able to explain why the rate of polymerization

for miniemulsion polymerization in a CSTR is substantially higher than for macroemulsion polymerization in the same reactor. All of the models discussed have been particle number models, containing no information about droplet size distribution or particle size distribution. None have attempted to model the formation of droplets during the miniemulsification stage.

Cunningham and coworkers [65–68] have completed detailed modeling of nitroxide mediated radical polymerization in miniemulsion. They found that issues of distribution of the control agent between the aqueous and organic phases can be critical to maintaining livingness.

3
Properties of Miniemulsion Polymerization

After having described the mechanism of miniemulsion polymerization and how it differs from macroemulsion polymerization in the previous section, this section will focus on the various mechanisms and properties of miniemulsion polymerization.

3.1
Shear Devices

Miniemulsions are produced by the combination of a high shear device to break up the emulsion into submicron monomer droplets with a water-insoluble, monomer-soluble component to retard monomer diffusion from the submicron monomer droplets. Both steps are necessary to effect predominant droplet nucleation. In the absence of a high-shear device, miniemulsion systems revert to macroemulsion polymerizations, indicating that the presence of a costabilizer alone is not sufficient to cause predominant droplet nucleation. The formation of submicron droplets is accomplished by placing a coarse emulsion (of monomer in water) in a high shear field. In general, it is best to form a coarse pre-emulsion before subjecting the system to high shear. This is because most devices that impart high shear are poor mixers, so unless a coarse emulsion is created first, the monomer and water phases may not be in close proximity when they enter the high shear field. A coarse pre-emulsion may be formed by vigorous stirring of the monomer, water, surfactant mix, as would be done to create a macroemulsion. For reasons of practicality, the costabilizer should be dissolved in the monomer before pre-emulsification.

For laboratory investigations of miniemulsions, a variety of high-shear devices have been used, although sonication has been the most popular. Sonication, however, may not be very practical for the large-scale production of commercial miniemulsion polymers. An effective alternative to sonication is also driven by the need to design an efficient miniemulsion polymerization process. A continuous process places greater demand on the shear device in terms of energy consumption and dissipation.
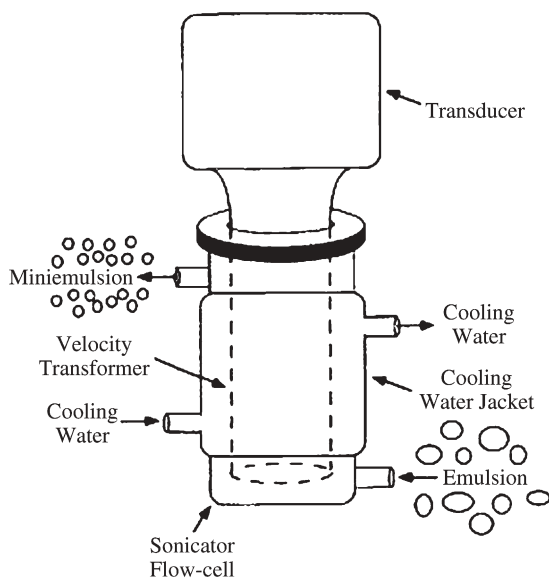
Fig. 4   Sonicator with cooling jacket (from [69])

The mechanism for ultrasonic emulsification is primarily that of cavitation. A typical sonicator for emulsification consists of a velocity transformer coupled to a transducer, capable of oscillating in a longitudinal mode, where the velocity transformer is immersed in the liquid. Figure 4 illustrates the basic parts of a sonicator with a continuous flow attachment, like the one used in this work. In this case, the flow cell is secured to the velocity transformer by a flange and a Teflon O-ring. The intensity of cavitation depends on the power delivered to the velocity transformer, which is relayed to the transducer from a variable transformer or some other control device not shown in Fig. 4.

The word homogenization is somewhat inconclusive and is typically defined as used in context. Two processes are considered here; the first is a fine clearance valve homogenizer, and the second is a rotor-stator-type mechanical homogenizer. Homogenization is similar to sonication and produces submicron droplets by a combination of mechanical shearing and cavitation.

The fine clearance valve homogenizer has been in use for nearly 100 years for the homogenization of milk and milk products. Raw milk is an emulsion of fat globules dispersed in a continuous skim milk phase. Without homogenization, the fat globules would rise to the top of the milk and form a cream layer. Homogenization reduces the average diameter of these fat globules and subsequently reduces their creaming rate, extending the shelf-life of the product. The MicroFluidizer used by many miniemulsion investigators is an example of this type of shear device.

The rotor-stator-type mechanical homogenizer generates submicron droplets by forcing the emulsion through small openings in the stationary
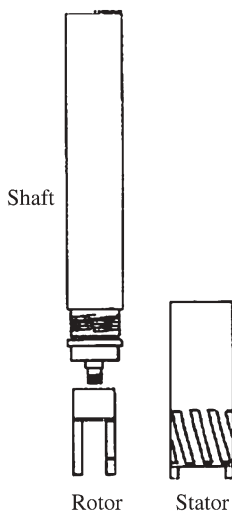
Fig. 5 Rotor-stator homogenizer (from [69])

stator at very high speeds, as illustrated in Fig. 5. The intensity of shearing depends on the rotor speed, which can be set anywhere from 5–35 krpm for most modern equipment. However, at higher speeds the shearing action generates a significant amount of heat, which may harm the sample being emulsified or the machine itself. This device has been used by Samer and Schork [69] and others, and has been shown to be effective. However, in general, the miniemulsion droplet size achievable with a rotor-stator device is larger than that achievable with sonication or valve homogenizers.

3.2
Choice of Surfactant

The vast majority of miniemulsion polymerizations reported in the literature have been stabilized with anionic surfactants, probably because of the widespread application of anionic surfactants in macroemulsion polymerization, and due to their compatibility with neutral or anionic (acid) monomers and anionic initiators. However, Landfester and coworkers [70, 71] have used the cationic surfactants cetyltrimethyl ammonium bromide (CTAB) and cetyltrimethyl ammonium tartrate for the production of styrene miniemulsions. They report that these surfactants produce similar particle sizes to anionic surfactants used at the same levels. Bradley and Grieser [72] report the use of dodecyltrimethyl ammonium chloride for the miniemulsion polymerization of MMA and BA.

Wang and Schork [73] miniemulsion polymerized vinyl acetate using the nonionic surfactant polyvinyl alcohol (PVA). They found that stable miniemulsions could be made with PVA and HD, but when the HD was removed, the PVA

alone was not capable of functioning as both surfactant and costabilizer. In general, the droplet diameter was greater with PVA than would be expected with an anionic surfactant. Chern and Chen [74, 75] used nonylphenol ethoxylate (40 ethylene oxides per molecule) with a monomeric costabilizer such as docecyl methacrylate or stearyl methacrylate to form stable miniemulsions of styrene. Wu and Schork [76] used polyoxyethylene-23 lauryl ether (BRIJ-35) as the surfactant with HD as the costabilizer to form stable miniemulsions of vinyl acetate. Landfester and coworkers [70, 71] also used polyethylene oxide for the miniemulsion polymerization of styrene. Luo and Schork used nonylphenyl ethoxylate (Triton X-405) and an interfacial initiation system to miniemulsion polymerize BA and BA copolymerized with cationic monomer. Graillat and Guyot [77] also used Triton X-405 to produce high solids vinyl acetate emulsions via miniemulsion polymerization.

Guyot and coworkers [78] have produced stable miniemulsions of styrene using the polymerizable surfactant, vinylbenzylsulfosuccinic acid sodium salt.

3.3
Choice of Costabilizer

Early work in miniemulsion polymerization [5, 48–50] used either cetyl alcohol (CA) or hexadecane (HD) to retard Ostwald ripening in submicron monomer droplets. Both CA and HD, referred to here as *costabilizers*, have the requisite properties for a costabilizer: high monomer solubility, low water solubility and low molecular weight. The need for these properties can be seen from Eq. 2. High monomer solubility will give a large Flory Huggins interaction parameter between the costabilizer and the monomer (χ_{ij}). Low water solubility will ensure a distribution coefficient for the costabilizer that very strongly favors the monomer drops, giving a higher volume fraction of costabilizer in the droplet. Low molecular weight will give a high ratio of costabilizer molecules to monomer molecules (m_{ij}) in the droplet. All of these factors will enhance swelling, or retard monomer loss via Ostwald ripening.

With cetyl alcohol, there is the complication that the polarity of the molecule may cause it to reside at the surface of the droplet, imparting additional colloidal stability. Here, the surfactant and costabilizer form an ordered structure at the monomer-water interface, which acts as a barrier to coalescence and mass transfer. Support for this theory lies in the method of preparation of the emulsion as well as experimental interfacial tension measurements [79]. It is well known that preparation of a stable emulsion with fatty alcohol costabilizers requires pre-emulsification of the surfactants within the aqueous phase prior to monomer addition. By mixing the fatty alcohol costabilizer in the water prior to monomer addition, it is believed that an ordered structure forms from the two surfactants. Upon addition of the monomer (oil) phase, the monomer diffuses through the aqueous phase to swell these ordered structures. For long chain alkanes that are strictly oil-soluble, homogenization of the oil phase is required to produce a stable emulsion. Although both costabilizers produce re-

latively stable emulsions, Azad et al. [80] have shown that the alkanes will produce emulsions of higher stability. A 1:3 molecular ratio of surfactant to costabilizer has been shown to provide optimal stability in emulsion systems where the costabilizer is a fatty alcohol. Shah [81] postulated that this ratio is due to an optimum alignment of surfactant and costabilizer molecules at the interface in microemulsions. Hallworth and Carless [82] have proposed that the stability of an emulsion containing long chain alkanes of fatty alcohols comes from a film at the interface which makes collisions at the interface more elastic.

Various researchers [83–88] have concluded from experimental data that liquid crystals of surfactants exist at the interface. These observations have been suggested through birefringence, interfacial tension, and viscosity measurements. Lack et al. [87] studied the formation of liquid crystals with fatty alcohol costabilizers as a function of concentration, chain length, and ratio of emulsifiers using birefringence measurements. Tertiary phase diagrams were presented which show two regions of normal micelle formation. There are also three regions of homogeneous anisotropic mesophases. These three mesophases, are (i) hexagonal rodlike aggregates of mixed micelles, (ii) lamellar double layers with overlapping tails, and (iii) lamellar double layers dispersed in the aqueous phase. The concentration of surfactants used in miniemulsions is found to fall within region (iii). These "liquid crystals" were shown to form more easily at higher emulsifier concentrations, with shorter chain alcohols, and with sonication.

Although evidence exists for liquid crystal formation with fatty alcohol costabilizers, it does not for systems with long chain alkanes. Delgado et al. [89] have presented evidence that the role of hexadecane costabilizer in miniemulsion polymerizations is one of diffusional control. Rodriguez [90] and Delgado [91] have reported that no optional ratio of hexadecane to SLS exists in the preparation of miniemulsions. This provides evidence for the lack of crystal formation. Ugelstad et al. [45] have presented evidence that alkanes are more likely to follow the diffusion mechanism.

3.3.1
Polymeric Costabilizers

The use of polymer as a costabilizer was first reported by Reimers et al. in 1995 [92]. Conventional thinking has been that effective costabilizers must be highly water-insoluble, highly monomer-soluble, and of low molecular weight, as required by Eq. 2. Polymer made from the same monomer from which the miniemulsion is to be made will be highly water-insoluble, and most polymers are quite soluble in their own monomers. The requirement that the costabilizer must be of low molecular weight is based on reported swelling experiments and theoretical swelling calculations [93]. Data from Schork and Reimers [94] demonstrate that it is possible to create miniemulsion latexes with a poor costabilizer (polymer). The inclusion of a small amount (~4%wt) of a monomer-

soluble polymer can significantly reduce the diffusional degradation of an emulsion. These emulsions are not *thermodynamically* stable, but they can be *kinetically* stable. This means that the droplets resist diffusional degradation long enough to allow nucleation to occur. The droplets are typically in the miniemulsion range of 100 to 500 nm in diameter. The polymeric costabilizer is thought to delay Ostwald ripening sufficiently to allow nucleation of the monomer droplets by water-phase radicals (primary or oligomeric). Once the droplets are nucleated, the polymer produced adds additional diffusional stability. It should be noted that the monomeric miniemulsions formed are not true miniemulsions in the sense that they are not stable over a period of months. However, Ostwald ripening can be reduced to permit the polymerization to be carried out. The latexes produced from polymer-stabilized emulsions have all the characteristics of miniemulsion latexes, and derive from droplet nucleation. The polymer has been shown to perform as well as hexadecane in stabilizing the droplets for the short periods necessary to ensure nucleation. It has the added advantages of being totally innocuous in the final product, very soluble in the monomer, and very water insoluble.

Reimers and Schork [94, 95] report the use of PMMA to stabilize MMA miniemulsions enough to effect predominant droplet nucleation. Emulsions stabilized against diffusional degradation by incorporating a polymeric costabilizer were produced and polymerized. The presence of large numbers of small droplets shifted the nucleation mechanism from micellar or homogeneous nucleation, to droplet nucleation. Droplet diameters were in the miniemulsion range and reasonably narrowly distributed. On-line conductance measurements were used to confirm predominant droplet nucleation. The observed reaction rates were dependent on the amount of polymeric costabilizer present. The latexes prepared with polymeric costabilizer had lower polydispersities (1.006) than either latexes prepared from macroemulsions (1.049) or from alkane-stabilized miniemulsions (1.037).

Wang and Schork [73] used PS, PMMA and PVAc as the costabilizers in miniemulsion polymerizations of VAc with PVOH as the surfactant. They found that, while PMMA and PS were effective kinetic costabilizers (at 2–4%wt on total monomer) for this system, PVAc was not. While the polymeric costabilizers did not give true miniemulsions, Ostwald ripening was retarded long enough for predominant droplet nucleation to take place.

Aizpurua et al. [96] have studied the kinetics of vinyl acetate miniemulsions stabilized with PS or PVAc. Guyot and coworkers [97] used PS as the costabilizer for the miniemulsion encapsulation of pigment. Samer [67] has used PMMA to stabilize MMA miniemulsions for continuous polymerization in a CSTR.

Various papers on hybrid miniemulsion polymerization have used alkyd [98, 99], polyester [100] or polyurethane [101] as both the costabilizer and a component of the hybrid particle. Since most of these materials were added far in excess of the levels normally used as costabilizers, it is not surprising that they are effective.

Polymeric materials are not costabilizers in the sense that costabilizers cause superswelling. Rather, they slow the onset of Ostwald ripening and preserve the number of monomer droplets, if not their size. However, this review will take a functional, rather than thermodynamic definition of a costabilizer, and include a discussion of the use of polymers as agents to enhance droplet nucleation under the heading of costabilizers.

3.3.2
Monomeric Costabilizers

Reimers and Schork [102] first used highly water-insoluble comonomers as costabilizers. Vinyl hexanoate, *p*-methyl styrene, vinyl 2-ethyl hexanoate, vinyl decanoate, and vinyl stearate were copolymerized with MMA at 10%wt on the total monomer. All formed stable miniemulsions with droplet diameters between 150 and 230 nm. All resulted in polymerization via predominant droplet nucleation (miniemulsion). Chern and coworkers [43, 74, 75,103] have used high molecular weight alkyl methacrylates at levels of 2–3%wt on the total monomer as both costabilizers and comonomers in the miniemulsion polymerization of styrene. The advantage, of course, is that, after polymerization, no low molecular weight costabilizer remains in the miniemulsion latex. Lauryl methacrylate and stearyl methacrylate have been used, since these high methacrylates have low water solubilities (10^{-8}–10^{-9} g/g) and high solubilities in styrene monomer. As might be expected, stearyl methacrylate is found to be better at retarding Ostwald ripening than lauryl methacrylate, but neither is found to be as effective as HD. Samer [104] found that 2-ethylhexyl acrylate (2EHA) as a comonomer was not an effective costabilizer in a continuous stirred tank (CSTR) copolymerization with MMA.

3.3.3
Other Costabilizers

The use of a chain transfer agent (CTA) as a costabilizer opens up new possibilities for molecular weight control. Macroemulsion polymerizations which utilize higher molecular weight mercaptan chain transfer agents exhibit retarded transport of the CTA from the monomer droplet into the growing polymer particles. This results in slower delivery of the mercaptan to the reaction sites over the course of the polymerization. (In some commercial recipes this retarded transport is used to "meter" the highly reactive CTA to the reaction site.) If the mercaptan were at the site of polymerization, as in a miniemulsion, new degrees of freedom in selecting chain transfer agents would exist. That is, the relative reactivities of chain transfer versus propagation can be used to select the CTA, without relying on retarded mass transfer. This may increase the efficiency of chain transfer (since CTA will not be "trapped" in the shrinking monomer droplets near the end of Interval II), or at least allow the chemist additional degrees of freedom in tailoring the molecular structure by manipulating the reaction conditions.

Mouran et al. [105] polymerized miniemulsions of methyl methacrylate with sodium lauryl sulfate as the surfactant and dodecyl mercaptan (DDM) as the costabilizer. The emulsions were of a droplet size range common to miniemulsions and exhibited long-term stability (of greater than three months). Results indicate that DDM retards Ostwald ripening and allows the production of stable miniemulsions. When these emulsions were initiated, particle formation occurred predominantly via monomer droplet nucleation. The rate of polymerization, monomer droplet size, polymer particle size, molecular weight of the polymer, and the effect of initiator concentration on the number of particles all varied systematically in ways that indicated predominant droplet nucleation.

For the MMA/DDM system, the value of the chain transfer constant (C_x) is 0.6–0.8, meaning that the chain transfer agent reacts slightly less rapidly than the monomer. Hence, the DDM will be present throughout the course of the reaction. In a system such as styrene/DDM, where C_x is 15–20, the rapid consumption of the DDM might leave the particles subject to Ostwald ripening before enough polymer is formed to stabilize the growing particles. In addition, the rapid consumption of CTA early in the course of the polymerization might give a clearly identifiable low molecular weight tail. Wang et al. [106] studied the miniemulsion polymerization of STY with DDM as the costabilizer. In this system, the chain transfer constant is at the other end of the kinetic spectrum.

The miniemulsion monomer droplets with dodecyl mercaptan as costabilizer were very stable. Shelf lives ranged from 17 hours to three months. The kinetics of miniemulsion polymerization were studied. Unlike other miniemulsion systems where the costabilizer does not act as a chain transfer agent, the polymerization rate fell with costabilizer level because the chain transfer agent enhances radical desorption from the particles. The polymerization rates in all of the miniemulsions were lower than those of the corresponding macroemulsions. Polymerized particles were larger than in the corresponding macroemulsions, but molecular weights were lower. Results indicate that DDM can serve as an effective costabilizer as well as a chain transfer agent, even when the chain transfer constant is quite high. The fact that the molecular weights were lower in the miniemulsion reactions indicates predominant droplet nucleation.

Reimers and Schork [107] used lauroyl peroxide (LPO) in the miniemulsion polymerization of MMA as a costabilizer as well as an initiator. They showed that lauroyl peroxide concentrations above 1 g/100 g of monomer are capable of stabilizing droplets against Ostwald ripening. The stable droplets produced were in the miniemulsion-size range and could then be nucleated. The ratio of the number of droplets to the number of particles was found to be close to unity. The overall rates of polymerization were high for the miniemulsions, as were the rates per particle. Once again, it was shown that components other than conventional costabilizers can stabilize small droplets against Ostwald ripening, causing droplet nucleation. Asua et al. [108] used LPO (in addition to the traditional costabilizer HD) to impart diffusional stability to styrene miniemulsions. They also evaluated a number of oil-soluble initiators (LPO, BPO, AIBN) as costabilizers, and concluded that only LPO was capable of acting as the sole costabilizer (without HD).

3.3.4
Enhanced Nucleation

Miller et al. [109–111] report that the addition of a small amount (as small as 0.05%wt) of polystyrene (PS) to the styrene phase of a miniemulsion polymerization of styrene causes an increase in both the rate of polymerization and the number of final polymer particles. This is not just a polymeric costabilizer effect, since these emulsions were also stabilized with what are known to be effective levels of HD or CA, although the effect was more pronounced with CA. With the addition of 1%wt styrene, the number of final particles was nearly the same as the original number of droplets, indicating 100% droplet nucleation. This was not the case for equivalent polymerizations without the PS. For polymerizations without the PS, the final particle number varied with the initial initiator concentration to the power of 0.31. With 1%wt PS, the particle number was independent of the initiator concentration, which is very clear evidence of 100% droplet nucleation. Miller hypothesized that miniemulsions prepared from polystyrene in styrene solutions resemble the polymer particles formed in normal (no polymer) miniemulsion polymerizations at early conversions. This being the case, these polymer-containing droplets would be able to effectively compete with growing polymer particles for free radicals, whereas their counterparts that contain no polymer are not, and as a result a greater fraction of the initial droplets become polymer particles. Based on this mechanism, Miller speculated that the presence of the polymer increases the capture efficiency of the droplets by modifying either their interior (by increasing the interior viscosity, thereby increasing the probability of a radical propagating rather than exiting) or the droplet/water interface (by disrupting the surfactant/CA interfacial barrier to radical entry). Experimental results were reported which support the latter explanation. (It should be noted that the effect was most pronounced with CA, and that other investigators have reported near 100% droplet nucleation with HD and without added polymer.)

In a follow-on set of papers, Blythe et al. [112–115] studied the effect on the polymerization kinetics of changing the properties of the polymer used to enhance nucleation. Miniemulsions were formed from CA with PS as the polymer additive, and CA as the costabilizer. Varying the molecular weight of the PS from 39,000 and 206,000 in systems containing 1% PS did not change the kinetics. Also, changing the end group of the polymer chain from a hydrophobic end group to a hydrophilic end group had no effect on the kinetics in 1% polymer systems. However, predissolving 1% PS in a miniemulsion always results in a significant enhancement in the kinetics compared to similar systems that do not contain predissolved polymer. The authors conclude that this enhancement in the kinetics is not due to either a change in the interior viscosity of the droplets or a disruption of the condensed phase formed by cetyl alcohol and sodium lauryl sulfate (since these effects would be altered by the variations in the PS above). Instead, it was suggested that the enhancement can primarily be attributed to a preservation of the droplet number due to the pre-

sence of polymer in each of the miniemulsion droplets formed during homo-genization. The authors rightly point out that the polymer is a poor costabilizer, due to its high molecular weight, but that it does act to preserve the droplet due to the thermodynamic balance between monomer and polymer. Therefore, they conclude that the polymer is unable to preserve the size of the droplets produced during ripening, only the number produced during homogenization. They support this by using 1% PS with no other costabilizer, where they are able to show that particle formation occurs via droplet nucleation. In other experiments, they show that there is no enhancement unless the shear rate is high enough to bring the droplet size down into the range where it is susceptible to Ostwald ripening.

In another paper, Blythe et al. [116] studied enhanced droplet nucleation when HD is used as the costabilizer. The enhancement in this case is much less. The authors conclude that, since HD is a very effective costabilizer (much more so than CA), the effect of the polymer in preserving the droplet number, if not the droplet size distribution, is not pronounced. Therefore, this effect appears to occur primarily in systems with CA (perhaps due to its polar nature, and so, its probable interfacial activity). Multiple investigators have reported effective (near 100%) droplet nucleation with HD and other costabilizers.

Blythe et al. argue (with justification) that polymer should not be termed a costabilizer since it does not cause super-swelling; however, this review will take a functional, rather than thermodynamic definition of a costabilizer, and treat polymer-stabilized miniemulsions under the heading of costabilizers.

3.4
Choice of Initiator

Following the common practice in macroemulsion polymerization, most miniemulsion polymerizations have been run using water-soluble initiators. However, a number of researchers have looked at the possibility of using an oil-soluble initiator instead. As discussed previously, Schork and Reimers [107] and Asua et al. [108] have used LP as both the initiator and the costabilizer. In addition, Asua et al. used other oil-soluble initiators in conjunction with HD (as the costabilizer) to carry out miniemulsion polymerization of styrene.

Ghazaly et al. [117] used both water-soluble and oil-soluble initiators in the copolymerization of n-butyl methacrylate (BA) with crosslinking monomers. Variations in the particle morphologies were found between the water-soluble and oil-soluble initiators, depending on the hydrophobicity of the crosslinking monomer. It would seem that if the crosslinking monomer is quite hydro-phobic, and therefore resides preferentially in the core of the particles (droplet), then the oil-soluble initiator is more effective at carrying out crosslinking, since the oil-soluble initiator will also reside preferentially in the core of the particle. Luo and Schork [118] carried out emulsion and miniemulsion polymerization using oil-soluble initiator in the presence of an aqueous phase free radical scavenger. They concluded that, for miniemulsion particles up to 100 nm in

diameter, even with an oil-soluble initiator, radicals originating in the aqueous phase play an important role in initiating polymerization. This is attributed to the fact that two radicals generated from the decomposition of an initiator molecular within the particle may recombine before initiating polymerization.

Choi et al. [53] have successfully used both water-soluble and oil-soluble initiators in the miniemulsion polymerization of styrene. Alducin and Asua [119] have studied the MWD of polystyrene miniemulsion polymerized with oil-soluble initiators. Rodriguez et al. [61] have developed a mathematical model of seeded miniemulsion polymerization with oil-soluble initiator. Blythe et al. [120] have successfully carried out miniemulsion polymerization of styrene with AMBN (oil-soluble). Ghazaly et al. [117] have used AIBN for the miniemulsion copolymerization of a hydrophobic bifunctional macromer. The polymerization progressed much faster when KPS was used than when AIBN was used. This may be due to the tendency of oil-soluble initiator radicals to recombine before initiating polymerization, as discussed by Luo.

Oil-soluble initiators have commonly been used in hybrid miniemulsion polymerization to improve monomer conversions. In most cases, the oil-soluble initiator was used as a *finishing initiator* to increase final monomer conversion, while a water-soluble initiator was used to carry out the majority of the polymerizations. These types of polymerizations will be discussed later.

3.5
Robust Nucleation

One of the problems with macroemulsion polymerization is the variability of the particle number with initiation rate, monomer quality, inhibition levels, and so on. This is a serious industrial problem, as shown by the fact that a great many industrial macroemulsion polymerizations are carried out as seeded polymerizations in which a known concentration of seed particles are added to the emulsion, and the polymerization is run under conditions that suppress nucleation of additional particles. The variance in particle number comes about because there is a competition for surfactant between the growth of existing particles (that need additional surfactant to stabilize their growing surface area), and the nucleation of new particles.

If a miniemulsion could be run at 100% droplet nucleation (or near to this), then a very robust nucleation system would result. The number of particles could be determined by the number of initial monomer droplets, and this can be controlled by adjusting surfactant, costabilizer and shear levels. In this case, the number of particles would be independent of radical flux. In fact, the most compelling evidence for droplet nucleation is experimental evidence that the number of polymer particles is independent of the initiator level. (Once the radical flux is high enough to nucleate all, or nearly all of the droplets, then changes in radical flux caused by inconsistent initiator or unknown inhibitors will not affect the final particle number.) We will discuss the results of such robust nucleation later.

3.6
Monomer Transport Effects

Macroemulsion polymerization relies on the transport of monomer from the monomer droplets to the polymer particles. This transport is driven by the equilibrium swelling of the polymer particles. This presumes rapid (relative to the rate of polymerization) transport of monomer. For most monomers, this is a good assumption. However, for monomers that are very water insoluble (VEOVA [vinyl versatatex] or DOM [dioctyl maleate]), this may not be true. In making this determination, the following assumptions can be made:

(i)   The limiting resistance is the transport from the monomer droplets into the aqueous phase.
(ii) Transport across the aqueous phase is by forced convection (stirring) and it is not the rate-determining step.
(iii) Transport from the aqueous phase into the polymer particle may (or may not) have an overall mass transfer coefficient equal to that for exit from the monomer droplets, but the very large interfacial area of the particles (relative to the monomer droplets) will ensure that this is not the limiting step.
(iv) Transport out of the monomer droplet can be modeled with an overall mass transfer coefficient and a driving force based on the difference between the saturation concentration of monomer in the aqueous phase and the concentration in the aqueous phase in equilibrium with the particle.

For monomers that are highly water insoluble, the driving force in (iv) will be small, since the saturation value will be extremely small. Since accurate overall mass transfer coefficients are hard to determine accurately, the likelihood of transport limitation with highly water-insoluble monomers is an open question. Some data (which will be discussed later) indicate the presence of transport limitations in the copolymerization of highly water-insoluble monomers. These potential transport limitations can be avoided by using miniemulsion polymerization.

In the case of nanoencapsulations of solids, or the incorporation of high molecular weight, highly water-insoluble additives (such as polymers, oligomers, alkyds) into polymer particles, macroemulsion polymerization will not work, since the high molecular weight material will remain in the monomer droplet as the monomer is transported out. At the end of the reaction, the additive will remain in the depleted monomer droplets, rather than in the polymer particles. Clearly, these products can only be made via miniemulsion polymerization.

3.7
Droplet Stability

Different techniques are available to carry out a free radical polymerization in emulsion. In spite of the fact that their names (macro-, mini- and microemul-

sion) seem to indicate a correlation between process and final particle size of the polymer particle dispersion, this is usually not the case. On the contrary, these techniques should rather be distinguished by either their nucleation process or the stability of the initial oil (the monomer) dispersion. These two aspects of the emulsion polymerization processes, nucleation and stability, are strictly related and depend upon each other.

To clarify this point, let us first discuss the case of a conventional emulsion recipe, or macroemulsion. In this case, the monomer is initially dispersed in water under agitation in the presence of surfactants [121], resulting in a rather coarse oil dispersion. Droplet size typically depends upon rate of stirring, and the resulting droplet size is generally in the 1–10 µm range (the reason for the name "macroemulsion"). This dispersion is unstable and, if the stirring is stopped, the monomer phase separates very quickly. Because of the large sizes of the droplets, the total surface area of the dispersion is small (the surface-to-volume ratio for spherical droplets is proportional to the inverse of the droplet diameter) and most of the surfactant is not used to stabilize the droplets; it aggregates in water to form micelles. These micelles, and not the droplets, are the main loci for polymerization, while the droplets just act as monomer reservoirs. In other words, the final particles in the macroemulsion do not correspond to the initial droplets. The most important consequence is that, in order to have a successful process, the monomer, as well as all other possible comonomers and coreactants, must be water-soluble enough to diffuse from droplets to particles.

For historical reasons [122], a stable dispersion of sub-micron droplets is called a miniemulsion. Miniemulsions do not form spontaneously and require high shear devices to form. The resulting dispersion is usually quite fine, with the droplet size ranging from 50 to 500 nm [3], a large droplet surface area, with all of the surfactant used to stabilize the droplets and with no more micelles present in the system. As a result, the droplets become the predominant loci for nucleation and polymerization. That is, in an ideal miniemulsion, there is a 1:1 correspondence between initial monomer droplets and final polymer particles. (This 1:1 correspondence is not always attained, and remains a point of controversy [1].) This was experimentally demonstrated for the first time by Ugelstad and coworkers in 1973 [5]. The consequence of this virtual copying process from droplets to particles is twofold: (i) final particle size is given by the initial droplet dispersion, and both surfactant coverage and surface tension do not significantly change during the process; (ii) any kind of hydrophobic component can be conveniently included in the recipe, since we can be sure that it is going to participate to the polymerization process.

A third type of emulsion process is the so-called microemulsion [123]. In microemulsions, the polymerization starts in droplets as well. However, these are thermodynamically stable and, in contrast to miniemulsions, they form spontaneously by gentle stirring. They consist of large amounts of surfactants or mixtures of them, and they possess an interfacial tension close to zero at the water/oil interface, with droplet sizes usually ranging between 5 and 50 nm. In

contrast to miniemulsions, the high amount of surfactant needed to prepare the microemulsions leads to a complete coverage of the droplets surface. Given the huge number of droplets initially present in the system, nucleation cannot take place in all of the droplets, and a large number of empty micelles can still be found in the final product.

Besides the similarities between mini- and microemulsions, especially with respect to the nucleation process, microemulsions are characterized by very peculiar thermodynamics; in this respect, there are many similarities between a macro- and a miniemulsion. Accordingly, we should focus on the reason why monomer dispersions are unstable in macroemulsions, while they are stable in miniemulsions.

3.7.1
Stability of Monomer Dispersions

There are two ways by which a dispersion of monomer droplets can degrade: (i) by droplet coalescence, and (ii) by diffusion degradation (often referred to as Ostwald ripening). While the first mechanism of degradation can be avoided by adding enough surfactant to the system, when two monomer droplets of different sizes, and stabilized by a surfactant, are put in water, they will start exchanging monomer without even making direct contact – through monomer diffusion across the water (continuous) phase.

This process of molecular diffusion is governed by the difference in chemical potentials of the monomer in the two droplets. Morton's equation has been successfully used to describe the swelling of polymer particles with monomer [32]. According to this equation, the chemical potential of the monomer in a droplet of radius $r_p (\mu_m^{(d)})$ in the presence of polymer is given by:

$$\frac{\mu_m^{(d)}}{RT} = \ln(\varphi_m) + \left(1 - \frac{1}{m_{pm}}\right)\varphi_p + \chi_{m,p}\varphi_p^2 + \frac{2\gamma \bar{V}_m}{r_p RT} \tag{3}$$

where φ_m and φ_p represent the volume fraction of monomer and polymer, respectively, in the particle (so $\varphi_m + \varphi_p = 1$); m_{pm} is the ratio of equivalent number of molecular segments between monomer and polymer; $\chi_{m,p}$ is the interaction parameter between monomer and polymer; γ is the interfacial tension at the water/oil interface; $\bar{V}_m$ is the molar volume of the monomer; R is the universal gas constant; T the temperature. In the case of pure monomer droplets, the partial molar free energy of mixing is zero, which is represented in Eq. 3 by the first two terms, accounting for the entropy of mixing, and by the third term, accounting for the enthalpy of mixing. Ugelstad and Hansen showed that this expression could be satisfactorily extended to the case where any other species, not necessarily a polymer, is involved [11]. Accordingly, we will use Eq. 3 to conveniently describe the monomer chemical potential in a miniemulsion droplet.

According to Eq. 3, in the case of a macroemulsion of pure monomer droplets, the monomer chemical potential is given by the last term with ($\varphi_m = 1$),
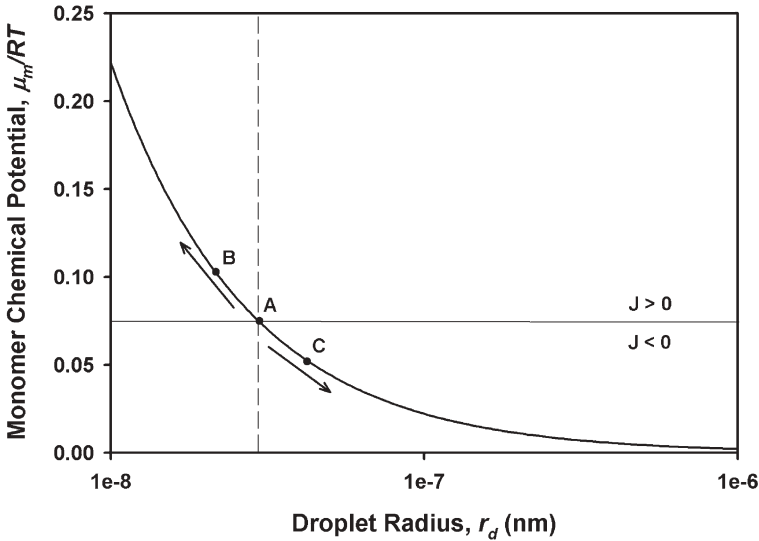
Fig. 6 Monomer chemical potential for a pure monomer droplet as a function of droplet radius (γ=25 Mn/M; $\bar{V}_\mathrm{m}$=1.1·10^{-4} m^3 mol; T=298.15 K). Point A represents an unstable equilibrium

accounting for the contribution of the interfacial energy. Therefore, given two droplets with the same interfacial tension (we assume that surface tension is a function of the degree of coverage only, and that this is the same for the two droplets), their chemical potential is a function of the droplet radius only and it is only the same if the two droplets have the same size. Therefore, when two droplets of different radii $r_{\mathrm{d},1}$ and $r_{\mathrm{d},2}$ are put together, the difference in their chemical potential is given by:

$$\frac{\Delta\mu_{\mathrm{m},1-2}^{(\mathrm{d})}}{RT} = \frac{2\gamma\tilde{V}_m}{RT}\left(\frac{1}{r_{\mathrm{d},1}} - \frac{1}{r_{\mathrm{d},2}}\right) = \psi\left(\frac{1}{r_{\mathrm{d},1}} - \frac{1}{r_{\mathrm{d},2}}\right) \tag{4}$$

In other words, if $r_{\mathrm{d},2} > r_{\mathrm{d},1}$, the difference in chemical potential is positive and the monomer will diffuse from 1 to 2. This process is schematically represented in Fig. 6. Point A represents the initial size of the monomer droplets. Equilibrium exists only if all of the droplets have the same size. In the case where a smaller droplet is created (symbolized by point B), monomer will flow from B to A (positive flux to A, or J>0) as a result of the difference in chemical potential, making B smaller and smaller. The opposite happens for a bigger droplet (point C), which will become bigger and bigger. In other terms, point A is an unstable equilibrium. This process is usually referred to as monomer ripening.

The ripening process characteristic of oil dispersions is avoided in miniemulsions by introducing a so-called costabilizer in the oil phase (a species with no or very low water phase solubility). The mechanism that halts the
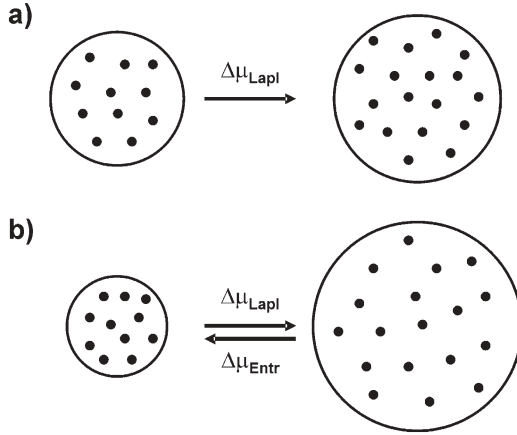
Fig. 7 Schematic representation of the role of the hydrophobe in halting the ripening process in a miniemulsion

ripening in a miniemulsion is sketched in Fig. 7. Let us suppose that the oil phase is initially comprised of the monomer and a perfectly water insoluble costabilizer. Let us also suppose that the system is initially made of two droplets with different sizes but the same compositions (or monomer volume fractions). Finally, let us suppose, for the sake of simplicity, that the mixture of monomer and costabilizer behaves like an ideal mixture, so that $\chi_{m,h}=0$. Under such hypotheses, the difference in chemical potential between the two droplets of Fig. 7a is given by the following equation:

$$\frac{\Delta\mu_{m,1-2}^{(d)}}{RT} = \ln\frac{\varphi_{m,1}}{\varphi_{m,2}} + (1-m_{m,h})(\varphi_{m,2}-\varphi_{m,1}) + \psi\left(\frac{1}{r_{d,1}} - \frac{1}{r_{d,2}}\right) \tag{5}$$

where the indexes 1 and 2 refer to the first and the second droplet, respectively, subscript h identifies the costabilizer, and ψ is defined as in Eq. 4. Knowing that $\ln\varphi_m \approx -(1-\varphi_m)$ for small volume fractions of the costabilizer, it is possible to simplify the previous equation as follows:

$$\frac{\Delta\mu_{m,1-2}^{(d)}}{RT} = m_{m,h}(\varphi_{m,1}-\varphi_{m,2}) + \psi\left(\frac{1}{r_{d,1}} - \frac{1}{r_{d,2}}\right) \tag{6}$$

Since the two droplets have the same initial composition ($\varphi_{m,1}=\varphi_{m,2}$), it follows from this equation that the difference in chemical potential is given by the difference in size only, and (as in a macroemulsion) monomer will flow from the smaller to the bigger droplet. The main consequence of this process is that the costabilizer is concentrated in the smaller droplet, while the big droplet becomes more and more dilute. This creates a gradient in composition (see Fig. 7b), which is represented by the first term on the right hand side of Eq. 6.

Therefore, an opposite flow of monomer is generated, which eventually leads to an equilibrium between the two terms of Eq. 6 (to a stable situation).

Just for completeness, these two contributions to the monomer equilibrium in a miniemulsion are often expressed in terms of pressures in the literature. The droplet composition gives rise to a so-called osmotic pressure:

$$\Pi_{osm} = RTc_m \tag{7}$$

while the presence of an interface generates a so-called Laplace pressure inside the droplet, defined as follows:

$$\Pi_{Lapl} = \frac{3\gamma}{r_d} \tag{8}$$

Note that, when accounting for the differences in osmotic and Laplace pressures between the two droplets, one obtains the same equation as Eq. 6, with $m_{m,h}=8/3$.

This same process is described in Fig. 8 in terms of the different contributions to the monomer chemical potential. In this figure, the initial droplet size (r_d) and monomer volume fraction (φ_m) have been fixed, and the corresponding volume of costabilizer inside the droplet has been computed ($V_h = 4/3\,\pi\,r_d^3$ $(1-\varphi_m)$. Assuming that the costabilizer cannot diffuse out of the particle, in Fig. 8 it is possible to observe how chemical potential of the monomer changes by increasing or decreasing the monomer volume fraction in the droplet. In particular, two contributions to the global potential (entropy of mixing and surface tension) have been reported. It is clear that if a second droplet is inserted into the system, these two terms will act in opposite ways until the difference in chemical potential between the droplets is compensated for.

Even though two droplets are always able to find an equilibrium when put together, because of the presence of the costabilizer, it is useful to check whether this equilibrium is stable or not. Going back to the case of the macroemulsion depicted in Fig. 6, point A is an unstable point because, if the system is perturbed and a new droplet is formed, it will diverge from the equilibrium point. Clearly, the necessarily condition to have a stable equilibrium is that the slope of the chemical potential versus radius is positive at the point of equilibrium [122, 124]. For a macroemulsion, this condition leads to the following expression:

$$\frac{\partial}{\partial r_d}\left(\frac{\mu_m^{(9)}}{RT}\right) = -\frac{\psi}{r_d^2} \tag{9}$$

which is always a negative function. This is not true for a miniemulsion. Referring to Fig. 8, we observe that the equilibrium point of the system is stable. In fact, if a larger droplet is generated by perturbing the equilibrium, this has a larger chemical potential and the monomer will flow back, bringing the droplet back to the original equilibrium point. The opposite happens when producing a smaller droplet.
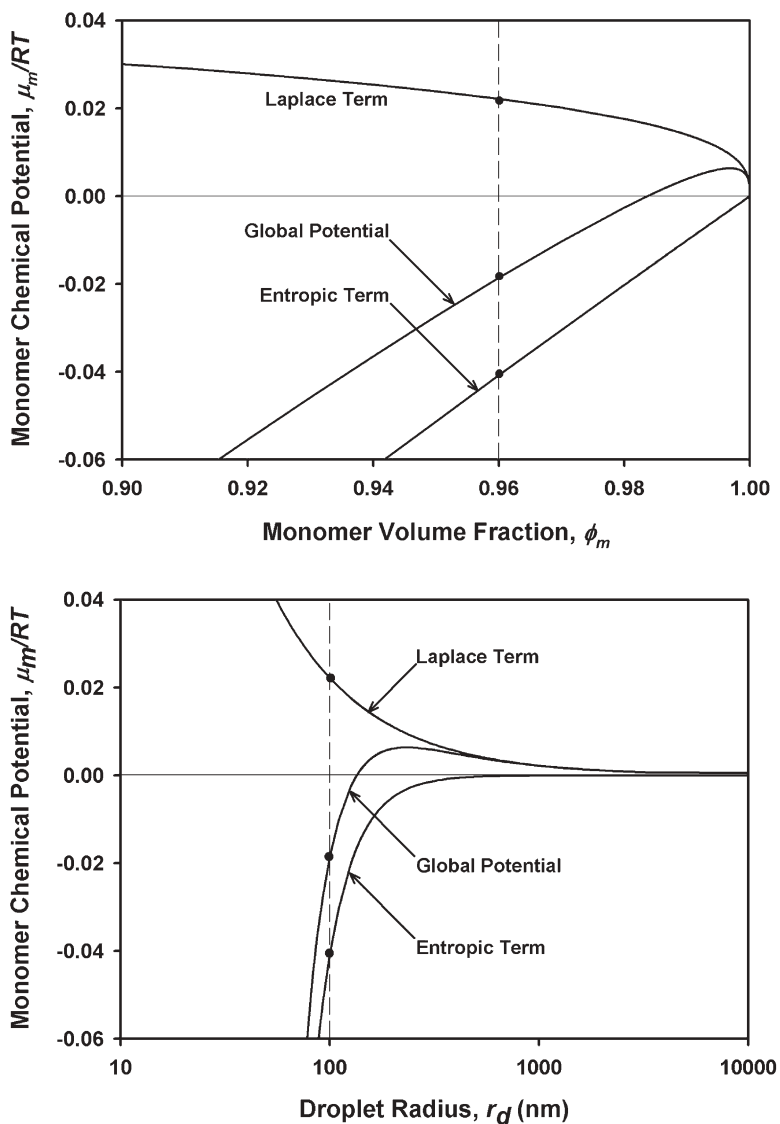
Fig. 8 Monomer chemical potential in a droplet comprising monomer and hydrophobe as a function of the monomer volume fraction (top) and droplet radius (bottom). The global potential (as given by Ugelstad's equation) is given, as well as the entropic term due to mixing and the Laplace term due to surface tension. Parameters: $m_{m,h}=1$; $\chi_{m,h}=0$; $\gamma=25$ mN/m; $\tilde{V}_m=1.1 \cdot 10^4$ m^3 mol; $T=298.15$ K; $\varphi_m=0.96$; $r_d=100$ nm

Let us check the conditions under which the derivative of the chemical potential is positive in a miniemulsion. Under the hypothesis of small concentrations of costabilizer in the droplet ($\varphi_m \to 1$), and of ideal behavior of the mixture ($\chi_{m,h}=0$), the condition of local stability leads to the following expression:

$$\frac{\partial}{\partial r_d}\left(\frac{\mu_m^{(9)}}{RT}\right)=\frac{9m_{m,h}V_h}{4\pi r_d^4}-\frac{\psi}{r_d^2} \tag{10}$$

and in turn to:

$$r_d < \bar{r}_d = \left(\frac{9m_{m,h}V_h}{4\pi\psi}\right) \tag{11}$$

The previous expression returns the value of the droplet radius corresponding to the maximum of the monomer chemical potential curve ($\bar{r}_d$), and says that, for a given amount of costabilizer in the particle (V_h), the droplet radius must be smaller than $\bar{r}_d$ in order to be locally stable. The same equation can be expressed in terms of the critical costabilizer volume fraction, $\bar{\varphi}_h$, as follows:

$$\varphi_h > \bar{\varphi}_h = \left(\frac{\psi}{3mr_h}\right)^{3/2} \tag{12}$$

where $r_h=(3V_h/4\pi)^{1/3}$. Both these two critical quantities, $\bar{r}_d$ and $\bar{\varphi}_h$, are functions of costabilizer concentration, costabilizer type and surface tension, as well as the corresponding value of the monomer chemical potential, which is given by the following simple expression:

$$\left.\frac{\mu_m^{(d)}}{RT}\right|_{r_d=\bar{r}_d}=2\left(\frac{\psi}{3}\right)^{3/2}\left(\frac{1}{m_{m,h}r_h}\right)^{1/2} \tag{13}$$

Therefore, it is important to show how these quantities depend upon the parameters involved, and what their effects are, in order to understand the stability of the droplet.

This analysis is shown in Fig. 9, where the parameters ψ, $m_{m,h}$, r_d and φ_m have been varied systematically. Let us start with the analysis of Fig. 9a. In this figure, the volume of the droplet has been varied while the volume fraction of the costabilizer is kept constant (the vertical dashed line represents the corresponding monomer volume fraction). This, in turn, changes the volume of the costabilizer inside the droplet, and the monomer chemical potential curve changes accordingly. As predicted by Eq. 12, when the droplet size is decreased, the maximum of the chemical potential curve shifts to smaller monomer volume fractions, and the height of the maximum increases. In other terms, as droplet size decreases (or costabilizer volume fraction decreases) the system approaches the unstable region. Figure 9b is conceptually identical to Fig. 9a,
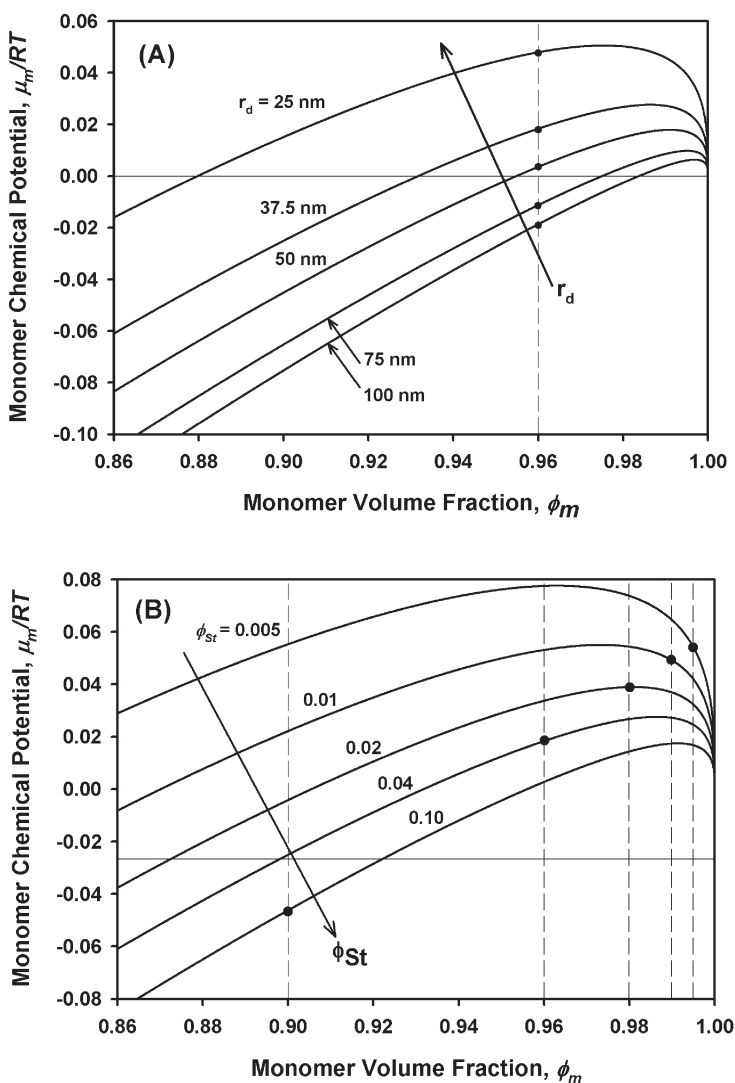
Fig. 9 Monomer chemical potential in a droplet comprising monomer and hydrophobe as a function of the monomer volume fraction. (A) Effect of droplet size (r_d=25, 37.5, 50, 75 and 150 nm); (B) effect of hydrophobe volume fraction (φ_h=0.005, 0.01, 0.02, 0.04 and 0.1)

but the amount of costabilizer in the droplets is varied while the droplet radius is kept constant and the costabilizer volume fraction varies. Again, as the costabilizer concentration decreases, the system moves from a region of complete stability to a region of instability. By observing Fig. 9b, it is also possible to distinguish between local and global equilibrium stability. The curve corresponding to φ_h=0.04 clearly satisfies the requirements of local equilibrium stability. In fact, if the system is slightly perturbed, the equilibrium point is always
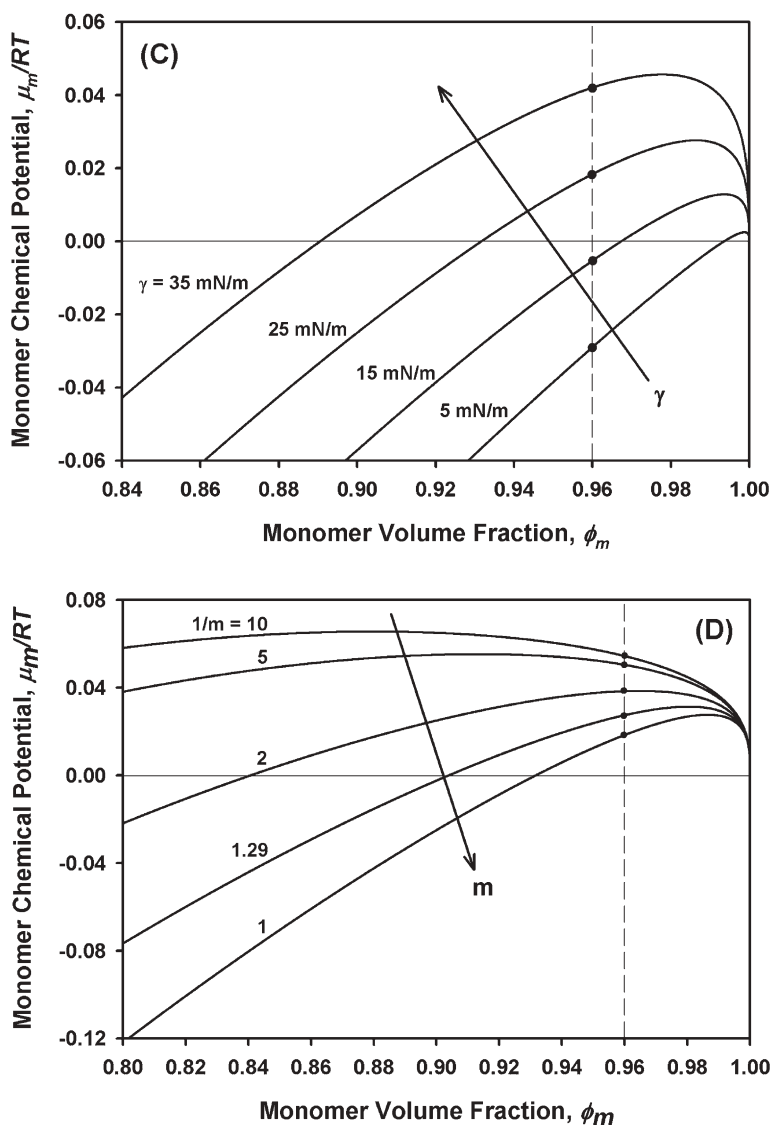
Fig. 9c,d (C) effect of surface tension (γ=5, 15, 25 and 35 mN/m); and (D) effect of hydrophobe to monomer segment ratio ($1/m_{m,h}$=1, 1.29, 2, 5 and 10). Other parameters (otherwise differently indicated): $m_{m,h}$=1; $\chi_{m,h}$=0; γ=25 mN/m; $\tilde{V}_m$=1.1·10^4 m^3 mol; T=298.15 K; φ_h=0.04; r_d=100 nm

convergent. However, in the case of large perturbations, it is possible to create droplets large enough to fall to the right of the maximum of the monomer chemical potential curve; these droplets have chemical potentials lower than that corresponding to equilibrium. Such a droplet will receive monomer from the droplets at the equilibrium point and will grow indefinitely. On the other hand, the same cannot happen for the equilibrium point corresponding to the curve for φ_h=0.10. In fact, in this case, all of the droplets that are larger than those at the equilibrium point also have larger monomer chemical potentials. Therefore, these droplets will always shrink back to the equilibrium point.

In Fig. 9c, the effects of different surface tension values on the equilibrium are examined. By decreasing the interfacial tension, the Laplace term becomes less significant than the contribution given by the entropy of mixing, and therefore ripening is decreased and stability is enhanced. Theoretically, in a system with zero surface tension at the oil/water interface, the total monomer chemical potential is given solely by the entropic terms, and it is always stable.

Finally, in Fig. 9d, the influence of the ratio of the equivalent number of molecular segments in the costabilizer to that of the monomer, $m_{m,h}$ is shown. This value can be thought of as the ratio between the molecular weights of the two components, and for oligomers and polymers this can be replaced by the average chain length. If we look closely at this figure, as well as Eqs. 12 and 13, we can see that the maximum of the chemical potential curve becomes smaller and shifts to larger droplet sizes as $m_{m,h}$ approaches unity, which facilitates the formation of a stable equilibrium. When dealing with very bulky costabilizers (such as a polymer), the maximum increases and shifts to low droplet sizes, making the equilibrium unstable.

There are two issues we should remark upon at this point. First, even though we have shown that the presence of a costabilizer in the system can lead to complete thermodynamic stability, we have also shown that costabilizers with smaller molecular weights are more effective. Therefore, even though these species are hydrophobic, they always have a small but finite solubility in water. As a result, the differences in costabilizer chemical potentials among the droplets will lead to a very slow diffusion of the costabilizer and eventually to the destabilization of the system. Second, Eqs. 11 and 12 do not contradict those reported by (for example) Sood and Awasthi, that point to a minimum droplet diameter below which there is no stability [124]. In our analysis, we set the equilibrium and the corresponding volume of costabilizer, and then we perturbed the system by changing the monomer concentration, and observed what happened. In their work, they computed the corresponding equilibrium point as a function of droplet radius for a given costabilizer concentration, and they checked the conditions at which this point corresponds to a stable equilibrium. As in our analysis, they conclude that decreasing droplet radius sufficiently eventually pushes the system into the region of instability.

3.7.2
Experimental Validation

Our understanding of miniemulsion stability is limited by the practical difficulties encountered when attempting to measure and characterize a distribution of droplets. In fact, most of the well-known, established techniques used in the literature to characterize distributions of polymer particles in water are quite invasive and generally rely upon sample dilution (as in dynamic and static laser light scattering), and/or shear (as in capillary hydrodynamic fractionation), both of which are very likely to alter or destroy the sensitive equilibrium upon which a miniemulsion is based. Good results have been obtained by indirect techniques that do not need dilution, such as soap titration [125], SANS measurements[126] or turbidity and surface tension measurements [127]. Nevertheless, a substantial amount of experimental evidence has been collected, that has enabled us to establish the effects of different amounts of surfactant and costabilizer, or different costabilizer structures, on stability.

This work has been summarized very effectively by Landfester and co-workers [127]. They showed that many costabilizers act as osmotic agents, blocking monomer ripening. All of these costabilizers have relatively low molecular weights and, according to the analysis above, the polymers can barely be used to prevent ripening, even though the resulting miniemulsion can be stable for enough time to run the polymerization.

However, the most significant result of their work was that they clearly demonstrated the role of surfactant in the formation of miniemulsions. They showed that it is possible to effectively control droplet size by tuning the surfactant concentration. The more surfactant, the smaller the droplets one can obtain. They also showed that, apart from the case where extremely large amounts of surfactant are used, the surfactant coverage of the droplets is always incomplete. In particular, larger droplets exhibit very low coverage and, therefore, large interfacial tensions at the oil/water interface. On the other hand, small droplets need large surfactant coverage in order to be stable.

In the same work, it is also supposed that colloidal stability, rather than monomer ripening, plays an effective role in determining the final droplet size. Such a conclusion was supported by two different experimental results. First, it was noticed that droplet size increases right after the emulsification process stops, and a stable situation is typically achieved after just a few hours. However, if surfactant is added immediately after, this growth in size does not occur. Second, it is shown that there is a clear correlation between final droplet size and amount of oil phase used in the recipe. In particular, when the oil fraction in the system increases, droplet size also increases.

These results can be effectively explained by supposing that colloidal stability plays a major role in determining miniemulsion stability. In fact, it is clear that addition of surfactant stops the droplet growth, which is explained by the enhanced colloidal stability. Moreover, in more concentrated systems, where the rate of droplet coalescence is larger, one obtains larger droplets, as

expected. However, some droplet flocculation or the formation of a limited layer of monomer at the water/air interface is commonly observed in many miniemulsion recipes. Moreover, there are well documented cases in the literature where either a bimodal distribution has been obtained at the end of the polymerization [124], or instability problems are evident at the beginning of the polymerization [128].

When speculating about the colloidal stability of a monomer droplet dispersion in water, one could use the Deryaguin-Landau-Verwey-Overbeek theory, also known as DLVO theory, to analyze the stability of the system. This has been done in Fig. 10a, where we show the effect of different surface potentials upon the rate of coagulation, β, defined in the case of two droplets of the same size as:

$$\beta = \frac{8\,k_b T}{3\mu W} \tag{14}$$

where μ represents the water viscosity and W is Fuch's stability ratio (see [129] for a further explanation of how this value has been computed). In Fig. 10b, the quantity $1/\beta N_d$ is reported, which expresses the characteristic time for coalescence. We can see that even small surface potentials are enough to give great colloidal stability. These values correspond to rather low surfactant coverage (around 5%) [124, 129], which is well below the typical coverage measured experimentally for miniemulsions [127]. It is therefore apparent that colloidal stability is a very strong function of droplet size, and it is quite difficult to explain the formation of bimodalities or monomer separation by colloidal stability only.

On the other hand, previous analyses of the monomer chemical potential in miniemulsions may justify some of the previous results. In Fig. 8, it is shown that miniemulsion formulations are often very close to instability, with positive monomer chemical potentials (which corresponds to conditions of monomer oversaturation, or superswelling). Experimental proof of this was reported by Landfester et al. [127], who said that the Laplace pressure is much larger than the osmotic pressure at equilibrium. We must also consider that, in reality, we are never dealing with perfectly monodispersed distributions of droplets, as the previous analysis supposed. Therefore, it is realistic to suppose that in the presence of a droplet size distribution, a fraction of the droplets lie in the unstable region and can lead to the formation of either pronounced bimodalities, monomer phase separation, or droplet flocculation [124]. Moreover, from the analysis of Fig. 9a to d, we observe that critical stability is almost reached when small droplets are formed. Therefore, it is not surprising to observe that smaller droplets require larger surfactant coverage to be stable, since lower surface tension helps the droplets to move away from the instability region. The same influence of surface tension on the chemical potential of the monomer could also explain why, on the addition of surfactant, the sizes of the droplets do not change significantly after emulsification. In fact, by adding surfactant, one decreases the interfacial tension and stabilizes the miniemulsion ripening.
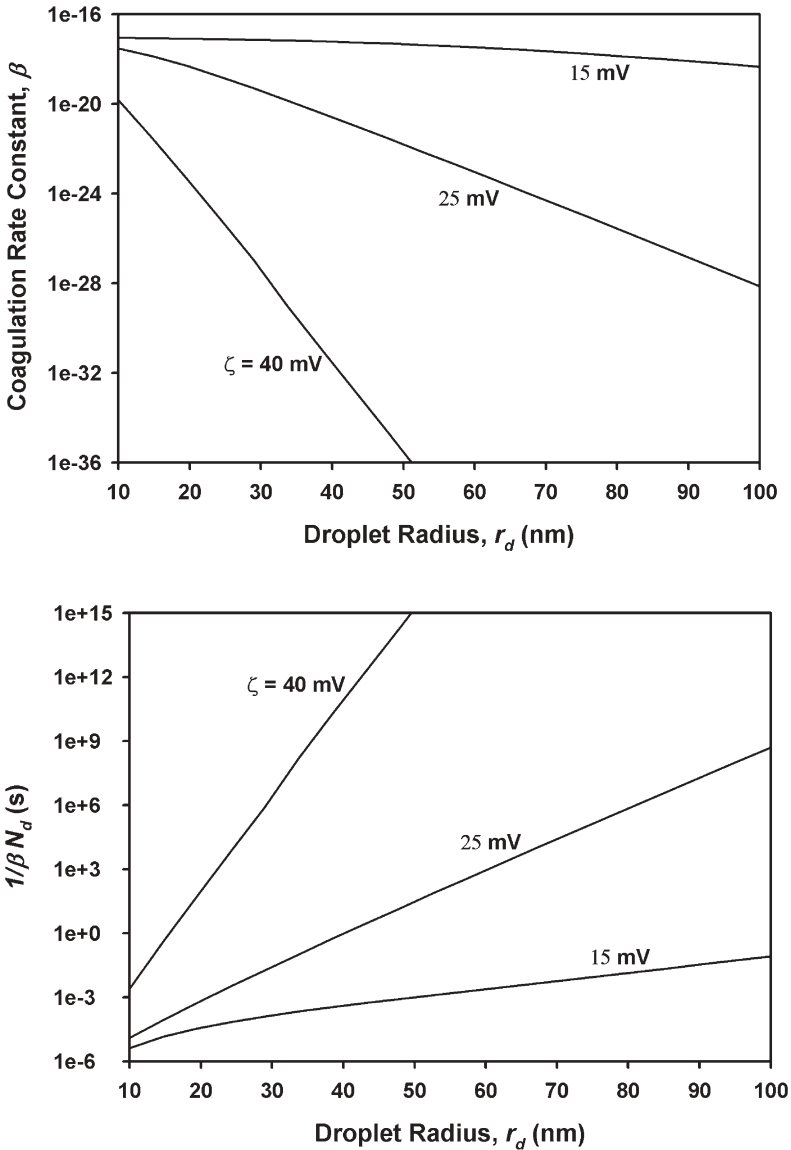
Fig. 10 Coagulation rate constant (β) and characteristic time for coagulation ($1/\beta N_d$) as a function of droplet size for various droplet surface potential values ($\zeta=15, 25$ and 40 Mv), as computed by DLVO theory. In order to compute N_d, a system with 20% oil fraction was supposed

It is certain that we do not know what the leading effect in determining droplet stability and droplet distribution in miniemulsion is at this point; both colloidal and ripening effects probably play a role. Future work is therefore needed to clarify these problems.

3.8
Semibatch and Plug Flow Reactors

Semibatch (also known as *semicontinuous*) reactors are used commercially for two primary reasons: to limit the rate of polymerization by effecting some level of monomer starvation, or to correct for copolymer composition drift in copolymerization. Since the use of semibatch reactors for miniemulsion co-polymerization involves important concepts (relative rates of mass transfer and reactivity ratios), a discussion of semibatch copolymerization reactions will be deferred until the section on copolymerization. In the area of semibatch homopolymerization, Tang et al. [116] studied seeded semibatch polymerization of BA. They found that when the monomer was added neat, a small number of new particles were formed. However, when the semibatch feed was a miniemulsion, a large number of new particles were formed, presumably by droplet nucleation. Monomer droplet nucleation decreased with increasing seed concentration, presumably because of monomer transport to the existing particles. Leiza, Sudol and El-Aasser [130] used semibatch miniemulsion polymerization (starting from a seed latex) to prepare high solids (>60%) lattices of BA. It is well-known that semibatch polymerization can be an effective method for making high solids latex. Part of the advantage of semibatch when making high solids is the broad PSD brought on by nucleation of particles over most of the reaction time. Miniemulsion can be effective in this regard, since a miniemulsion feed is likely to produce additional polymer particles, as shown by Tang et al. [131].

Sajjadi and Jahanzad [132] have used semibatching to study the effects of monomer-starved and monomer-flooded conditions on the seeded polymerization of styrene. Seed particles were grown via macroemulsion polymerization and added to the initial charge of the reactor. Feeds of styrene miniemulsion (using HD as the costabilizer) were then added, either batch-wise or in a semibatch mode. Under starved conditions, the miniemulsion droplets were depleted of their monomer by transport into the growing particles. (Even though HD prevents the loss of monomer to droplets of a larger size, it cannot prevent monomer depletion to polymer particles with a low degree of monomer saturation, as would be found in a starved reactor; this same effect will be seen later in experiments where fresh miniemulsion droplets are introduced into a CSTR at high monomer conversion.) When the miniemulsion was added batch-wise (flooded conditions) the final particle number was greater, since a greater portion of the miniemulsion droplets were nucleated before being depleted of monomer. When polymer was predissolved in the monomer prior to miniemulsion formation, the final number of particles was indepen-

dent of the method of addition, and was equal to the seed particles plus the number of miniemulsion droplets added. Therefore, with predissolved polymer, the droplet number (but not the droplet size distribution as inferred from the final PSD) was preserved. This result reinforces the idea of polymer as an agent for preserving droplet number.

Macro- and miniemulsion polymerization in a PFR/CSTR train was modeled by Samer and Schork [64]. Since particle nucleation and growth are coupled for macroemulsion polymerization in a CSTR, the number of particles formed in a CSTR only is a fraction of the number of particles generated in a batch reactor. For this reason, their results showed that a PFR upstream of a CSTR has a dramatic effect on the number of particles and the rate of polymerization in the CSTR. In fact, the CSTR was found to produce only 20% of the number of particles generated in a PFR/CSTR train with the same total residence time as the CSTR alone. By contrast, since miniemulsions are dominated by droplet nucleation, the use of a PFR "prereactor" had a negligible effect on the rate of polymerization in the CSTR. The number of particles generated in the CSTR was 100% of the number of particles generated in a PFR/CSTR train with the same total residence time as the CSTR alone.

Durant [133] has used a PFR to achieve a miniemulsion with a solids content in the industrially relevant range. Ouzineb and McKenna [134] have used a PFR to obtain miniemulsion latexes with high solids contents.

3.9
Continuous Stirred Tank Reactors

The first work on continuous miniemulsion polymerization was by Chen, Gothjelpsen and Schork [55]. Theirs was a very simple model of CSTR miniemulsion polymerization using an oil-soluble initiator. The first experimental work was that of Barnette [35, 135]. This work showed two significant facts:

(i) Miniemulsion polymerization in a CSTR is not subject to the sustained or decaying oscillations very often found in CSTR macroemulsion polymerization. The sustained oscillations in macroemulsion take place at low surfactant concentration due to the competition for micellar surfactant between existing particles requiring additional surfactant to stabilize the increased interfacial area produced by particle growth, and nucleation of new particles from micelles. Since, in miniemulsion polymerization, the nucleation occurs from monomer droplets, and micelles do not exist, no such competition exists, and the monomer conversion climbs monotonically on start-up to its steady-state value.

(ii) In miniemulsion polymerization, the steady-state monomer conversion is approximately twice that found in macroemulsion polymerization (after the oscillations have died away). This means that a single CSTR will yield approximately twice as much polymer as the same reactor carrying out a macroemulsion polymerization.

Observation (i) above can be understood in terms of droplet nucleation and the lack of competition between nucleation and growth. A mechanistic understanding of observation (ii) above was provided by Samer and Schork [64]. Nomura and Harada [136] quantified the differences in particle nucleation behavior for macroemulsion polymerization between a CSTR and a batch reactor. They started with the rate of particle formation in a CSTR and included an expression for the rate of particle nucleation based on Smith Ewart theory. In macroemulsion, a surfactant balance is used to constrain the micelle concentration, given the surfactant concentration and surface area of existing particles. Therefore, they found a relation between the number of polymer particles and the residence time (reactor volume divided by volumetric flowrate). They compared this relation to a similar equation for particle formation in a batch reactor, and concluded that a CSTR will produce no more than 57% of the number of particles produced in a batch reactor. This is due mainly to the fact that particle formation and growth occur simultaneously in a CSTR, as suggested earlier.

An approach similar to that taken by Nomura and Harada was used by Samer to quantify the effects of droplet nucleation on emulsion polymerization kinetics in a CSTR. In their simplified analysis, it was assumed that radical capture by particles and droplets is proportional to the ratio of particle and droplet diameters. This assumption is reliable at low to moderate residence times, when polymer particles still closely resemble monomer droplets with respect to composition and surface characteristics. For predominant droplet nucleation, the maximum particle generation is limited by the concentration of monomer droplets in the feed. In Fig. 11 the steady state particle generation is given as a function of the residence time and temperature. Nucleation efficiency is defined as the number of particles divided by the number of droplets in the
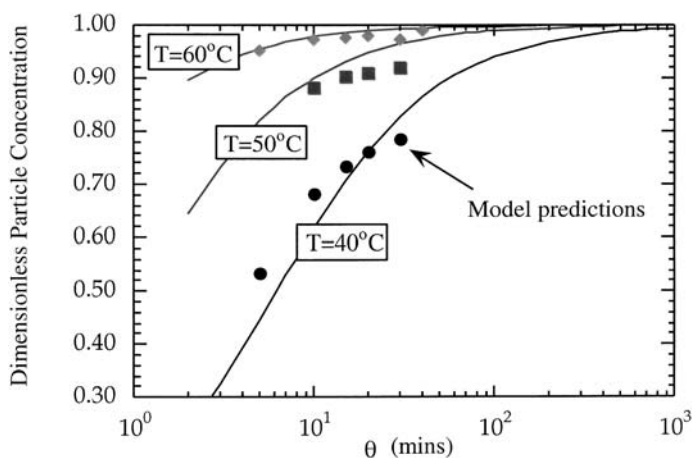
Fig. 11 Model predictions for the number of particles in CSTR miniemulsion polymerization expressed as the number of particles divided by the number of droplets in the feed (from [64])

feed and is shown to increase with increasing temperature. It can be seen in this figure that the nucleation efficiency approaches unity for residence times greater than 30 minutes. Therefore, whereas the particle number is limited by surfactant in macroemulsion emulsion polymerization in a CSTR, in miniemulsion polymerization, the particle number is limited by monomer droplet concentration, *but to a much smaller extent*. Therefore, since nucleation efficiencies in miniemulsion polymerization approach 100%, rather than the 57% predicted for macroemulsion polymerization, the steady-state conversion in a miniemulsion (proportional to particle number) found by Barnette [36] is approximately twice that in a macroemulsion.

Samer and Schork [69, 137] confirmed Barnette's findings on the lack of oscillations in the CSTR miniemulsion polymerization of MMA. Aizpurua and Barandiaran [138] confirmed the lack of oscillations in CSTR miniemulsion polymerization over a wide range of surfactant and initiator concentrations for VAc. They also observed near-identical MWD for macroemulsion and miniemulsion polymerizations under the same conditions. This is understandable, since MWD should be determined by particle size (and number of radicals per particle) rather than by particle nucleation mechanism. Aizpurua et al. [139] successfully used polymeric costabilizers in the CSTR miniemulsion polymerization of VAc at high solids levels. Neither sonication alone, nor the presence of costabilizer alone, was able to eliminate the oscillations found in macroemulsion polymerization. However, sonication and costabilizer together were capable of eliminating oscillations, indicating droplet nucleation. The results cited above are particularly significant, since, as fresh miniemulsion droplets are introduced into a CSTR, they must compete to retain their monomer with existing particles that may contain more than 50% polymer (50% conversion). Therefore, for instance, miniemulsion droplets stabilized with 5% polymer would need to compete with existing particles containing 50% polymer. The fact that the particle number approaches the droplet number in the feed suggests that the droplet number (if not droplet size distribution) is conserved.

Samer also demonstrates the existence of multiple steady states in isothermal miniemulsion polymerization in a CSTR. This is not surprising, since multiplicity is a function of gel or Trommsdorf effect, and not of nucleation mechanism.

Miniemulsion copolymerization in a CSTR involves some very interesting features. However, in the interest of clarity, these systems will be discussed along with results for batch copolymerization.

4
Applications

It should be apparent by now that miniemulsion polymerization systems have some properties that ought to be exploitable when making polymer colloidal products with unique or improved properties. This section will discuss some of these documented and potential applications.

Overall, there are two areas in which miniemulsion polymerization differs significantly from macroemulsion polymerization. First, miniemulsions exhibit a significant robustness of nucleation. Macroemulsion polymerization relies heavily on micellar nucleation. Micellar nucleation is notoriously nonrobust. It has been called "near-chaotic", because final particle number depends on the operating variables (temperature, initiator concentration and addition method, mixing, and so on) and on the quality of the reagents (including initiator purity and level of inhibitor in the monomer). As stated above, this is due to the competition for surfactant between the nucleation of new particles from micelles and the adsorption of surfactant onto the surface of growing polymer particles. In fact, the sensitivity to inhibitor levels has actually been used to manipulate particle size: addition of an oil-soluble initiator is known to result in the nucleation of more particles, and hence smaller particles. The introduction of a water-phase inhibitor is known to extend Interval I, allowing particle growth to occur simultaneously with particle nucleation, producing fewer and hence smaller particles. Finally, the use of seeded systems to control particle number and size in commercial macroemulsion polymerization highlights the poor robustness of particle nucleation in macroemulsion polymerization. This should be contrasted with miniemulsion polymerization where, *if* droplet nucleation efficiency can be driven close to unity, the number of particles is determined by the levels of surfactant and costabilizer, and so should be controllable independent of the initiation system. While the number of particles is often preserved during miniemulsion polymerization, we have seen before that the PSD may not be. We have also seen the effect of robustness on CSTR polymerization, in that CSTR miniemulsion polymerization exhibits a substantially higher rate of particle nucleation *and* a lack of oscillations. This section will explore the ramifications of robust nucleation in miniemulsions.

The second property of miniemulsions that makes them unique when compared to macroemulsions is the virtual lack of monomer transport. Recall that, during Interval II of a macroemulsion polymerization, monomer must diffuse from the monomer droplets, across the aqueous phase, and into the growing polymer particles. Most macroemulsions are presumed to be reaction-limited. In other words, the rate of monomer diffusion is rapid in comparison with the rate of propagation, so that polymerization is reaction-limited. This is certainly true for monomers with water solubilities as low as that of styrene, but for monomers of much lower water solubility, this assumption may be questioned. Also, if any sort of non-monomeric materials are to be incorporated into the polymer particles, these are not likely to be transported easily across the aqueous phase. Examples of such systems would be preformed polymers or oligomers in hybrid miniemulsion polymerization, or solid particles in the case of nanoencapsulation. Certainly high molecular weight prepolymers or solid particles will not traverse the aqueous phase, and so, if introduced into a macroemulsion system, they will remain outside the loci of polymerization. In addition, in living radical polymerization, the molecular weight control agents are often only sparingly soluble in water. If the control agent is not at the locus

of polymerization, the polymerization will proceed by uncontrolled free radical polymerization, and any advantages of livingness are lost. This section will explore areas where miniemulsion polymerization may be superior to macroemulsion polymerization because of its virtual lack of interphase mass transfer.

4.1
Robust Nucleation

4.1.1
Effect of Initiation and Inhibition

Reimers [95] used polymeric costabilizer to carry out miniemulsion polymerization of MMA. Droplet nucleation was found to be the dominant nucleation mechanism in the polymerization. As a result, the nucleation was more robust, and the polymerizations were less sensitive to variations in the recipe or contaminant levels. This was evident in the rates of polymerization and in the particle numbers. The miniemulsion polymerizations were subjected to changes in initiator concentration, water-phase retarder, and oil-phase inhibitor, and were shown to be significantly more robust.

Batch miniemulsion polymerization of MMA using PMMA as the costabilizer was carried out with SLS as the surfactant and KPS as the initiator. Solids content was kept at ~30%. A low surfactant level was used with the miniemulsions to ensure droplet nucleation. The initiator concentration of the polymer-stabilized miniemulsion polymerizations was varied from 0.0005 to 0.02 M_{aq}, based on the total water content. An aqueous phase retarder, (sodium nitrite) or an oil-phase inhibitor (diphenylpicrylhydrazol [DPPH]), was added to both the miniemulsions and the macroemulsions prior to initiation. Particle numbers and rates of polymerization for both systems were determined.

4.1.1.1
Results

Results from the polymer-costabilized miniemulsion polymerizations are shown in Table 2. Droplet sizes were found to vary between 115.1 and 121.0 nm. These are in accord with measurements made by Fontenot [140] for MMA miniemulsions stabilized with hexadecane. The sizes of the particles in the final products were close to the sizes of the droplets, ranging from 102.6 to 108.1 nm, with polydispersities ranging from 1.011 to 1.027. The ratio of the number of particles to the number of droplets (N_p/N_d) was found to be between 0.95 and 1.08. Therefore, the majority of the droplets were nucleated to form polymer particles. Droplet nucleation led to polymerization rates comparable to those for the corresponding macroemulsions. For equal concentrations of initiator, 0.01 M_{aq}, the rates are 0.199 and 0.233 gmol/min L_{aq} for the mini- and the macroemulsion polymerizations, respectively.

Table 2 Results from polymer-stabilized miniemulsion polymerizations (from [95])

		D_d (nm)	D_p (nm)	PDI$_p$	$N_p \times 10^{-17}$ (L^{-1})	N_p/N_d	R_p (mol/ min L$_{aq}$)
[I]=	0.0005	118.1	105.1	1.013	4.452	0.99	0.096
	0.001	117.5	104.3	1.015	4.508	1.00	0.102
	0.002	116.8	105.1	1.018	4.428	0.98	0.151
	0.005	120.2	103.1	1.017	4.328	1.04	0.263
	0.01	117.4	105.1	1.016	4.548	1.01	0.199
	0.02	–	–	–	–	–	0.176
[NaNO$_2$]=	0.0	117.4	105.1	1.016	4.548	1.01	0.199
	0.0001	115.1	103.3	1.027	4.432	0.99	0.253
	0.0005	117.3	104.1	1.016	4.780	1.06	0.203
	0.001	118.7	102.7	1.011	4.840	1.08	0.201
	0.002	117.1	102.9	1.017	4.640	1.03	0.180
	0.005	118.2	118.4	1.014	3.304	0.47	0.016
[DPPH]=	0.0	117.4	105.1	1.016	4.548	1.01	0.199
	0.00005	118.2	103.2	1.013	4.704	1.05	0.155
	0.0001	118.4	103.3	1.012	4.720	1.05	0.149
	0.0005	117.8	102.6	1.014	4.732	1.05	0.146
	0.001	117.3	102.1	1.017	4.752	1.06	0.090
RPM=	100	119.2	107.0	1.012	4.328	0.95	0.086
	200	120.2	103.1	1.017	4.096	1.04	0.111
	300	120.8	108.1	1.012	4.096	0.97	0.138
	400	120.8	107.9	1.015	4.072	0.98	0.144
	500	121.0	107.4	1.012	3.996	0.95	0.143

The effects of the (water-soluble) initiator concentration on the polymerization of polymer-stabilized miniemulsion are shown in Table 2. An increase in the initiator concentration does not change the number of particles, but does increase the rate of polymerization. This is due to an increase in the number of radicals per particle. However, the number of radicals per particle ranged from just 0.5 to 0.8, indicating that the kinetics (after nucleation) are still essentially Smith Ewart Case II. The number of particles was found to be proportional to the initiator concentration raised to the power of 0.002±0.001. Macroemulsion polymerizations, in contrast, show a dependence of 0.2 and 0.4 for methyl methacrylate and styrene, respectively [141]. The fact that the exponent approaches zero indicates that all or nearly all of the droplets are being nucleated.

A water-phase retarder (sodium nitrite) was added to both the mini- and macroemulsion polymerizations. The rate of polymerization was reduced with increasing level of retarder, as would be expected. However, the number of particles *increased* with increasing retarder concentration. This result would only be expected with an *oil-soluble* retarder. The reason for this anomaly is
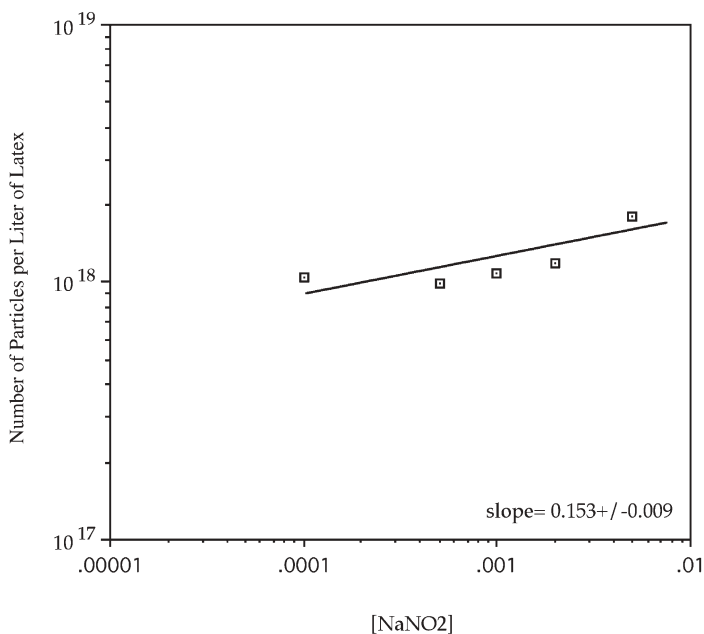
Fig. 12 The effect of a water-phase retarder on the number of particles in macroemulsion polymerization (from [95])

unknown. If we plot the log of the nitrite concentration against the log of the number of particles, we find a linear relationship between them, as depicted by Fig. 12. The slope of this line is 0.153±0.009. This value is close to the value of 0.2 reported for the initiator dependence, perhaps implying that the function of the water-phase retarder is simply to reduce the effective radical flux to the particles. The polymer-stabilized miniemulsions are far less sensitive to the presence of the retarder than are the macroemulsions. The retarder has little effect on the particle number. Particle numbers remained fairly constant up to a concentration of 5 mM$_{aq}$. Up to this amount, the dependence of the retarder concentration on the number of particles was calculated to be 0.020±0.007 (Fig. 13). This is significantly less than the value found for macroemulsions. (It is presumed that the highest level of retarder prevents a large fraction of the droplets from ever being nucleated.) Monomer conversions exhibit prolonged nucleation periods, but the rates are not significantly affected. Again the nitrite is acting as a retarder, since no induction period is observed.

Macroemulsion polymerizations carried out in the presence of an oil-phase inhibitor (DPPH) resulted in an increase in the number of particles. Presumably initiator radicals that enter droplets are terminated by the inhibitor, resulting in dead particles. These particles do not grow, and hence do not consume surfactant to stabilize their increasing surface area, until they absorb another radical. The surfactant not adsorbed by dead particles is available to
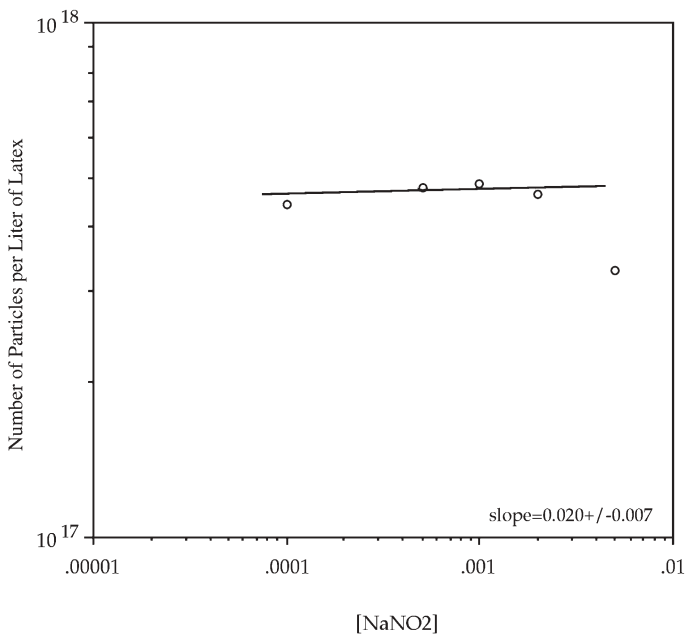
Fig. 13 The effect of a water-phase retarder on the number of particles in a polymer-stabilized miniemulsion polymerization (from [95])
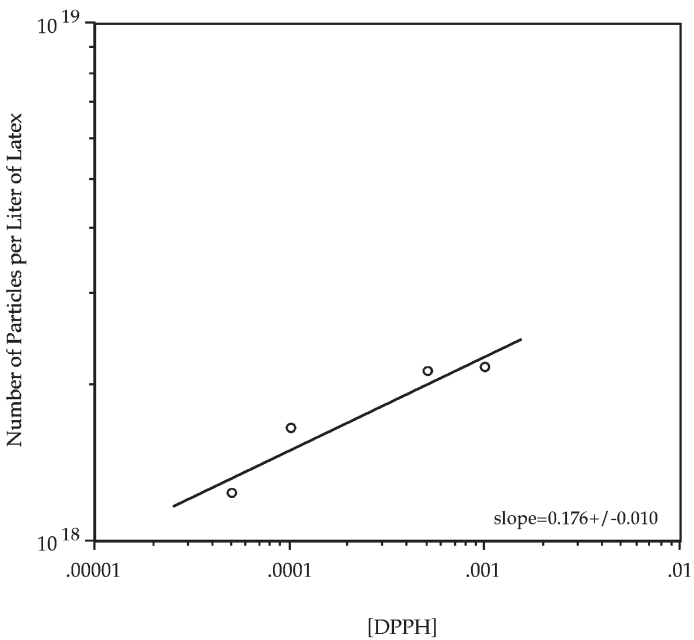
Fig. 14 The effect of an oil-phase inhibitor on the number of particles in macroemulsion polymerization (from [95])
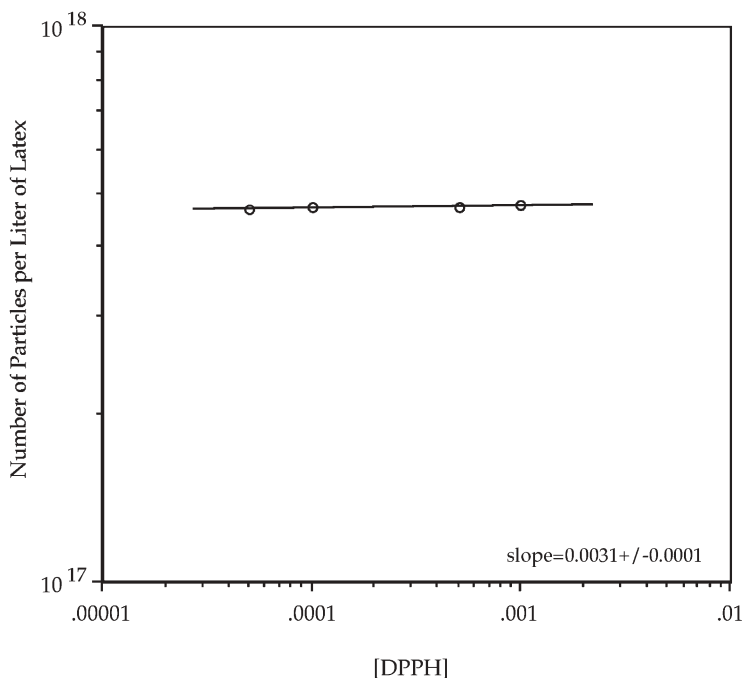
Fig. 15 The effect of an oil-phase inhibitor on the number of particles in miniemulsion polymerization (from [95])

stabilize new particles, thereby increasing the total number of particles. Since the nucleation period is lengthened, the polydispersity increases. Figure 14 shows that the dependence of the inhibitor concentration on the number of particles is 0.176±0.010. Conversion time curves indicate that an induction period results from the presence of the inhibitor. Since polymer-stabilized miniemulsion polymerization occurs via droplet nucleation, it should be less sensitive to oil-phase inhibition. Initiator radicals will enter the droplet one after the other until all of the inhibitor is used up, and the monomer polymerizes. This does not affect the number of droplets or particles. As seen in Fig. 15, the number of particles is proportional to the DPPH concentration raised to the power of 0.0031±0.0001. Therefore, the number of particles is essentially independent of the presence of inhibitor.

4.1.1.2
Summary

Shifting the site of nucleation to the droplets greatly enhances the robustness of the nucleation process to recipe variations, inhibition levels, and changes in operating procedure (initiation rate and/or agitation rate). As a result of droplet nucleation, polymer-stabilized miniemulsion polymerizations are far less sen-

Table 3 Summary of dependence of particle number on impurities and operational variations ([95])

X	a (macroemulsion)	a (miniemulsion)
[I][a]	0.2^3	0.002 ± 0.001
[NaNO$_2$]	0.153 ± 0.009	0.020 ± 0.007
[DPPH][b]	0.176 ± 0.010	0.0031 ± 0.0001
RPM	–	-0.026 ± 0.001

[a] [I] and [NaNO$_2$] in gmol/L$_{aq}$.
[b] [DPPH] in gmol/L$_{mon}$.

sitive to these variations in operation. The dependence of the particle number on the concentration of initiator, water-phase retarder, oil-phase inhibitor, and agitation are shown in Table 3. The exponents for the variation of particle number with each of these variations were 0.002, 0.02, 0.0031, and –0.026, respectively. The corresponding values for the macroemulsions were one to two orders of magnitude larger. Therefore, nucleation in polymer-stabilized miniemulsion polymerizations was found to be more robust than in macroemulsion polymerizations.

An enhanced robustness can benefit a process in a number of ways. Since the polymer-stabilized miniemulsions are less susceptible to disturbances, their polymerization is less likely to be affected by operator error, fluctuations in feed stream concentrations and residual contaminants in the reaction vessel. Many monomers contain species that can act as inhibitors or retarders as a result of monomer production, storage, or processing. These contaminants also cause batch-to-batch variability in particle number in macroemulsions. Therefore, miniemulsion polymerization may be an alternative to seeded polymerization as a way of maintaining robust control of particle number.

4.1.2
Particle Size Distribution

There has been a belief that, due to the fact that the original miniemulsion droplets are formed by a shear process, the droplet size distribution will be broad, and so the resulting PSD will have a large polydispersity (as measured by the *polydispersity index*, defined as the mass average over the number average particle radius). In a recent note [142] Landfester et al. discuss particle size polydispersity in miniemulsions and attempt to dispel the idea that miniemulsions necessarily have broader PSD than the equivalent macroemulsions. Rather, they argue that the PSD of a miniemulsion can be either broader or narrower than its macroemulsion counterpart, and that, in most cases, the miniemulsion will have a polydispersity equal to, or only very slightly greater than, the equivalent macroemulsion.

4.1.2.1
Hexadecane as Costabilizer

Fontenot and Schork [140] studied the miniemulsion polymerization of methyl methacrylate using hexadecane as the costabilizer. A portion of their results are shown in Table 4. Polydispersities are listed for macroemulsion, and miniemulsions subjected to varying durations of sonication, at two levels of initiator. In this and all cases following, the macroemulsions and miniemulsions were made from the same recipe, but with the costabilizer left out of the macroemulsion. The miniemulsions and macroemulsions were polymerized by the same procedure except that the sonication was eliminated for the macroemulsions. It may be seen that at both initiator levels, the macroemulsion is slightly more narrow than some of the miniemulsions, but broader than others. An estimate of the standard deviation of the polydispersity measurement is given as ±0.01–0.02, and may be applied to all of the polydispersity data reported. With this standard deviation estimate, it may be seen that the differences in polydispersity between the macro- and miniemulsions are not likely to be significant.

Landfester et al. [143] studied the miniemulsion polymerization of styrene using hexadecane as the costabilizer. When styrene miniemulsions were subjected to varying sonication times (see Table 5), very similar trends are seen as for the MMA miniemulsions. The particle size and the polydispersity of miniemulsion droplets rapidly polymerized after sonication either do not depend on the amount of the costabilizer, or are very weak functions of the amount of costabilizer (see Table 6). It was found that doubling the amount of costabilizer does not decrease the radius nor have any effect on the polydis-

Table 4 Polydispersity index as a function of initiator concentration and sonication time, with hexadecane as costabilizer and MMA as monomer ([140])

Sonication time	Polydispersity index
[I] 0.005 mol/L(aq)	
Macroemulsion	1.05
2 min	1.08
4 min	1.06
6 min	1.04
12 min	1.05
[I] 0.01 mol/L(aq)	
Macroemulsion	1.05
2 min	1.07
4 min	1.06
6 min	1.05
8 min	1.07
12 min	1.04

Table 5 Polydispersity index as a function of sonication time, with hexadecane as costabilizer, styrene as monomer, and [I]=0.3 mol/L (aq) (from [143])

Sonication time	Diameter d_i (nm)	Polydispersity index
Macroemulsion	–	1.04
0.5 min	135	1.01
1 min	112	1.03
2 min	96	1.00
5 min	87	1.03
10 min	84	1.02
20 min	83	1.01

Table 6 Hexadecane as costabilizer, with styrene monomer (from [143])

Hexadecane level (gm)	Particle diameter d_i (nm)	Polydispersity index
Macroemulsion	98	1.04
0.33	109	1.03
0.66	108	1.01
1.66	108	1.01
3.33	102	1.04
5	100	1.03
6.66	99	1.05
8.33	95	1.01

persity. It was also found that the droplet size is initially a function of the amount of mechanical agitation. The droplets are rapidly reduced in size throughout sonication in order to approach a pseudo-steady state [143]. Once this state is reached, the size of the droplet does not change. Higher sonication time causes a slight reduction in polydispersity.

After halting sonication, a rather rapid equilibration process must occur. Since the droplet number after sonication is fixed, this process does not influence the average size, but the droplet size distribution usually undergoes very rapid change. It was found that steady-state miniemulsification results in a system "with critical stability"; in other words the droplet size is the product of a rate equation of fission by ultrasound and fusion by collisions, and the droplets are as small as possible for the timescales involved. The equality of droplet pressures makes such systems insensitive against net mass exchange by diffusion processes (after the very fast equilibrium process at the beginning), but the net positive character of the pressure makes them sensitive to all changes in the droplet size. Steady-state homogenized miniemulsions, which are critically stabilized, undergo droplet growth on a timescale of hundreds of hours, presumably by collisions or by costabilizer exchange. As can be seen from Table 7, during this growth, the polydispersity does not change significantly.

Table 7 Influence of time delay between the ultrasonication and the polymerization (from [143])

Time delay between start of polymerization and sonication (h)	Particle diameter d_i (nm)	Polydispersity index
0	82	1.01
1	87	1.05
6	108	1.03
48	152	1.03
96	164	1.04

Therefore, we may conclude that there is indeed no significant difference in polydispersity between the miniemulsion and the equivalent macroemulsion.

4.1.2.2
Dodecyl Mercaptan as Costabilizer

Mouron et al. [105] and Wang et al. [106] have used dodecyl mercaptan (DDM) as the costabilizer in styrene and MMA miniemulsion polymerizations, respectively. Some of the results are shown in Table 8 and Table 9. For styrene (Table 8), the macroemulsion is compared with miniemulsions containing varying levels of DDM (costabilizer). In this case, the macroemulsion has a broader particle size distribution than all but one of the miniemulsions. For MMA (Table 9), miniemulsions and the equivalent macroemulsions have been compared at varying initiator concentrations. In this case, the macroemulsions

Table 8 Dodecyl mercaptan as costabilizer with styrene monomer (from [106])

DDM level (gm)	Polydispersity index
Macroemulsion	1.02
1	1.01
2	1.01
3	1.02
4	1.04

Table 9 Dodecyl mercaptan as costabilizer with methyl methacrylate monomer (from [105])

Initiator (mol/L(aq))	Macroemulsion PDI	Miniemulsion PDI
0.005	1.02	1.02
0.01	1.01	1.02
0.02	1.01	1.02

all have narrower particle size distributions, although the difference is hardly significant.

4.1.2.3
Polymethyl Methacrylate as Costabilizer

Reimers and Schork [144] have used polymethyl methacrylate as the co-stabilizer for methyl methacrylate miniemulsion polymerization. A portion of the results are shown in Table 10. In this case, the miniemulsion has a narrower particle size distribution than the equivalent macroemulsion.

4.1.2.4
Influence of the Amount of the Surfactant

Colloidal stability is usually controlled by the type and amount of surfactant employed. In miniemulsions, the fusion-fission rate equilibrium during soni-cation, and therefore the size of the droplets directly after primary equilibra-tion, depends on the amount of surfactant. For styrene miniemulsions that use SLS as surfactant, droplet sizes between 180 nm down to 32 nm can be obtain-ed. The polydispersity slightly increases with decreasing size, but is still quite low (see Table 11). Using similar molar amounts of the simple cationic surfac-

Table 10 Polymethyl methacrylate as costabilizer with methylmethacrylate monomer (from [144])

	Polydispersity index
Macroemulsion	1.02
Miniemulsion	1.01

Table 11 Polydispersity index as a function of SDS concentration (from [105])

SDS concentration (% compared to monomer)	Particle diameter d_i (nm)	Polydispersity index
0.3	180	1.03
0.5	134	1.07
1.0	108	1.02
1.5	94	1.02
2.1	89	1.08
3.5	82	1.08
4.9	82	1.03
6.8	65	1.03
10.3	55	1.05
17.0	46	1.06
25.2	42	1.07

Table 12 Polydispersity index as a function of CTAB concentration (from [70])

CTAB concentration (% compared to monomer)	Particle diameter d_i (nm)	Polydispersity index
0.4	347	1.01
0.7	159	1.05
1.2	125	1.05
2.4	102	1.04
3.6	86	1.01
10.0	59	1.09
16.7	59	1.13

tant cetyltrimethylammonium bromide (CTAB) or the anionic surfactant SLS results in similar particle sizes, showing that the particle size is essentially controlled by the limit of the surfactant coverage of the latex particles [71, 145]. Again, the polydispersity increases with decreasing size (see Table 12), but is only slightly higher than in the SDS miniemulsions.

4.1.2.5
Summary

Based on the data above, it would appear that it is possible, via miniemulsion polymerization, to make a polymer latex with a particle size distribution that approaches that made by macroemulsion polymerization. In some cases, the miniemulsion product may be even narrower than the macroemulsion. There are two significant mechanisms leading to this narrowness. First, the monomer droplet size distribution is to some extent determined by the thermodynamics of swelling, and not solely by the droplet size distribution induced by the sonicator or homogenizer. For this to be true, the process should include a *ripening time* between sonication and polymerization. During this ripening time, the droplets will come to swelling equilibrium. Studies show that the ripening time is of the order of seconds to minutes, and is naturally included in the preparation of batch polymerizations. Second, the narrowness of the particle size distributions depends on the ability to nucleate nearly all of the droplets over a short period of time. If droplet nucleation takes place over a longer period of time, some particles will have polymerized for a longer time, and some droplets will lose monomer by mass transfer to growing particles before the droplets begin to polymerize. Using hexadecane or polymer as a costabilizer will facilitate one hundred percent droplet nucleation, while the use of cetyl alcohol does not. Miller et al. [109] have shown that a small amount of polymer dissolved in the monomer droplets enhances droplet nucleation. Also, the initiator flux must be high enough to nucleate all of the droplets within a short time interval.

In summary, the miniemulsion route to polymer latexes should not be dismissed solely due to a requirement for narrow particle size distribution, par-

ticularly when the unique properties of the miniemulsion process may be of particular advantage.

4.1.3
Shear Stability

The shear stabilities of mini- and macroemulsion latexes were compared and quantitatively evaluated with respect to their particle size distributions by Rodrigues and Schork [146]. Although miniemulsion latexes exhibit many of the properties of macroemulsion latexes, there may be subtle differences in particle size distribution and surface characteristics due to differences in their polymerization mechanisms. To study the effects of these differences on the shear stabilities of the miniemulsions, a quantitative approach was developed where changes in the average diameter and total number of particles have been related to the particle size distribution before and after shearing.

Two pairs of MMA mini- and macroemulsion latexes were polymerized for this study. HD was used as the costabilizer for the miniemulsions, and the polymerizations were carried out at 60 °C. Efforts were made to make the main- and macroemulsion in each pair as similar as possible. The two pairs were:

Pair I

Macroemulsion (Sample A)
0.02 mol. SLS/L_{aq}; 0.0115 mol. KPS/L_{aq}; 2 g DDM;
PSD range: 141–188 nm (diameter)

Miniemulsion (Sample E)
0.02 mol. SLS/L_{aq}; 0.0115 mol. KPS/L_{aq}; 2 g DDM;
PSD range: 96–123 nm (diameter)

Pair II

Macroemulsion (Sample H)
0.01 mol. SLS/L_{aq}; 0.0115 mol. KPS/L_{aq}; 4 g DDM
PSD range: 167–241 nm (diameter)

Miniemulsion (Sample D)
0.01 mol. SLS/L_{aq}; 0.0115 mol. KPS/L_{aq}; 4 g DDM
PSD range: 145–209 nm (diameter)

The samples were sheared using a rotational viscometer with a coaxial cylinder system, based on the Searle-type, where the inner cylinder (connected to a sensor system) rotates while the outer cylinder remains stationary. The outer cylinder surrounding the inner one was jacketed, allowing good temperature control, and the annular gap was of constant width. The sensor system used was the NV type, with a rotor with a recommended viscosity range of 2×10^3 mPa, a maximum recommended shear stress of 178 Pa, and a maximum recommended shear strain rate of 2700 s^{-1}; this rotor could work with volumes from 10–50 ml. Flow was laminar.

The optimum shear rate for each pair was arrived at by trial and error, such that the shearing produced aggregation, but not massive coagulation. That is, the shear rate was not increased beyond the point at which the particle diameters stopped increasing (and maybe even started decreasing again). All the tests were conducted at 25 °C; each miniemulsion latex within a pair was sheared for the same time interval as its macroemulsion latex counterpart. Only changes in particle sizes were followed during these series of experiments, with the particle size distribution (analyzed by dynamic light scattering, DLS) recorded before and after shearing for each of the shear experiments.

The ratio of total number of particles initially present to the total number of particles after shearing (N_i/N_f) was computed and used both to compare the two types of latexes, and to determine the extent of aggregation and the nature of the aggregates formed.

4.1.3.1
Relative Shear Stability of Miniemulsion and Macroemulsion Latexes

The particle size range and average particle diameter before and after shearing, and the shear rate and time of shear used for each of the sample pairs is shown in Table 13. For both pairs, the shifts in the particle size range and in the average diameter are substantially greater for the macroemulsion latex than the corresponding miniemulsion latex. In all cases, the particle size distribution broadened after shearing. The percentage change in average diameter is greater for the macroemulsions as well.

The ratio of the initial total number of particles to the final total number of particles after shearing (N_0/N_f) is shown in Table 14. It is clear that the macroemulsion latexes showed greater shear instability. The ratio N_o/N_f gives an indication of the extent of aggregation in each of the latexes; a N_o/N_f ratio of two would indicate that average aggregation up to doublet formation has taken place, and so on. It can be seen from Table 14 that aggregation has taken place in all the latexes essentially up to doublet formation, with slightly higher

Table 13 Particle size ranges and average particle diameters before and after shearing, and the shear rates and times of shear for samples A, E, H, and D (from [146])

Sample	Shear rate (s^{-1})	Time of shear (s)	Initial PSD range (diameter) (nm)	Average diameter before shearing (nm)	PSD range after shearing (nm)	Average diameter after shearing (nm)	% Change in average diameter (nm)
A (macro)	200	1260	141–188	155	181–244	204	31.61
E (mini)	200	1260	96–123	108	106–143	121	12.04
H (macro)	200	1260	167–241	195	218–319	264	35.38
D (mini)	200	1260	145–209	168	170–223	195	16.07

Table 14 Ratio of the initial total number of particles to the final number of particles after shearing for samples A, E, H, and D (from [146])

Sample	% Solids	N_i/N_f
A (macro)	27.2	2.28
E (mini)	25.9	1.41
H (macro)	20.9	2.87
D (mini)	24.8	2.43

aggregate formation in the macroemulsion latexes than in the miniemulsion latexes, as evidenced by their correspondingly higher N_o/N_f values.

4.1.3.2
Effect of Large Particles

The effects of a few externally-added large particles on the shear stabilities of miniemulsion- and macroemulsion latexes were also investigated. This was done to determine if the greater shear instability of the macroemulsion latex was due to the presence of a few large particles, possibly formed by droplet nucleation during the synthesis of the latex itself. To test this, portions of a larger particle size macroemulsion (Sample C) were added to the two macroemulsion latexes (Samples A and H), and portions of a larger miniemulsion (Sample G) were added to the two miniemulsion latexes (Samples E and D) used in the first part of this analysis. The large particles were as follows:

Macroemulsion Seed Latex (Sample C)
PSD range: 252–298 nm (diameter)
Average diameter: 276 nm

Miniemulsion Seed Latex (Sample G)
PSD range: 320–380 nm (diameter)
Average diameter: 344 nm

The percentages by weight of the larger particle size latexes used were 2, 5, 10 and 25% of total sample weight. The latexes were then sheared, and the shift in the particle size distribution range and average particle diameter, the percent change in this average diameter after shearing, and the N_o/N_f values were determined for both sets of samples. These results are shown in Tables 15 and 16.

Table 15 shows that, for all four samples analyzed, the percent change in average diameter increases with the fraction of larger particles, reaches a maximum, and then decreases. In all cases, the maximum shear aggregation occurs at approximately 5–10% large particles. This supports (but by no means proves) the hypothesis that macroemulsion latexes are more susceptible to shear coagulation than miniemulsion latexes due to the presence of a small fraction of large particles originating from droplet nucleation. It is important to remember

Table 15 Particle size ranges and average particle diameters before and after shearing, and the shear rates and times of shear for samples A, E, H, and D with large particles added (from [146])

Sample	Shear rate (s⁻¹)	Time of shear (s)	Initial PSD range (diameter) (nm)	Average diameter before shearing (nm)	PSD range after shearing (nm)	Average diameter after shearing (nm)	% Change in average diameter (nm)
A (original-macro)	200	1260	141–188	155	181–244	204	31.61
A (2% big C)	200	1260	143–310	170	194–334	228	34.12
A (5% big C)	200	1260	144–317	176	208–358	249	41.48
A (10% big C)	200	1260	143–312	182	202–344	246	35.16
A (25% big C)	200	1260	143–308	199	196–333	250	25.63
E (original-mini)	200	1260	96–123	108	106–143	121	12.04
E (2% big G)	200	1260	102–372	118	114–380	153	29.66
E (5% big G)	200	1260	103–379	124	124–389	168	35.48
E (10% big G)	200	1260	106–384	131	130–397	177	35.11
E (25% big G)	200	1260	105–377	140	123–394	186	32.86
H (original-macro)	250	1740	167–241	195	233–348	277	42.05
H (2% big C)	250	1740	169–323	199	236–352	290	45.73
H (5% big C)	250	1740	171–338	207	264–388	324	56.52
H (10% big C)	250	1740	170–333	212	253–369	305	43.87
H (25% big C)	250	1740	170–312	222	242–355	297	33.78
D (original-mini)	250	1740	145–209	168	197–281	226.00	34.52
D (2% big G)	250	1740	149–370	179	224–377	247.00	37.99
D (5% big G)	250	1740	151–374	193	233–381	266	37.82
D (10% big G)	250	1740	154–373	208	242–399	284	36.54
D (25% big G)	250	1740	155–375	226	237–389	305	34.96

that in all four latexes used here, the size differential between these latexes and the two latexes used as large particles (Samples C and G) is not very large. Therefore, the particles that qualify as large particles by definition lie at the upper end of the particle size distribution of samples C and G; in other words, only a small fraction of the externally-added larger latex actually functions as large particles in terms of influencing shear stability.

The results shown in Table 16 support the observations drawn from Table 15. For all of the latexes, there is an increase in N_o/N_f value as the percentage of externally added large particles increases, up to approximately 5–10%wt of large particles. Any further addition of large particles decreases the N_o/N_f value.

Table 16 Ratio of the initial total number of particles to the final number of particles after shearing for samples A, E, H, and D with large particles added (from [146])

Sample	% Solids	N_i/N_f
A (original-macro)	27.2	2.28
A (2% big C)	27.1	2.41
A (5% big C)	26.9	2.83
A (10% big C)	26.7	2.47
A (25% big C)	26.2	1.98
E (original-mini)	25.9	1.41
E (2% big G)	25.7	2.18
E (5% big G)	25.6	2.49
E (10% big G)	25.3	2.47
E (25% big G)	25.2	2.34
H (original-macro)	20.9	2.87
H (2% big C)	21.1	3.09
H (5% big C)	21.2	3.83
H (10% big C)	21.2	2.98
H (25% big C)	21.3	2.39
D (original-mini)	24.8	2.43
D (2% big G)	24.9	2.63
D (5% big G)	25.3	2.62
D (10% big G)	25.5	2.55
D (25% big G)	25.6	2.46

4.1.3.3
Summary

Under controlled shearing conditions, miniemulsions were shown to be more shear stable than similar conventional or macroemulsions. This *may* be due to macroemulsion shear instability resulting from the presence of a small number of large particles (derived from droplet polymerization) that act as seeds for aggregation. Intentional seeding of mini- and macroemulsions with larger particles induced increased shear instability, supporting this hypothesis. However, it may be that miniemulsion polymerization avoids the burying of some of the initiator end groups. For KPS initiation, these end groups, if on the surface of the particle, will add substantially to the colloidal stability of the particles. Due to the nature of macroemulsion polymerization (particle growth at the expense of monomer droplets), end groups tend to become buried in the particle where they contribute nothing to colloidal stability. Since there is less particle growth (none in the ideal case) for miniemulsion polymerization, most of the initiator end groups should remain on particle surfaces.

While the mechanism is an open question, there clearly seems to be a difference in shear stability between miniemulsions and macroemulsions.

4.2
Monomer Transport Effects

One of the most unique properties of miniemulsion polymerization is the lack of monomer transport. Recall from Fig. 1 that with macroemulsion polymerization, the monomer must diffuse from the monomer droplets, across the aqueous phase, and into the growing polymer particles. In contrast, in an ideal miniemulsion (nucleation of 100% of the droplets), there is no monomer transport, since the monomer is polymerized within the nucleated droplets. This lack of monomer transport leads to some of the most interesting properties of miniemulsions. For most monomers, macroemulsion polymerization is considered to be reaction, rather than diffusion limited. However, for extremely water insoluble monomers, this might not be the case. In this instance, polymerization in a miniemulsion might be substantially faster than polymerization in an equivalent macroemulsion. For copolymerization in a macroemulsion, where one of the comonomers is highly water insoluble, the comonomer composition at the locus of polymerization might be quite different from the overall comonomer composition, resulting in copolymer compositions other than those predicted by the reactivity ratios.

4.2.1
Polymerization of Highly Water-Insoluble Monomers

Balic [147] has made a complete study of the macroemulsion polymerization of vinyl neo-decanoate (vinyl versatate or VEOVA). This monomer is highly water-insoluble (4×10^{-5} mol/L at 25 °C). Balic reports low rates of polymerization and long inhibition periods in macroemulsions. He asserts that this is not due to monomer transport limitations, and provides calculations to support this. He attributes the low rates to impurities in the monomer, although he could not remove these. It could be that the extremely low solubility of the monomer in the aqueous phase retards the formation of oligomeric radicals of sufficient length (hydrophobicity) to enter the polymer particles. Under these conditions of very slow aqueous phase polymerization, the oligomers might be particularly susceptible to low levels of aqueous phase inhibitor. With the resultant low radical flux into the particles, the rate of polymerization would be low. It could also be that the rate of monomer diffusion is not sufficient to allow the polymerization to be reaction limited, since Balic's arguments do not necessarily rule out this possibility. It would be interesting to see the same polymerizations run in miniemulsion, since this would rule out the monomer transport effect.

Kitzmiller et al. [148] have found the rate of copolymerization for VAc and vinyl 2-ethylhexanoate to be much slower in macroemulsion than in miniemulsion. They attribute this to monomer transport effects for the less water-soluble monomer.

4.2.2
Copolymer Composition Distribution

While the rate of monomer transport in macroemulsions may or may not limit the rate of polymerization, it is quite possible that unequal rates of diffusions for comonomers may make the comonomer composition at the locus different (richer in the more water-soluble monomer) from the overall composition.

Copolymerization refers to the process by which two monomers (M_1 and M_2) are simultaneously polymerized. Mayo and Lewis [149] developed the following equation to describe copolymerization kinetics

$$\frac{dM_1}{dM_2} = \frac{M_1(r_1M_1 + M_2)}{M_2(M_1 + r_2M_2)} \tag{15}$$

where M_i is the molar concentration of monomer i at the site of propagation. The reactivity ratios, r_1 and r_2, are the homopropagation rate constants divided by the cross propagation rate constants, such that

$$r_1 = \frac{k_{p11}}{k_{p12}} \qquad r_2 = \frac{k_{p22}}{k_{p21}} \tag{16}$$

where r_1 and r_2 are determined experimentally, typically from bulk or solution polymerization experiments. Different types of copolymerization behavior are observed, depending on the values of r_1 and r_2. Equation 15 is rewritten in a more useful form, where the comonomer compositions (f_1 and f_2) are related to the instantaneous copolymer compositions (F_1 and F_2):

$$\frac{dM_1}{dM_2} = \frac{F_1}{F_2} = \frac{\dfrac{r_1f_1}{f_2} + 1}{\dfrac{r_2f_2}{f_1} + 1} \tag{17}$$

Equation 17 is known as the *copolymerization or Mayo Lewis equation.*

Schuller [150] and Guillot [98] both observed that the copolymer compositions obtained from emulsion polymerization reactions did not agree with the Mayo Lewis equation, where the reactivity ratios were obtained from homogeneous polymerization experiments. They concluded that this is due to the fact that the copolymerization equation can be used only for the exact monomer concentrations at the site of polymerization. Therefore, Schuller defined new reactivity ratios, $r'1$ and $r'2$, to account for the fact that the monomer concentrations in a latex particle are dependent on the monomer partition coefficients (K_1 and K_2) and the monomer-to-water ratio (ψ):

$$r'1 = r_1 \frac{1 + \dfrac{1}{K_2 \psi}}{1 + \dfrac{1}{K_1 \psi}} \qquad r'2 = r_2 \frac{1 + \dfrac{1}{K_1 \psi}}{1 + \dfrac{1}{K_2 \psi}} \tag{18}$$

The Mayo Lewis equation, using reactivity ratios computed from Eq. 18, will give very different results from the homogenous Mayo Lewis equation for mini- or macroemulsion polymerization when one of the comonomers is substantially water-soluble. Guillot [151] observed this behavior experimentally for the common comonomer pairs of styrene/acrylonitrile and butyl acrylate/vinyl acetate. Both acrylonitrile and vinyl acetate are relatively water-soluble (8.5 and 2.5%wt, respectively) whereas styrene and butyl acrylate are relatively water-insoluble (0.1 and 0.14%wt, respectively). However, in spite of the fact that styrene and butyl acrylate are relatively water-insoluble, monomer transport across the aqueous phase is normally fast enough to maintain equilibrium swelling in the growing polymer particle, and so we can use the monomer partition coefficient.

Schuller's equation is appropriate when one of the monomers has significant water solubility and the other does not. In the case where one monomer is water insoluble, and the other is *extremely* water insoluble, Schuller's equation does not hold. For the comonomer pair of MMA/VS (vinyl stearate), $K_1 \ll K_2$, so Schuller's equation predicts that, for macroemulsion polymerization, the polymer formed early in a batch reaction will be richer in vinyl acetate (VA) than in the homogenous case. The opposite was found by Reimers [102]. It has long been accepted that monomer transport is not a rate-limiting step in the conventional emulsion polymerization of *relatively water-insoluble* monomers, such as MMA, styrene, and butyl acrylate (BA). However, the water solubility of VS is as much as three orders of magnitude smaller than these typical emulsion polymerization monomers. In this case, VS cannot readily cross the aqueous phase to saturate the growing polymer particles. (The major transport resistance is actually from the monomer droplets into the aqueous phase.) Therefore, Schuller's partition coefficient model cannot be used here, since it assumes that the particles are saturated with both monomers. The homogeneous polymerization model is not useful either since the monomer concentration in the particles is not identical to the bulk monomer concentration. Therefore, a pseudo-partition coefficient κ_2 was proposed by Samer [137] for *extremely water-insoluble* comonomers in order to interpret the experimental data. κ_2 is not a partition coefficient and does not have any physical significance. As defined by Samer, it is simply an adjustable parameter that replaces K_2 in Eq. 18. If K_1 is set to infinity and κ_2 is set to unity, Eq. 17 and Eq. 18 can be used to correlate the copolymer composition with the total monomer conversion data in the MMA/VS (and other) systems.

Extremely water insoluble comonomers are only selectively used in emulsion polymerization because of concerns about monomer transport limitations.

Typically, copolymer composition can be manually adjusted by slowly feeding the more reactive monomer in throughout the reaction; but this may not be helpful when trying to overcome monomer transport limitations. Therefore, Reimers and Schork [102] performed identical copolymerization experiments in miniemulsions, where monomer transport is less significant, in order to determine what effect this would have on the evolution of the copolymer composition. Data on the MMA/VS (and other) copolymerizations indicate that the Schuller equation (and not the Samer adaptation) fits the copolymer composition data. This points to the effect of extremely low monomer water solubility on copolymer composition in macroemulsion polymerization, and the relative insensitivity of miniemulsion polymerization to this effect.

We will now look at the type of reactor system (batch, semibatch or CSTR) from the point of view of miniemulsion copolymerization.

4.2.2.1
Batch Copolymerization

Reimers [102] carried out batch copolymerizations in both macro- and equivalent miniemulsions. MMA was used as the main monomer. The MMA was copolymerized in macroemulsion- or miniemulsion with p-methylstyrene (pMS), vinyl hexanoate (VH), vinyl 2-ethylhexanoate (VEH), vinyl n-decanoate (VD) or vinyl stearate (VS). The comonomers were copolymerized at 10%wt comonomer, 90%wt MMA. SLS was used as the surfactant and KPS as the initiator. The comonomers (all highly water insoluble) were used as the co-stabilizer. Miniemulsions were sonicated, while equivalent macroemulsions were only subjected to vigorous mixing. Polymerizations were carried out at 60 °C.

Copolymer composition was obtained by integrating characteristic peaks in the ^{1}H NMR spectra. The integrated peaks correspond to signals produced by the methyl ester protons (three) of MMA, 3.56 ppm, the aromatic protons (four) of pMS, 6.7 ppm, and the α-proton of the vinyl esters at 4.8 to 5.6 ppm. The relative ratios of the peaks allowed the mole fraction of each comonomer in the copolymer to be assessed. Samples were taken throughout the reaction at different times to monitor the incorporation of comonomer as a function of the extent of total monomer conversion. These results were then compared with the results for average comonomer fraction given by an integrated copolymer (Mayo Lewis) equation [149], using r_1 and r_2 from bulk polymerization. The mole fractions used were based on the total moles of monomer in the droplets and were corrected for the water solubility.

Both the mini- and macroemulsion copolymerizations of pMS/MMA tend to follow bulk polymerization kinetics, as described by the integrated copolymer equation. MMA is only slightly more soluble in the aqueous phase, and the reactivity ratios would tend to produce an alternating copolymer. The miniemulsion polymerization showed a slight tendency to form copolymer that is richer in the more water-insoluble monomer. The macroemulsion formed a copolymer that is slightly richer in the methyl methacrylate than the co-

polymer equation would predict. This may be explained by different nucleation mechanisms operating in each polymerization. Droplets would have a higher concentration of the less water-soluble comonomer throughout the reaction. Therefore their nucleation should yield a copolymer with a higher pMS fraction. In contrast, micellar nucleation should lead to a copolymer with a higher methyl methacrylate content, because it can cross the aqueous phase more readily.

As the water solubility of the comonomer decreases, the difference in incorporation of the hydrophobic monomer between the mini- and macroemulsion polymerization becomes more pronounced. This was seen in the copolymerization of VH/MMA. The fraction of the hexanoate in the copolymer formed in the miniemulsion polymerization was substantially higher than that found with the macroemulsion. This incorporation closely follows the copolymer equation. The VEH/MMA miniemulsion copolymerization also followed the copolymer equation. Differences between the mini- and macroemulsion polymerization are not as pronounced in this system. For the VD/MMA and VS/MMA systems there were large differences between the two copolymerizations. In addition, none of the mini- or macroemulsion copolymerizations of vinyl decanoate or vinyl stearate are predicted by the copolymer equation. The miniemulsion copolymerizations fall above the prediction curve (more hydrophobic monomer incorporation than predicted), and the macroemulsions fall below. In these cases, both micellar and droplet nucleation took place in the miniemulsion polymerizations, and the presence of micelles tended to enrich the concentration of the hydrophobic monomer in the droplets, since the micelles would likely be richer in the more water-soluble MMA.

Samer [104] carried out similar copolymerizations with similar results. An example of his data is given in Fig. 16. Here 2-ethylhexyl acrylate (EHA) was copolymerized with MMA in batch. The miniemulsion polymerizations (two are shown) follow the copolymer equation, while the macroemulsion polymerization gives EHA incorporation that is lower than predicted by the copolymer equation, presumably due to the low concentration of EHA at the locus of polymerization. The dotted line in Fig. 16 is for a model derived by Samer that accurately predicts the copolymer composition. Samer derived this model by adapting the work of Schuller [149]. Schuller modified the reactivity ratios for the macroemulsion polymerization of *water-soluble* monomers to take into account that the comonomer concentration at the locus of polymerization is different from the comonomer composition in the reactor due to the water solubilities of the monomers. Samer used the same approach to account for the fact that the comonomer concentration at the locus of polymerization might be different from that of the reactor due to transport limitations of *water insoluble* comonomers.

Delgado et al. published a series of papers [56, 58, 91, 153–157] on the miniemulsion copolymerization of vinyl acetate and butyl acrylate. A very comprehensive mathematical model of the polymerization system was developed. Equilibrium swelling was accounted for, since the model did not presume complete droplet nucleation, and so monomer transport from unnucleated mini-
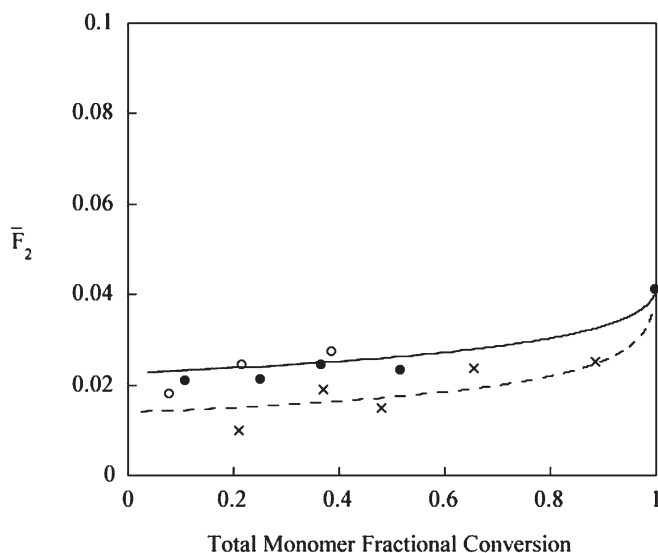
Fig. 16 Copolymer composition during the batch miniemulsion copolymerization of methyl methacrylate with 2-ethylhexyl acrylate (from [104])

emulsion droplets to polymer particles occurred. Monomer transport limitations were minor, but with these two monomers, that is not surprising. Delgado did report [91] a higher BA content (up to 70% conversion) for miniemulsion-polymerized copolymers relative to those polymerized in an equivalent macroemulsion. Since BA is significantly less water-soluble than VAc, this result is in agreement with Reimers. Rodriguez et al. [60, 61] developed a comprehensive model of the miniemulsion copolymerization of styrene and MMA. This system presumes significantly less than 100% nucleation of monomer droplets, and so there was significant monomer transport from the monomer droplets to the polymer particles. However, since neither of these monomers are extremely water insoluble, no effects on copolymer composition were observed. Ghazaly et al. [117] studied the miniemulsion copolymerization of n-butyl methacrylate with crosslinking macromonomers (two double bonds per molecule). Since the comonomers were macromers, presumably, it was important to use a miniemulsion to avoid common transport issues. Wu and Schork [152] studied the batch and semibatch miniemulsion copolymerization of VAc with BA. They found the copolymer composition for batch miniemulsion polymerization to be in good agreement with the copolymer equation. However, there was significant deviation for batch macro-emulsion polymerization, especially at low conversion. Delgado [157] attributed this effect to the small amount of water that exists in the monomer-swollen polymer particles. Because of the high water solubility of VAc, the particles then contain a higher level of VAc, and so BA incorporation is suppressed.

4.2.2.2
Semibatch Copolymerization

Controlling copolymer composition has long been of prime interest in polymer reaction engineering. Because of possible differences in reactivity ratios, the copolymer composition distribution may be broad, and only the overall (average) copolymer composition at full conversion need be at the ratio of monomer feeds. As noted above, Mayo and Lewis [149] studied the kinetics of copolymerization and developed an equation to describe the relationship between the molar concentrations at the site of propagation and reactivity ratios of monomers for homogeneous copolymerization, such as bulk or solution polymerization. Semibatch polymerization (both solution and macroemulsion) has long been used to produce copolymers of desired copolymer composition distribution. This may be done on one of two ways. First, in a binary polymerization the more reactive monomer may be fed in a semibatch manner. This will result in a high concentration of the less reactive monomer at the locus of polymerization, and the formation of polymer that is higher in the less reactive monomer than would be the case for batch polymerization. Alternatively, the reaction may be run monomer-starved. In this case, the monomers are fed into the system in the desired ratio, but at a slow rate. The rate of polymerization is then controlled by the rate of monomer feed. Since polymerization occurs under monomer-starved conditions, the copolymer composition will be that of the comonomer feed. Obviously, monomer-starved conditions will result in low rates of polymerization. If either policy for semibatch monomer feeding is to be used, issues of relative transport of the monomers must be considered. Also, the decision must be made as to whether to feed in neat monomer, a macroemulsion of monomer droplets, or a miniemulsion of monomer droplets. In general, neat monomer feed will result in the least nucleation, while miniemulsion feed will result in the most. Depending on the goals of the polymerization, nucleation of new particles during the semibatch feeding may be desirable or undesirable.

In 1993, Unzue and Asua [158] studied the semibatch miniemulsion terpolymerization of BA, MMA and VAc. The aim was to produce a miniemulsion of 65% solids. It is well known that semibatch polymerization can be an effective method of making high solids latex. Part of the advantage of semibatch in making high solids is the broad PSD brought on by nucleation of particles over most of the reaction time. Miniemulsion can be effective in this regard, since a miniemulsion feed is likely to produce additional polymer particles, as shown by Tang et al. [131].

Wu and Schork [152] compared batch and semibatch and mini- and macroemulsion polymerization for three monomer systems, VAc/BA, VAc/dioctyl maleate (DOM) and VAc/n-methylol acrylamide (NMA), with large differences in reactivity ratios and water solubilities. HD was used as the costabilizer. (It should be noted that DOM could function as a costabilizer itself, but for the sake of consistency, HD was added to the DOM polymerizations.) KPS and the

emulsifier SLS was used as the initiator. The semibatch miniemulsion polymerization involved two stages, a miniemulsion batch stage and semibatch stage. The miniemulsion batch stage was performed as above. When the monomer conversion was estimated to be about 80%, the feeding stage was initiated by pumping monomer emulsion (miniemulsion or macroemulsion, which was continuously formed while feeding) and initiator solution at set flow rates simultaneously into the reactor. The composition of the monomer feed was identical to the composition of the monomer in the batch stage. Copolymer composition was determined by NMR, MWD by GPC and PSD by dynamic light scattering.

Miniemulsion and macroemulsion copolymerizations of VAc and comonomers with extremely different physical and kinetic properties (BA, NMA and DOM), were investigated in batch and semibatch systems. The results for polymer particle size and number, monomer conversion, composition and molecular weights of copolymers indicated that there was an obvious divergence between macroemulsion and miniemulsion copolymerization. In all cases, the particle size was smaller and the particle number was higher in macroemulsion copolymerization than in miniemulsion copolymerization. For the systems VAc/BA and VAc/DOM, the particle number increased with increasing conversion throughout the reaction for both batch macroemulsion and miniemulsion runs. This was taken to indicate that the nucleation of new particles takes place via homogeneous nucleation throughout these reactions. For the batch runs, the rate of polymerization of the macroemulsion polymerization runs was faster than that of the miniemulsion.

An investigation of the copolymer composition demonstrated the important effect of monomer transport on the copolymerization. The droplets in the macroemulsion act as monomer reservoirs. In this system, the effect of monomer transport will be predominant when an extremely water-insoluble comonomer, such as DOM, is used. In contrast with the macroemulsion system, the miniemulsion system tends to follow the integrated Mayo Lewis equation more closely, indicating less influence from mass transfer.

Likewise, for the semibatch operation, the influence of monomer was seen in the differences between macro- and miniemulsion feeds. For extremely water-insoluble monomers, the miniemulsion-feed mode lessens the departure of the copolymer composition from the feed composition during semi-starved semibatch polymerization. However, this is accomplished by simultaneously broadening the PSD. Results from the GPC analysis indicated that the polymers with lower molecular weight and broader distribution were formed in the semibatch process, in contrast to the batch run.

Wu [159] also investigated the miniemulsion and macroemulsion copolymerization of VAc and vinyl versitate (VEOVA). At room temperature, the water solubility of VAc is 2.58%wt, and vinyl versitate (also known as neodecanoate, one of the isomers in VEOVA-10) is 7.5×10^{-4}%wt. The extreme difference in water solubility between the two comonomers may impact on copolymer composition and the properties of the final polymer, due to the mass

transfer of monomer. In this work, mini- and macroemulsion polymerizations of VAc/vinyl versatate were designed to investigate the effects of monomer transport and feeding strategies (for semibatch runs) on the reaction rate, particle size distribution, molecular weight distribution, copolymer composition, and glass transition temperature (T_g) of the resultant polymer. Polymerizations were run at 55 °C. HD was used as the costabilizer, and SLS as the surfactant. The initiator was KPS. VEOVA was added either as an emulsion with the vinyl acetate, or as a neat liquid stream. In the polymerization of VAc miniemulsion (or macroemulsion) plus neat vinyl versatate, the VAc miniemulsion (or macroemulsion) was pre-formed. The neat vinyl versatate was then injected into the polymerization system at the same time as the injection of initiator solution. For the semibatch processes, 20%wt of the polymer solids was in the form of seed and the remaining 80% was fresh monomer emulsion. The seed latex was prepared as a miniemulsion polymerization. The miniemulsion was made (sonicated) in-line, immediately prior to feeding into the reactor. The first shot of initiator solution was introduced when the feed of monomer emulsion started. A subsequent shot followed the removal of each latex sample for analysis.

In the semibatch runs of VAc miniemulsion (or macroemulsion) plus neat VEOVA, with simultaneous feeding of VAc miniemulsion (or macroemulsion), the neat vinyl versatate was injected into the polymerization system two (for the feedrate of 0.6 ml/min) or three (for 0.3 ml/min) times during each sampling interval. Copolymer composition was determined by NMR, MWD by GPC, T_g by DSC, and PSD by dynamic light scattering.

The effect of mass transfer of vinyl versatate on the mini/macroemulsion polymerization of VAc/VEOVA in batch and semibatch systems was explored. For the batch experiments, the addition of neat VEOVA formed poor dispersions of VEOVA, which resulted in smaller particles, lower polymerization rates and different polymer composition tracks compared to normal mini/macroemulsion polymerization of VAc/VEOVA. The well-dispersed VEOVA seemed to help the monomer-swollen particle to gain more radicals in the nucleation period.

In the semibatch experiments, the particle size distributions of the final latexes were affected by the residual surfactant in the seed latex, which tended to facilitate homogeneous nucleation during the entire feed period. The monomer feedrate determined the polymerization rate and had little effect on copolymer composition. The polymer compositions for the runs with different monomer feeding modes tended to be identical at very low feedrate.

For all runs, thermal analysis of the resulting polymers showed that only one glass transition temperature could be found. This corresponded to the T_g of the VAc/VEOVA copolymer. Lower glass transition temperatures were found for the semibatch runs, perhaps due to slightly improved VEOVA incorporation.

In summary, the semibatch feeding of neat monomer or a macroemulsion of monomer to a miniemulsion does not differ substantially from the equivalent semibatch feeding into a macroemulsion. The semibatch feeding of a

miniemulsion tends to cause an increase in the particle number (due to partial nucleation of the monomer droplets in the feed) and copolymer compositions that more closely follow the Mayo Lewis Equation (due to the ability of the miniemulsion droplets to, at least partially, retain their monomer, rather than being depleted of monomer to feed the existing higher conversion polymer particles).

4.2.2.3
Copolymerization in a Continuous Stirred Tank Reactor

Samer [137] studied miniemulsion copolymerization in a single CSTR. Two separate feed streams, miniemulsion (or macroemulsion for comparative studies) and initiator were fed at constant rates into the reactor. SLS was used as the surfactant, HD as the costabilizer, and KPS was the initiator. In the miniemulsion configuration (costabilizer included in recipe), the emulsion stream was continuous. Constant volume was provided by an overflow outlet. Salt tracer experiments were used to validate the ideal mixing model assumed for a CSTR. Total monomer conversion was measured via in-line densitometry, and copolymer composition via offline NMR.

Continuous macroemulsion copolymerization of MMA with 0.033–0.05mol% 2-ethylhexyl acrylate (EHA): On the basis of the batch copolymerization experiments for this system, one would expect the average compositions to follow the relation $F_{2\,Mini} > F_{2\,Macro}$. (The subscript 2 refers to the EHA.) However, this behavior was not observed in a CSTR. Although the steady-state conversion was significantly greater (as expected) for miniemulsions than for macroemulsions, the copolymer composition is nearly identical for both reactions. In this case, it does not appear that droplet nucleation leads to an increase in the amount of the *extremely water-insoluble* comonomer incorporated into the copolymer, as observed in batch reactors. The experimental copolymer compositions were compared with the predicted copolymer compositions calculated from the Mayo Lewis equation where the reactivity ratios were obtained from homogeneous copolymerization experiments and where the pseudo-partition coefficient κ_2 was adjusted to fit the data. Surprisingly, both the macroemulsion and miniemulsion data showed good agreement with Samer's modification of Schuller's modified reactivity ratio model. This included both mini- and macroemulsion copolymer compositions at different initial comonomer compositions. Since the water solubility cannot change, it was suggested that monomer transport, or at least the relative difference in monomer transport between MMA and EHA, changes between batch and continuous miniemulsion copolymerization reactions.

The difference in copolymer composition between miniemulsion and macroemulsion copolymerization in a batch reactor was not observed in a CSTR. In this case, the copolymer composition for the *extremely water insoluble* comonomer in a miniemulsion recipe decreases from a batch reactor to a CSTR. This difference can be attributed to the fact that monomer transport is

enhanced in the steady-state CSTR where fresh monomer droplets are in contact with "monomer-starved" particles. The comonomers cannot cross the aqueous phase at similar rates because of their water-solubility differences, which favors incorporation of the more water-soluble comonomer. All of the droplets are nucleated at roughly the same time in a batch reactor, so little monomer is available to quench monomer-starved particles.

However, this does not preclude miniemulsion copolymerization in a CSTR for *extremely water-insoluble* comonomers. In spite of the fact that the copolymer composition in the continuous miniemulsion is less than that predicted using the homogeneous copolymerization reactivity ratios, the miniemulsion copolymer might be more uniform than the macroemulsion copolymer, where the possibility of significant droplet nucleation could lead to two separate homopolymers or, at the very best, copolymers of various composition. Therefore, it is very important to use CSTR data to scale up a continuous miniemulsion copolymerization product to take into account the different particle growth kinetics for batch and continuous reactors.

4.2.3
Interfacial Polymerization

Interest in the design and controlled fabrication of composite nanoparticles consisting of hydrophobic polymer cores coated with hydrophilic polymer shells continues to increase. These particles have potential technological applications in diagnostic testing, bioseparations, controlled release of drugs, gene therapy, catalysis, and water-borne coatings and adhesives [160–170]. Emulsion copolymerization of hydrophobic and hydrophilic monomers seems to be a straightforward approach to fabricating such nanoparticles. However, this kind of emulsion copolymerization presents a big challenge, because the hydrophilic monomer resides almost exclusively in the aqueous phase while the hydrophobic monomer resides almost exclusively in the organic phase. AIndeed, most of the studies made so far have been limited to a very low hydrophilic monomer level. In all cases, the incorporation of water-soluble monomer was very limited, regardless of the initial amount of water-soluble monomer loaded into the system [171]. It was proposed that interfacial graft-polymerization of hydrophilic monomer onto hydrophobic polymer should be possible in an emulsion process by selecting an appropriate initiator system [172]. In the work of Luo et al. [170], the idea of interfacial polymerization was used to develop a novel repulpable pressure-sensitive adhesive. In order to maximize the incorporation of cationic monomer (hydrophilic monomer), an interfacial redox initiator system was used. In this initiator system, oil-soluble cumene hydroperoxide (CHP) was used as the oxidizer while hydrophilic tetraethylenepentamine was employed as the reducer. It was hoped that by using CHP/TEPA, the hydrophobic CHP would meet the hydrophilic TEPA at the particle-water interface, where hydrophobic and hydrophilic monomer are both present. In the meanwhile, non-ionic surfactant (Triton X-405) was used to facilitate the adsorption of cationiccomonomer at the interface.

In order to gain evidence for interfacial initiation, the redox initiator system was compared with a water-soluble initiator (VA-044) in terms of the emulsion polymerization behavior of butyl acrylate (BA)/[2-(methacryloyoxy)ethyl]trimethyl ammonium chloride (MAETAC). It was found that for the water-soluble initiator system, only homopoly(MAETAC) was formed and BA did not polymerize at all. In the case of VA-044, it was suggested that it may be difficult for polymeric free radicals in the aqueous phase to penetrate the viscous surfactant layer to initiate the polymerization of the BA monomer. On the other hand, it has also been found that BA could be rapidly polymerized under the same conditions if VA-044 is replaced with CHP/TEPA, indicating that radicals are formed in the interface, where they do not need to penetrate through viscous surfactant layer.

The polymerization kinetics of BA/MAETAC macroemulsion and miniemulsion copolymerization was investigated with the interfacial redox initiator system. It was found that adding MAETAC had a complex effect on the polymerization kinetics of BA, as shown in Figs. 17 and 18 [170].

In comparison with the homopolymerization of BA, adding 5%wt MAETAC greatly increases the BA polymerization rate for both macroemulsion and miniemulsion polymerization. However, when the MAETAC level is increased further, the polymerization rate begins to decrease. At higher MAETAC levels, the effect of MAETAC is different for macroemulsion and miniemulsion polymerizations. For macroemulsion polymerization at high MAETAC level, there seems to be an induction period before polymerization begins. At higher MAETAC levels, the length of the induction period increases. For miniemulsion polymerization, there is no induction period; instead, the BA polymerization rate decreases to zero at less than full conversion. BA homopolymerization with CHP/TEPA levels off at ~30% conversion. At higher MAETAC levels, the BA conversions levels off at substantially higher conversion. The leveling-off has
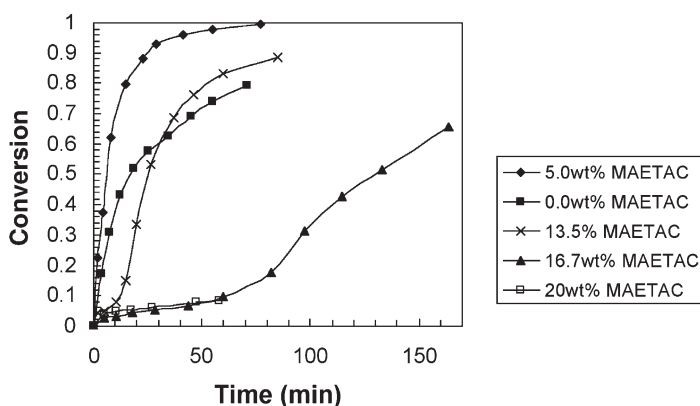
Fig. 17 BA monomer conversion for macroemulsion copolymerization with varying levels of MAETAC (from [170])
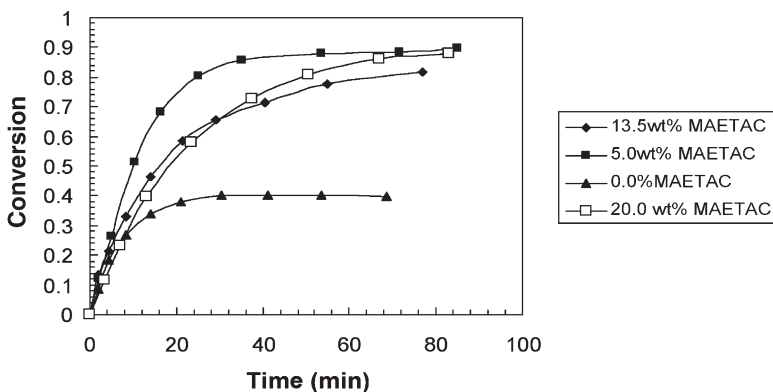
Fig. 18 BA monomer conversion for miniemulsion copolymerization with varying levels of MAETAC (from [170])

been ascribed to the depletion of TEPA. Comparing Fig. 17 with Fig. 18, it is clear that the influence of MAETAC levels on macroemulsion polymerization is much greater than on miniemulsion polymerization, especially in the early stage of polymerization. With increasing MAETAC levels, the polymerization rate of BA, especially in the early stage of polymerization, rapidly drops off in the macroemulsion polymerization. It is suggested that adding MAETAC would interfere with the nucleation of macroemulsion polymerization. At low MAETAC levels, introducing MAETAC leads to homogeneous nucleation, so the polymerization rate increases. However, at high MAETAC level, adding MAETAC did not result in homogeneous nucleation but suppressed micellar nucleation. It has been suggested that polymer formed in the aqueous phase is too hydrophilic to lead to homogeneous nucleation at high MAETAC. The suppression of micelle nucleation can be illustrated by Fig. 19. The hydrophobic molecules such as BA and CHP will be present in the micelles at the beginning of the polymerization. When TEPA was added to the reactor, many of the free radicals will be formed by the following mechanism in the surface of a micelle, where CHP and TEPA meet each other [173].

Because of their different hydrophilicities, the two free radicals formed at the same time can separate from each other quickly which can eliminate the cage effect. In a micelle, the local BA concentration may be quite high. Once a micelle is initiated, a number of BA molecules may be added quickly. As a result, some short BA blocks would be incorporated into a poly(MAETAC) chain to form something like multi-block copoly(MAETAC-BA), as shown in Fig. 19 [170]. Surfactant should stabilize the BA blocks so that the block copolymer remains in the aqueous phase.

The BA blocks in the copolymer, which is surrounded by surfactant, swell with BA monomer, which polymerizes there until particles form. Therefore, micellar nucleation is diminished or even eliminated. As a result, micellar nucleation is retarded, and N_p decreases. It is clear that the nucleation is very
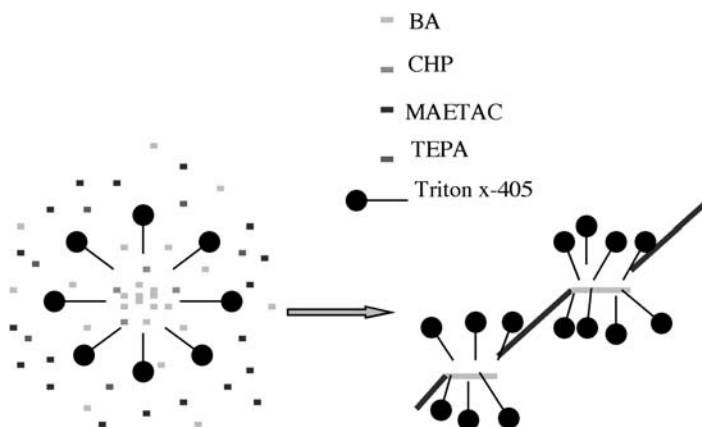
Fig. 19 Schematic of the formation of multi-block poly(MAETAC-BA) (from [170])

sensitive to the level of hydrophilic monomer for macroemulsion polymeriza-
tion. As a result, the polymerization rate and particle size change dramatically
with changes of hydrophilic monomer level. For miniemulsion polymerization,
the monomer is dispersed into droplets of 50–500 nm prior to polymerization
and no micelles exist. Therefore, TEPA comes into contact with CHP at the
droplet-water interface. MAETAC and BA copolymerize at the interface. The
number of BA molecules in a monomer droplet is far larger than that in a
micelle, so the resultant copolymer has a much higher composition of BA and
is anchored at the interface. Therefore, droplet nucleation during miniemulsion
polymerization is hardly affected, although it was found that when the hydro-
philic monomer was low, homogeneous nucleation could occur in the mini-
emulsion polymerization, as shown in Fig. 20 [170]. As a result, there is little
initial dependence of the polymerization rate on the hydrophilic monomer level
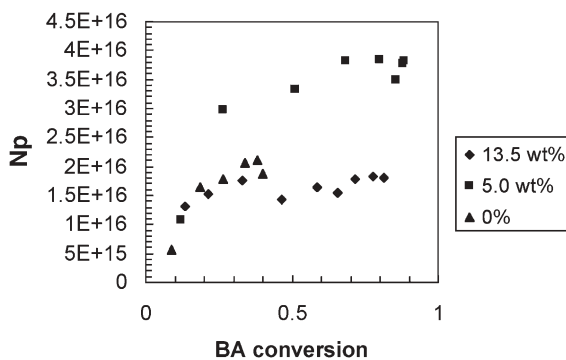
Fig. 20 Particle number development for miniemulsion copolymerization with varying
levels of MAETAC (from [170])

during miniemulsion polymerization, in sharp contrast to macroemulsion polymerization, as shown in Figs. 17 and 18. Clearly, nucleation during miniemulsion polymerization is highly robust to the level of hydrophilic comonomer.

4.3
Multiphase Particles

4.3.1
Hybrid Miniemulsion Polymerization

It would often be desirable to create submicron particles containing two or more polymers. These could be in the form of a blend or in the form of a graft copolymer. In a simple blend, the two polymers may or may not be compatible. If they are compatible, the particle will be homogenous. If the polymers are not compatible, then microphase separation is likely. However, if the phase separation occurs in submicron particles, the phase domains will be small, and decent dispersion of the two polymers will occur. Homogenous, grafted, or phase-separated morphologies might conceivably be of practical value.

One method of creating such polymer blends or grafts in submicron particles is through *hybrid miniemulsion polymerization*. In this technology, a preformed polymer (or oligomer) is dissolved into a monomer (or monomer solution). A miniemulsion is then created from the monomer-polymer solution, and this miniemulsion is polymerized via standard techniques. Care must be taken in creating the miniemulsion, because the polymer solution will likely have a high viscosity (higher than for a simple monomer miniemulsion) and so the droplet break-up by the shear device may be more difficult. On the other hand, the preformed polymer may act as the costabilizer, eliminating the need for HD or other costabilizers. For some chemistries, grafting will take place during the polymerization of the monomer, and for some polymers phase separation will occur. In any case, the product is a submicron dispersion of one polymer in another, and may well have practical value. Since most of the oligomers or prepolymers are polymeric and probably highly water-insoluble, macroemulsion polymerization will not result in a graft copolymer or an intimate blend. Since the prepolymer is not transported from the monomer droplets to the polymer particles, the prepolymer does not reach the locus of polymerization. Macroscopic phase separation and colloidal instability often result.

Details of the chemistry and process (and the product) are very specific to the choice of prepolymer and monomer; for this reason, each system will be discussed separately here.

4.3.1.1
Alkyds

Water-based coatings have become more widely used over the past few decades because they are environmentally friendly, offer easy clean-up, and their properties and application performance characteristics have improved. Solvent-based systems such as alkyd resins and polyurethanes have remained important for some applications because of superior properties, such as gloss and hardness. This is due to the curing mechanism of oil-based coatings in which the oils react with atmospheric oxygen to form very hard crosslinked materials. This mechanism is generally lacking in water-based coatings, which tend to be soft and pliable, due to the fact that the coatings are made soft to allow film formation, and since there is no curing chemistry available, remain soft on drying. Several researchers have focused on the use of the hybrid miniemulsion polymerization of acrylic monomers in the presence of alkyd and polyurethane resins to develop alternative coatings which have the advantages of water-based systems (like low VOC) with the drying (air cure) properties of solvent-based systems. Alkyd/acrylate coatings are targeted as replacements for solvent-based architectural coatings, and oil-modified polyurethane (OMPU)/acrylate coatings may provide a low VOC alternative to solvent-based clear coats. Since U.S. architectural coating sales in 1995 amounted to 625 million gallons [174], a conservative estimate of the VOC reduction if all of these coatings were water-based is approximately 500 million pounds of solvent that would not be released into the air.

Nabuurs and German [175] developed an alkyd-acrylic hybrid system via emulsion polymerization. They were able to produce a stable product using MMA as the acrylic. When the alkyds were functionalized by sulfonation, there was no evidence of heterogeneity in the particles. When unfunctionalized alkyd was used, the MMA appeared as microdomains within the particles. Grafting of acrylic to alkyd was low. The presence of the alkyd led to low rates of polymerization and limited conversion that were both attributed to retardation through radical delocalization following radical transfer to the unsaturated groups in the fatty acids of the alkyd. Although this work was not reported to be miniemulsion polymerization, the emulsions were subjected to high shear prior to polymerization. No costabilizer was added, but the alkyd presumably functioned as such. Since the alkyd-acrylic droplet size was probably quite small, droplet nucleation was probably the dominant nucleation mechanism. This would explain the good colloidal stability of the resulting system, and the fact that both alkyd and acrylic domains were found in the same particles.

Wang et al. [98] carried out macroemulsion and miniemulsion polymerization of acrylic monomers in the presence of alkyd resins. Miniemulsion and macroemulsion polymers were produced using a commercial medium soya-linseed alkyd and a mix of acrylic monomers consisting of 50% BA, 49% MMA, and 1% acrylic acid (AA). PMMA polymer with a weight average molecular weight of 100,000 was used as the costabilizer. Alkyd levels were 5, 30, 60 or

100% based on total acrylic monomer. SLS was used as the surfactant, and sodium persulfate (SPS) was used as the initiator. The miniemulsions were prepared by dispersing the desired amount of monomer-PMMA-alkyd solution in the aqueous SLS solution by mixing with stirring at room temperature. The resulting emulsion was sheared further by sonication. Polymerization was carried out at 60–80 °C. The reaction was followed by gravimetric conversion analysis. Macroemulsion polymerizations were carried out in the same manner except that no sonication process was used and the PMMA costabilizer was not employed. Droplet and particles sizes were determined by dynamic light scattering, and double bond content of the alkyd by NMR. Grafting was determined by extraction, and degree of crosslinking by exhaustive extraction.

The monomer miniemulsions with PMMA as costabilizer were prepared with different amounts of alkyd resin. The PMMA costabilizer was effective in the preparation of stable miniemulsions, especially in conjunction with the alkyd. The size of monomer droplets was below 300 nm. After five days, the unpolymerized macroemulsions with alkyd separated into three phases, monomer on the top, clear water in the middle, and alkyd resin on the bottom. The miniemulsion without alkyd showed two phases, monomer and water. All miniemulsions with alkyd resin appear to remain uniform. Very stable miniemulsions were obtained when the alkyd content was higher than 30%. The shelf life of macroemulsions was only 2–8 minutes.

The polymerization rate in the presence of alkyd was slower than that without alkyd. Doubling the initiator and emulsifier concentration increased the reaction rate, but not to the level achieved with the miniemulsion polymerization without alkyd. This retardation (as reported also by Nabuurs) increased with increasing alkyd level. The latexes obtained from the miniemulsion polymerization of the alkyd-acrylate mixtures were uniform emulsions, and no coagulation occurred during polymerization. Macroemulsion polymerization with alkyd resulted in colloidal instability, probably due the inability of the alkyd to reach the locus of polymerization.

NMR analysis indicated that approximately 30% of the alkyd double bonds had been consumed in the polymerization process. This is important in that it indicates that a substantial fraction of the double bonds remain for oxidative crosslinking while a coating made from this material is dried. Selective extraction indicated that approximately 60% of the acrylate was grafted to alkyd. Exhaustive extraction indicated less than 5% crosslinked material. The polymerized latex formed good films with acceptable hardness.

On the whole, the miniemulsion polymerization process proved to be effective for incorporating an alkyd resin into acrylic coated copolymers. The reaction produced stable, small particle size latexes that contain graft copolymer of the acrylic and alkyd components. Attempts at macroemulsion hybrid polymerization were unsuccessful.

Van Hamersveld et al. [176, 177] carried out hybrid miniemulsion polymerization of MMA, using HD as the costabilizer. In an attempt to encourage grafting, oxidized triglycerides (such as sunflower oil) were used as initiators.

This produced homogenous particles (presumably due to higher levels of grafting), whereas the use of conventional initiators resulted in particle inhomogeneity due to phase separation of the alkyd and acrylic.

Wu et al. [99, 174] further investigated the hybrid miniemulsion polymerization of alkyd-acrylic systems, using the same monomer mix as Wang [98]. Retardation by the alkyd was reported; high polymerization temperature and mixed (oil and water-soluble) initiators were used to improve monomer conversion. The polymers obtained had a very wide molecular weight distribution, with polydispersities of more than 19 and a number average molecular weight slightly larger than alkyd. This indicates that a fraction of the alkyd remains in the ungrafted form. On the other hand, extraction results indicate that a large fraction of polyacrylate chains contain at least some grafted alkyd. Approximately 20% of the double bonds in the alkyd are consumed in grafting reactions. Two glass transition temperatures were observed, indicating the presence of at least two forms of polymer. The two glass transition temperatures correspond to those of poly(acrylate-graft-alkyd) and polyacrylate respectively. The proportion of the two kinds of polymers in the samples was determined by extraction, and this indicated that poly(acrylate-graft-alkyd) is the predominant form.

Tsavalas et al. [178] studied the limiting conversion phenomenon brought on by alkyd retardation. He concluded that retardive chain transfer to the alkyd double bonds was not adequate, especially for systems that graft through addition through double bonds (acrylates, but not methacrylates) as well as through chain transfer via hydrogen abstraction at alkyd double bonds (acrylates and methacrylates). Without transfer, no radicals of low activity would be created, and so the dramatic reduction in polymerization rate would have to be attributed to another cause. He concluded that there are two mechanisms for limiting conversion, one kinetic, and one physical. MMA, which has a high T_g, and grafts primarily through chain transfer, was found to produce a plateau in the kinetic profile of monomer conversion when the monomer glass transition temperature was near the reaction temperature. However, simple calculations suggest that transfer alone could not produce such a dramatic change in kinetics. The physical mechanism is thought to play a significant role, particularly since MMA/alkyd particles display core shell morphology, with the possibility of residual monomer trapped in the alkyd-rich core.

Butyl acrylate has a low T_g and no steric hindrance to prevent direct addition to alkyd double bonds. In this case, the limiting conversion is not absolute, but more of a very significant reduction in the rate of polymerization at high conversion. Again, simple calculations suggest that retardive chain transfer alone could not produce such a dramatic change in kinetics. Instead, the physical mechanism was found to be significant as well. PBA and alkyd both have glass transitions well below the reaction temperature, so a barrier to entry is never formed in that type of system. However, a viscous environment forms after appreciable conversion that slows the mobility of both monomer and initiator. BA monomer is thought to be dissolved in small alkyd domains dis-

tributed throughout a continuous BA particle phase. These islands eventually act as reservoirs diffusing monomer to the polymerization of BA in the continuous particle phase. The viscosity and diffusion rate are then what retard the rate in this type of hybrid system. This is evidenced by the fact that although there is a point of dramatic rate change, afterwards the new rate continues to complete conversion. That point of rate change likely corresponds to a morphology transformation to those alkyd island domains. Butyl methacrylate exhibits a reduced rate of polymerization like that of BA, rather than a true limiting conversion like that of MMA. The grafting kinetics of BMA are similar to those of MMA, but its limiting conversion behavior is similar to that of BA. Therefore it was concluded that the physical mechanism (based on T_g) is dominant over the kinetic mechanism (retardive chain transfer) for all three monomers.

Tsavalas [179] also studied the grafting of alkyd-acrylic hybrid systems. He attributed differences in levels of grafting for different monomers to differences in grafting mechanism. Grafting was observed between methacrylates and typical alkyds, but steric hindrance at the methacrylate reactive center directs addition to an alkyd double bond. This method was shown to give optimal grafting efficiency. Instead, methacrylates tend towards allylic hydrogen abstraction, a process that creates a relatively stable and unreactive radical on the resin along with terminating the abstracting methacrylate chain. These effects degrade both the grafting efficiency and the rate of polymerization. Acrylate monomers were found to produce high levels of grafting. Direct addition to resin double bonds is facilitated and virtually complete grafting of the component is observed. This was attributed to the lack of steric hindrance of the acrylate reactive center. The double bond content of the resin was shown to be important to grafting. Double bonds are needed, even in systems where abstraction is the dominant route of attack, since hydrogens allylic to them are good leaving groups. The double bond density correlates directly with the concentration of possible grafting sites and was shown to lead to higher levels of grafting. Tsavalas showed that the choice of monomer(s) is the most important variable in determining the level of grafting. Chain transfer dominates the interaction of methacrylate with resin, and so there is less opportunity for grafting. Conversely, the interaction of acrylate with resin is dominated by direct addition to a resin double bond, a highly efficient mode of grafting. In a third paper, Tsavalas [180] confirmed the differences in particle morphologies between acrylates and the methacrylates described above.

Shoaf and Stockl [181] optimized the formulations for hybrid miniemulsion polymerization. By adjusting the T_g of the polymer phase (acrylate-styrene), they were able to create latex that gave good film formation with little coalescing aid, and hence, very low VOC. By adding a latent oxidative functional monomer, they were able to get very hard film. Latexes containing up to approximately 50% alkyd (based on total solids) were produced. The coatings exhibited high gloss, which is sometimes unattainable with water-based systems. No information on the heterogeneity of the particles was provided.

4.3.1.2
Polyester

Tsavalas et al. [100] carried out hybrid miniemulsion polymerization with a three component acrylic system of methyl methacrylate, butyl acrylate, and acrylic acid in the presence of a Bayer Roskydal TPLS2190 unsaturated polyester resin. Latexes were obtained in which the polyester resin was grafted to the acrylic polymer, forming a water-based crosslinkable coating. Both emulsions and latexes were shelf stable for over six months, shear stable, and resistant to at least one freeze/thaw cycle. Resin to monomer ratios as high as 1:1 (wt:wt) and total emulsion solids as high as 45% were studied. The sizes of the monomer droplets and latex particles were similar, suggesting predominant droplet nucleation. A high level of crosslinking (>70%) during polymerization was observed in this particular hybrid system in contrast to those involving alkyd, as reported above. Homogeneous and hard films were achieved with exceptional adhesion. Electron microscopy showed the hybrid particle morphology to have internal domains of polyester resin in an acrylic matrix. Kinetic studies showed that as resin content increased in comparison to monomer content, the polymerization rate decreased, suggesting retardive chain transfer as found with the alkyds.

4.3.1.3
Polyurethane

Oil-modified polyurethanes (OMPU) are, in terms of volume produced and sold, the most important polyurethane coatings, with superior properties such as gloss, chemical resistance and film formation. Most urethane coatings are solvent-based, and solvent-based coatings are less than desirable due to the environmental impact of their high VOC. To meet the increasing concern for health, safety and the environment, there has been a strong preference in recent years for water-borne coatings. Dong et al. [101] carried out hybrid miniemulsion polymerization with acrylic monomers (methyl methacrylate, butyl acrylate and acrylic acid) in the presence of oil-modified polyurethane resin. The OMPU served as the costabilizer. Latexes with different ratios of resin to acrylic monomer were synthesized. The monomer emulsions prepared for hybrid miniemulsion polymerization showed excellent shelf-life stability (more than five months) and the polymerization was run free of coagulation. Solvent extraction indicated that the grafting efficiency of polyacrylates was greater than 29% for all of the samples produced. The ^{13}C solution NMR spectrum showed that a substantial fraction of the original carbon double bonds (>61%) in oil-modified polyurethane remained after polymerization for film curing. Films obtained from the latexes presented good adhesion properties and fair hardness properties.

Li et al. [182] used hybrid miniemulsion polymerization to prepare urethane/BMA latexes with particle sizes of about 50 nm. Hexadecane was used as the

costabilizer. In this case, the presence of the prepolymer (polyurethane, MW <10,000) resulted in an increase, rather than a decrease, in the rate of polymerization due to the fact that the presence of the polyurethane prepolymer resulted in smaller initial droplet sizes. (Presumably there was no retardive chain transfer, since there was no significant unsaturation in the polyurethane.) Free isocyanate groups remaining on the polyurethane reacted with the aqueous phase, causing an increase in particle size over several days due to flocculation.

Wang et al. [183] carried out hybrid miniemulsion polymerization of acrylates in the presence of polyurethane. The polyurethane was used as the costabilizer, and SLS as the surfactant. When MMA was used as the monomer, some homogenous nucleation was observed. This is in agreement with Tsavalas [179] who reported evidence of homogenous nucleation in the hybrid miniemulsion of MMA in the presence of alkyd.

Barrere and Landfester [184] prepared a hybrid miniemulsion in which isophorone diisocyanate was condensation polymerized with dodecanediol to form polyurethane at the same time that the polystyrene or polyBA was free radical polymerized. Unlike previous work, the polyurethane was not prepared in organic solvent in advance. Therefore, in this one-pot synthesis, polyaddition and free radical polymerization both take place in the same particle. HD was used as the costabilizer. After miniemulsification, the polycondensation was allowed to take place, and then a free radical initiator was added to polymerize the styrenic or acrylic monomer. Molecular weight distributions were bimodal; the PU had a substantially lower molecular weight than the polyacrylate. Neither intra- nor interparticle phase separation could be detected by TEM; the particles appeared to be homogeneous. No measurements of grafting were made, but since there was no unsaturation in the PU, none was expected.

4.3.1.4
Other Hybrids

El-Aasser and coworkers [185, 186] have carried out miniemulsion polymerization of styrene monomer in the presence of Kraton D1102 thermoplastic elastomer, to form hybrid composite latexes approximately 100–150 nm in size. A costabilizer other than the rubber was used. The miniemulsification was carried out via homogenization, and resulted in a very broad droplet size distribution. This resulted in the formation of inhomogeneous hybrid composite particles due to monomer diffusion during polymerization. When an oil-soluble initiator was used, an induction period was observed, resulting from the presence of radical scavengers such as antioxidants and UV stabilizers within the Kraton-styrene droplets. This also lead to inhomogeneous particles, but was eliminated with a water-soluble initiator. TEM showed domains of polystyrene within the rubber particles. Some evidence of homogeneous (or micellar) nucleation was found.

Kawahara et al. [187] prepared acrylic/epoxy composite latexes via hybrid miniemulsion polymerization. Landfester et al. [188] have incorporated PMMA

macromer as a phase capatibilizing agent in the core shell polymerization of styrene and MMA. Roberts et al. [189, 190] copolymerized vinyltriethoxysilane with various acrylates. Phase separation resulted. Hydrolysis of the triethoxy-silane and subsquent condensation resulted in a crosslinked siloxane phase, separate from the polyacrylate.

4.3.1.5
Artificial Miniemulsions

El-Aasser and coworkers [191–193] have used the miniemulsification process to create water dispersions of preformed polymers. In this technique, a polymer is dissolved in a volatile organic solvent. The polymer-solvent solution is then miniemulsified and the solvent is evaporated off. This leaves a submicron water dispersion of the polymer. This technology has some distinct advantages. First, it can be applied to any polymer that is insoluble in water, but soluble in an organic solvent. Second, the polymerization need not be via free radical poly-merization, since it is accomplished previous to miniemulsification. For this rea-son, polymerizations that are not water-tolerant may be used to form the poly-mer. This technique has been applied to a number of commercial applications.

4.3.2
Nanoencapsulation

Nanoencapsulation, or the encapsulation of solids within submicron particles, has been the subject of considerable work in recent years. Most have attempted nanoencapsulation via emulsion and miniemulsion polymerization techni-ques. Lee and coworkers [194, 195] have carried out emulsion polymerization in the presence of layered silicate. The term emulsion polymerization is un-fortunate, since the polymerization takes place between the layers of silicate rather than in latex particles, forming an intercalated silica nanocomposite. Garcés et al. [196] and many others have reported marked improvement in mechanical properties if the inorganic reinforcing material (such as silica) is dispersed on the nano-scale. None of these applications are truly nanoen-capsulation, since the polymer resides in the interstices of large inorganic particles, rather than having the inorganic fully encapsulated within a polymer particle.

Van Herk and German [197] have surveyed the true nano (micro) encapsu-lation of inorganic and organic pigments and fillers via emulsion polymeriza-tion. In this technique, small inorganic particles are used as nuclei for the for-mation of polymer particles. A number of materials have been encapsulated in this way, including clays, limestone, alumina, silica, carbon black, and magnetic materials. The practical challenges associated with these encapsulations include stabilizing the inorganic colloids, and controlling particle nucleation.

A more direct and reproducible route to nanoencapsulation is that of miniemulsion polymerization. If an organic or inorganic solid is contained

within the monomer droplets, nanoencapsulation can be accomplished; unlike in macroemulsion polymerization, no transport of solids from the monomer droplets to the locus of polymerization is required. Erdem et al. [198–200] have published a series of papers on the nanoencapsulation of titanium dioxide (TiO$_2$) particles in styrene. The challenges in this work involved getting the hydrophilic TiO$_2$ particles to reside in the hydrophobic environment of the interior of the miniemulsion monomer droplet, rather than in the hydrophilic environment of the continuous aqueous phase. This was accomplished through the use of specific surfactant systems. Landfester et al. [3, 201–204] studied the nanoencapsulation of solid materials via miniemulsion polymerization. They successfully encapsulated a wide variety of materials. For hydrophobic solids (like carbon black) that will easily transport into the monomer droplets, the technique is straightforward. For hydrophilic solids (like TiO$_2$) that prefer the aqueous phase, the authors used a combination of oil-in-water and water-in-oil surfactants to move the solids into the miniemulsion monomer droplets.

While the literature has demonstrated the viability of nanoencapsulation via miniemulsion technology, a great many issues remain. These include the use of surfactant systems to stabilize the solid colloidal particles and bring them into the monomer droplets, uniformity of encapsulation (a uniform [small] number of solid particles per polymer particle for a minimum number of polymer particles, not including the encapsulated solid), and complete coverage of the solids by the resultant polymer coating.

4.4
Controlled Free Radical Polymerization

4.4.1
Nitroxide-Mediated Polymerization

Nitroxide-Mediated Controlled Radical Polymerization (NMCRP) was first discovered by Solomon et al., who patented their discovery in 1985 [205]. This opened up new pathways in the field of free-radical polymerization. Polymer architectures, which were the domain of the anionic polymer chemist, became accessible to the free-radical polymer chemist. However, it was not until the work of Georges et al. [206] was published in 1993, that the world of polymer chemistry became aware of the possibilities of this new class of free-radical polymerization. This was the beginning of what is today one of the leading topics in free-radical polymer chemistry: Controlled or "Living" Free Radical Polymerization. This initiated the search for new Controlled or "Living" Free Radical Polymerization techniques, and soon afterwards other methods (which will be discussed later) were developed.

4.4.1.1
Mechanism

In processes based on reversible termination, like NMCRP and ATRP (Sect. 4.4.2), a species is added which minimizes bimolecular termination by reversible coupling. In NMCRP this species is a nitroxide. The mechanism of nitroxide-mediated CRP is based on the reversible activation of dormant polymer chains (P_n-T) as shown in Scheme 1. This additional reaction step in the free-radical polymerization provides the living character and controls the molecular weight distribution.

$$P_n\!\!-\!T \;\; \underset{k_{deact}}{\overset{k_{act}}{\rightleftharpoons}} \;\; P_n \cdot \;\; + \;\; T\cdot$$
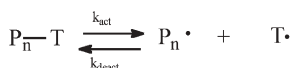
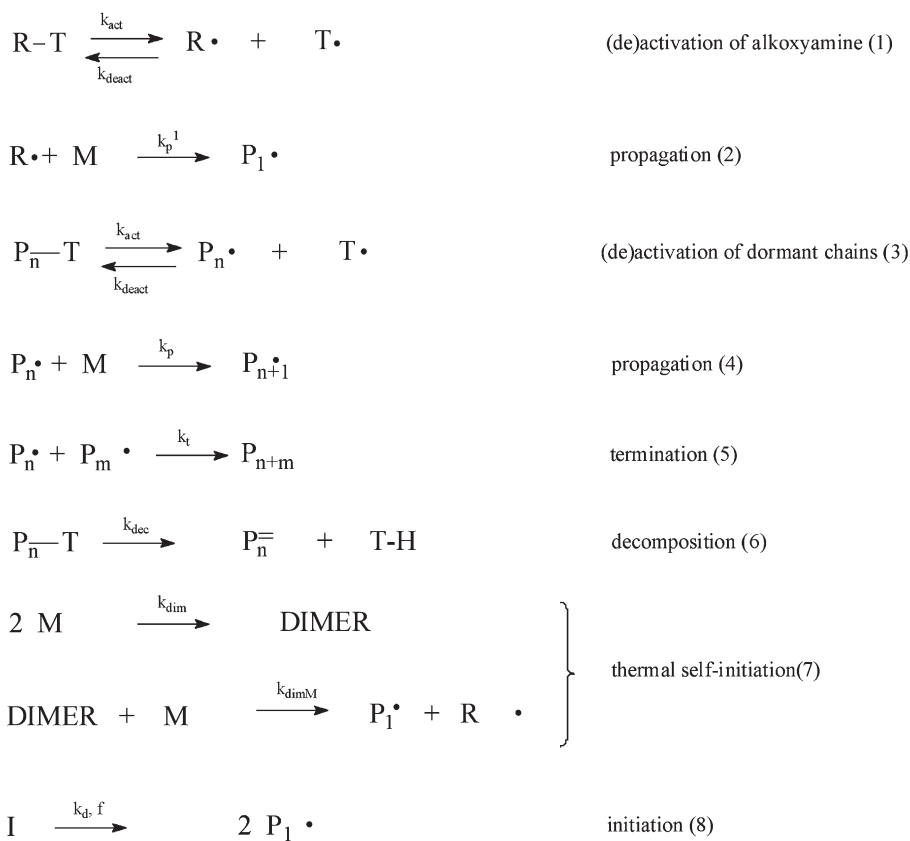**Scheme 1** Reversible activation of dormant polymer chains

When a dormant species or alkoxyamine dissociates homolytically, a carbon-centered radical and a stable nitroxide radical are formed (Scheme 2). This is a reversible process and the reversible reaction is very fast – close to diffusion-controlled rates. With increasing temperature, the dissociation rate will increase, which will increase the concentration of the polymeric radicals ($P_n^\cdot$). These will have a chance to add to monomer before being trapped again, which allows growth of the polymer chains. The nitroxide is an ideal candidate for this process since it only reacts with carbon-centered radicals, is stable and does not dimerize, and in general couples nonspecifically with all types of carbon-centered radicals (at close to diffusion-controlled rates).
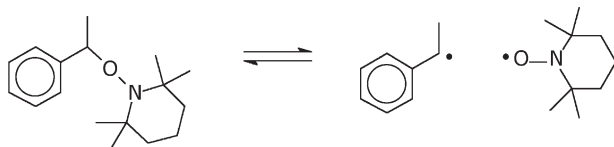
Scheme 2 Dissociation of a typical alkoxyamine into a carbon-centered radical (ethylbenzene radical) and a nitroxide (TEMPO)

Polymerization can be started using an alkoxyamine as initiator such that, ideally, no reactions other than the reversible activation of dormant species and the addition of monomer to carbon-centered radicals take place. The alkoxyamine consists of a small radical species, capable of reacting with monomer, trapped by a nitroxide. Upon decomposition of the alkoxyamine in the presence of monomer, polymeric dormant species will form and grow in chain length over time. Otherwise, polymerization can be started using a conventional free-radical initiator and a nitroxide. The alkoxyamine will then be formed in situ when an initiator molecule decomposes, and, after adding a monomer unit or two, is trapped by a nitroxide.

Since the nitroxide and the carbon-centered radical diffuse away from each other, termination by combination or disproportionation of two carbon-centered radicals cannot be excluded. This will lead to the formation of "dead" polymer chains and an excess of free nitroxide. The build-up of free nitroxide is referred to as the Persistent Radical Effect [207] and slows down the polymerization, since it will favor trapping (radical-radical coupling) over propagation. Besides termination, other side reactions play an important role in nitroxide-mediated CRP. One of the important side reactions is the decomposition of dormant chains [208], yielding polymer chains with an unsaturated end-group and a hydroxyamine, TH (Scheme 3, reaction 6). Another side reaction is thermal self-initiation [209], which is observed in styrene polymerizations at high temperatures. Here two styrene monomers can form a dimer, which, after reaction with another styrene monomer, results in the formation of two radicals (Scheme 3, reaction 7). This additional radical flux can compensate for the loss of radicals due to irreversible termination and allows the poly-

$$R-T \underset{k_{deact}}{\overset{k_{act}}{\rightleftharpoons}} R\cdot + T\cdot \qquad \text{(de)activation of alkoxyamine (1)}$$

$$R\cdot + M \xrightarrow{k_p^1} P_1\cdot \qquad \text{propagation (2)}$$

$$P_n-T \underset{k_{deact}}{\overset{k_{act}}{\rightleftharpoons}} P_n\cdot + T\cdot \qquad \text{(de)activation of dormant chains (3)}$$

$$P_n\cdot + M \xrightarrow{k_p} P_{n+1}\cdot \qquad \text{propagation (4)}$$

$$P_n\cdot + P_m\cdot \xrightarrow{k_t} P_{n+m} \qquad \text{termination (5)}$$

$$P_n-T \xrightarrow{k_{dec}} P_n^= + T\text{-}H \qquad \text{decomposition (6)}$$

$$2\,M \xrightarrow{k_{dim}} DIMER$$

$$DIMER + M \xrightarrow{k_{dimM}} P_1\cdot + R\cdot \qquad \left.\begin{array}{c}\\\\\end{array}\right\} \text{thermal self-initiation(7)}$$

$$I \xrightarrow{k_d,\,f} 2\,P_1\cdot \qquad \text{initiation (8)}$$

Scheme 3 Mechanism of nitroxide-mediated CRP. R-T represents an alkoxyamine, T· represents a nitroxide

merization to proceed successfully, providing that the number of initiating radicals is small compared to the number of nitroxide-trapped polymer chains [210]. Systems that do not show thermal self-initiation can also be controlled by using an additional initiator, which will provide the additional radical flux [210]. In addition, the dimer formed (Scheme 3, reaction 7) can react with a nitroxide molecule to provide the dimer radical and a hydroxyamine. The most important reactions in nitroxide-mediated CRP are shown in Scheme 3. An excellent overview of the kinetics and mechanism, supported by simulations, is given by Fukuda [211].

4.4.1.2
Effects Of Segregation And Heterogeneity

Similar to conventional free radical polymerization, heterogeneity and segregation effects make the kinetics of NMCRP more complex when applied in miniemulsions. This issue has also been discussed in a review article by Qiu et al. [212], which covers controlled free-radical polymerization in heterogeneous media up to 2001 (and so also covers miniemulsion polymerization). Butté et al. [213, 214] and Charleux [215] both discussed compartmentalization effects. Butté et al. came to the conclusion that the effects of segregation in NMCRP miniemulsions are very small, while Charleux predicted an increased polymerization rate for small (50–100 nm) particles. Both groups come to different conclusions, because Butté et al. did not account for the possibility that a nitroxide molecule exits a particle, while Charleux did. In summary, the segregation effect in NMCRP miniemulsions is not large unless the particles are small or a lot of the nitroxide partitions to the aqueous phase. This is nicely illustrated by work of Pan et al. [216], who performed NMCRP miniemulsions with varying surfactant concentrations. Although the surfactant concentration had a large effect on particle size, it hardly affected the polymerization rate.

Since both NMCRP and ATRP (Sect. 4.4.2) are based on reversible termination, the effects observed for these will be similar and are further discussed later.

4.4.1.3
Results

A review article by Qiu et al. [212] and references herein [217–226] covers NMCRP in miniemulsions up to 2001. Cunningham wrote a related review in 2002, also covering controlled radical polymerization in dispersed phase systems [227]. Here, the main results reported in the Qiu review will be summarized, and new developments in the field since then will be reviewed.

For several reasons, miniemulsion polymerization is the preferred technique for NMCRP in aqueous dispersed systems. Since NMCRP in general requires high reaction temperatures (above 100 °C) for the thermal polymerization of

styrene, the presence of a monomer phase is not desired. This would lead to colloidal instability. Furthermore, the presence of a large monomer reservoir makes the nitroxide partition out of the loci of polymerization, which will reduce control of the polymerization. Another reason for using miniemulsion polymerization is the fact that pre-formed alkoxyamines or nitroxide-terminated oligomers are often used. Generally, these are too water-insoluble to be transported through the aqueous phase, which excludes the use of conventional or seeded emulsion polymerization. Finally, the poorly understood and complex particle nucleation step is avoided in miniemulsion polymerization, which allows the use of oil-soluble initiators and makes results easier to understand.

The first results for NMCRP in miniemulsion were reported by Propdan et al. [218, 221] and Macleod et al. [219]. Both groups performed miniemulsion polymerizations of styrene at high temperatures (above the boiling point of water) using high pressure reactors. Propdan et al. used oil-soluble benzoyl peroxide (BPO) free-radical initiator and TEMPO, **1** (see Scheme 4), in a Dowfax 8390 surfactant system at 125 °C, while Macleod et al. used water-soluble potassium persulfate (KPS) initiator and sodium dodecylbenzene sulfonate (SDBS) surfactant at 135 °C. The Propdan system resulted in stable latexes and 90% conversion was reached in 12 hours. The polydispersity was 1.15–1.60 and molecular weights were up to 40 kg/mol. The Macleod system, if a proper nitroxide/initiator ratio was chosen, also gave stable latexes with good control, with polydispersities in the range of 1.1–1.2. Conversion reached 87% in six hours, although a later publication [225] showed that this relatively fast polymerization also resulted in a large proportion of dead chains.
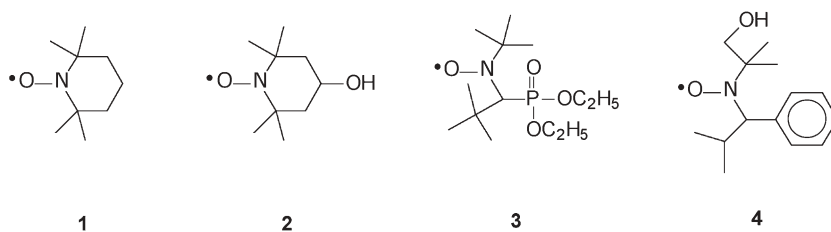
Scheme 4 Nitroxides used for NMCRP in miniemulsion

Later on, these same research groups started using pre-formed TEMPO-terminated polystyrene as a one component initiator system instead of a bicomponent nitroxide/initiator system. Pan et al. [224] prepared TEMPO-terminated polystyrene in bulk and isolated this to use it as the initiator in their miniemulsions. This led to slower polymerization rates, molecular weights lower than predicted and relatively broad molecular weight distributions. Keoshkerian et al. [225], on the other hand, reported very high conversions in six hours (99.6%) and narrow polydispersities (1.15) by preparing TEMPO-terminated polystyrene in bulk up to a conversion of about 5% and applying

the mixture directly in miniemulsion without purification. As a proof of livingness, they were able to extend the chains with styrene in bulk and to produce block copolymers with butyl acrylate (BA) by directly adding the BA to the miniemulsion, yielding a block copolymer with a polydispersity of 1.18.

A disadvantage of TEMPO mediated systems is that a high temperature (above the boiling point of water) is required and so conventional emulsion polymerization reactors cannot be used. Another disadvantage of TEMPO is the limited monomer choice. The use of the so-called SG1 nitroxide, **3** (see Scheme 4), partially overcomes these problems, since it has been reported to work at 90 °C and to work with both styrene and BA [217, 220, 223, 226, 228, 229, 230]. When AIBN, an oil-soluble initiator, was used, poor results were obtained in styrene miniemulsion polymerizations [217, 220]. Conversion was low and the polydisperity was around 1.6. On the other hand, the use of a water-soluble initiator was more successful [223, 226, 228]. Conversion reached 90% within eight hours. Another important observation was that the pH was a very important parameter in the SG1-mediated polymerizations. This was assigned to side-reaction of the SG1 nitroxide. The best results were obtained when the pH was close to 7. Also, the monomer/water ratio appeared to have an important effect on the controllability of the polymerizations. Increasing the monomer/water ratio led to better-controlled (lower polydispersity) reactions. This was assigned to the fact than at a higher monomer/water ratio, less nitroxide partitions to the aqueous phase.

As already mentioned, the SG1 nitroxide is also capable of controlling polymerizations other than styrene [226, 229, 230]. Farcet et al. showed that it also worked with BA, although it required higher reaction temperatures (above 100 °C) because of the lower activation rate constant of SG1-terminated polybutyl acrylate compared to polystyrene. Polydispersities as low as 1.19 were obtained for BA miniemulsion homopolymerizations, while M_n increased linearly with conversion. Addition of styrene, after the majority of BA had reacted, resulted in the formation of block copolymers with a narrow polydispersity of 1.27. Additional evidence for the livingness of the polybutyl acrylate chains was given by thorough analyses of the materials formed via ^{1}H NMR, ^{13}C NMR, SEC and MALDI-TOF [230]. These analyses showed that the majority of chains consisted of polybutyl acrylate with one initiator-derived and one SG1 chain-end. Besides block copolymers, gradient copolymers of styrene and BA were also synthesized [230] using miniemulsion copolymerization of styrene and BA. Due to the composition drift and the livingness of the chains, this gives gradient block copolymers that contain relatively more styrene in the beginning of the chain and relatively more BA closer to the chain end.

Keoshkerian et al. used another nitroxide, **4** (see Scheme 4), to perform miniemulsion polymerizations with acrylates [231]. First the nitroxide was reacted with styrene and BPO in bulk to form nitroxide-terminated oligomers. These oligomers were used in a miniemulsion polymerization of BA at 135 °C. 86% conversion was reached after three hours, and at this point the polymer

had a M_n of 12 kg/mol with a polydispersity of 1.27. When the same procedure was followed with TEMPO as the nitroxide, conversion was less than 8% and did not proceed any further. The addition of a small amount of ascorbic acid, which destroys free nitroxide, led to conversions close to 65% after three hours, although the polydispersity of 1.62 was broader than with **4**.

Tortosa et al. [228] tried to synthesize styrene/BA block copolymers using both TEMPO and OH-TEMPO, **2** (see Scheme 4). OH-TEMPO was used because of the aqueous phase partitioning of this nitroxide, which would reduce the nitroxide concentration in the particles and so result in higher polymerization rates. It was indeed found that the conversion in the OH-TEMPO-mediated polymerizations was much higher. However, it was also found that the TEMPO-mediated polymerizations showed a greater living character and that the OH-TEMPO-mediated polymerizations also gave pBA homopolymer. In a later publication, Cunningham et al. [232] studied the effects of camphorsulfonic acid (CSA), a nitroxide destroyer known to accelerate bulk polymerizations, on styrene miniemulsion polymerizations with TEMPO and OH-TEMPO. It was found that the CSA effectively accelerates the polymerization rate, especially at high nitroxide/initiator ratios, although the effects were not as large as seen in bulk experiments. This was ascribed to the aqueous phase partitioning of the CSA, which reduces the CSA concentration in the particles. Unlike the large differences in polymerization rate seen in the BA polymerizations with TEMPO and OH-TEMPO [228], the experiments with styrene showed about equal polymerization rates for both the TEMPO and OH-TEMPO-mediated systems. Also, the increase in rate caused by the addition of CSA was equal in both systems, despite the large difference in water-solubilities between TEMPO and OH-TEMPO.

In another publication, Cunningham et al. [233] studied the effects of the KPS concentration and the TEMPO/KPS ratio on conversion, molecular weight and particle size in styrene miniemulsion polymerizations. It was found that most characteristics were similar to those for bulk polymerizations, although some unique features for heterogeneous systems were identified. A much higher initiator efficiency (approaching 100% at TEMPO/KPS=4) compared to conventional emulsion and miniemulsion polymerization was also observed, which emphasized the role of aqueous phase TEMPO in deactivating aqueous phase radicals. These results inspired the authors to model these systems in order to gain an even better understanding and to identify the operating conditions for optimal process performance [234, 235]. Ma et al. were the first to model the interfacial mass transfer of TEMPO and they found that phase equilibrium is achieved before TEMPO has an opportunity to react with active polymer radicals, and this is fast enough to maintain phase equilibrium throughout the polymerization [234]. In a second publication [235], they modeled the whole system, and by varying the KPS and TEMPO concentration they were able to find operating conditions at which the polydispersity was minimized and the degree of polymer livingness was maximized. In addition, it was found that the polymerization rate and the degree of livingness could be further im-

Table 17 Different NMCRP miniemulsion systems, with associated references

Nitroxide	T	Monomers	Initiators	Surfactants	Reference
1	125	Sty	BPO	Dowfax 8390	[219, 222]
1	125	Sty	pSty-**1**	Dowfax 8390	[225]
1	135	Sty	KPS	SDBS	[220, 223, 234]
1	135	Sty, BA	pSty-**1**	SDBS	[226]
3	90	Sty	AIBN	SDS	[218, 221]
3	90	Sty	KPS/SPS	SDS	[218, 221, 224]
3	112–120	BA, Sty	**3**-alkoxyamine	SDS/Forafac Dowfax 8390	[227, 229, 230, 231]
1, 2	135	Sty, BA	BPO, KPS	SDBS	[229, 233]
1,4	135	BA	pSty-**1** pSty-**4**	SDBS	[232]
1	125	Sty	pSty-**1**	Dowfax 8390	[217]

proved by increasing the volume fraction of water, although from an industrial point of view this might not be desirable.

The final paper that will be discussed in this section is a kinetic investigation by Pan et al. [216]. They created a series of styrene miniemulsions, using TEMPO-terminated polystyrene, in which they varied the Dowfax 8390 surfactant concentration from 1.25 to 25 mM. Although this had a large effect on the particle size, the effect on molecular weight and polymerization rate was small, while for conventional miniemulsion polymerization the effect of the particle size on polymerization rate is generally very significant. This was explained by the low average number of radicals per particle as a result of the coupling between TEMPO and active radicals, which overwhelms the compartmentalization effect in this case.

All systems discussed are summarized in Table 17.

4.4.2
Atom Transfer Radical Polymerization

4.4.2.1
Mechanism

Atom Transfer Radical Polymerization (ATRP) was first reported in 1995 by Matyjaszewski et al. [236–238] who investigated its potential for copper complexes, and Sawamoto et al. [239–241] who utilized ruthenium complexes. ATRP belongs to a class of living polymerizations known as reversible termination, that includes nitroxide-mediated radical polymerizations (NMRP). They are so named because the growth of the chain is controlled by a reversible termination event where the chain-end is exchanged between an active and dormant species. The lifetime of the active species is very short, such that only a few monomer units are added during each active cycle, giving the reaction its living character.

To induce this reversible termination, ATRP employs a transition metal complex with sufficient redox potential to deactivate propagating radicals. A halide atom, typically Cl or Br, is transferred reversibly (hence the name "atom transfer") to the metal complex. In the process the metal alternates between a lower and higher oxidation state. A general mechanism is shown in Scheme 5.

$$P\text{-}X + M_t^n/L \underset{k_d}{\overset{k_a}{\rightleftarrows}} P^\bullet + X\text{-}M_t^{n+1}/L$$
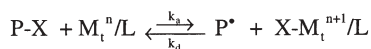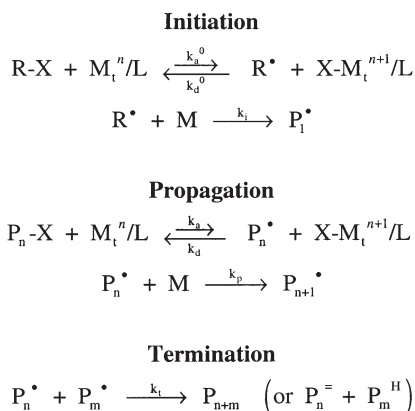
Scheme 5 General ATRP mechanism

The metal undergoes a one-electron oxidation with the simultaneous abstraction of the halogen, generating radicals via a reversible redox process. The success of the process depends upon the fact that the equilibrium is shifted heavily in the direction of the dormant species. While complexes of copper and ruthenium have been most widely studied, complexes of nickel, palladium and iron can also be used [242–244]. Molybdenum, rhenium and rhodium ATRP have also been reported [245–247]. ATRP reactions are very well behaved and can easily produce polymers of controlled molecular weight and narrow polydispersity. Most classes of monomers have been successfully polymerized via ATRP. These include styrenes, (meth)acrylates, (meth)acrylamides, dienes, acrylonitrile and other monomers containing radical stabilizing substituents [248, 249]. Ring-opening polymerizations are also possible with ATRP [250, 251]. The initiators used are typically alkyl halides, but any compound with a weak halogen-heteroatom bond will suffice. The halogen end-group has the advantage of offering the ability to add functionality to the polymer.

In general, reaction rates in ATRP are slower than conventional free radical polymerizations. The unique nature of the ATRP equilibrium, which is shifted strongly towards the dormant species, effectively lowering the active, propagating radical concentration as compared to the conventional analog, is the source of the lower rates. This can be overcome to a certain degree by adjusting the metal/ligand ratio or through the use of additives [252–254]. Another factor contributing to the rate is that each bimolecular termination event releases two metal complexes in the higher oxidation state. As such, a shift in equilibrium in order to increase the propagation rate results in increased termination and an increase in the concentration of the complex in the higher oxidation state. The system tends to self-regulate and maintain the rate of polymerization. ATRP with transition metal complexes is extremely sensitive to oxygen owing to its reliance on the redox reaction between the halide and the metal complex. Reactions must be conducted in an inert environment or the metal will oxidize, effectively killing the polymerization. Because the quantity of metal complex required is relatively large and much of it will remain in the polymer, its residue must be removed for both environmental and economic reasons.

Although ATRP behaves differently from conventional free radical polymerization, the fundamental reactions involved are very similar and include initiation, propagation, transfer and termination (see Scheme 6). Since chain termination does not occur in a truly living polymerization, the "living" character of the chains in ATRP derives from the fact that chain propagation is first order with respect to radical concentration and irreversible bi-molecular termination is second order. As such, the concentration of the radicals is kept very low, the rate of bi-molecular termination is greatly reduced, and typically less than 10% of all of the chains will terminate. Unlike conventional free radical polymerization, where the rate is dictated by a steady state between the initiation and termination rates, the rate and concentration of propagating radicals in ATRP is controlled entirely by the equilibrium between activation and deactivation [255].

Initiation

$$R\text{-}X + M_t^n/L \xrightleftharpoons[k_d^0]{k_a^0} R^{\bullet} + X\text{-}M_t^{n+1}/L$$

$$R^{\bullet} + M \xrightarrow{k_i} P_1^{\bullet}$$

Propagation

$$P_n\text{-}X + M_t^n/L \xrightleftharpoons[k_d]{k_a} P_n^{\bullet} + X\text{-}M_t^{n+1}/L$$

$$P_n^{\bullet} + M \xrightarrow{k_p} P_{n+1}^{\bullet}$$

Termination

$$P_n^{\bullet} + P_m^{\bullet} \xrightarrow{k_t} P_{n+m} \left(\text{or } P_n^{=} + P_m^{H} \right)$$

Scheme 6 Fundamental ATRP reactions

The initiators used are typically alkyl halides with similar structures to that of the monomer being employed. Of the halogens, chlorine and bromine have been shown to produce the best overall results with respect to molecular weight control [256]. However, iodine works well in certain cases, for example, rhenium-mediated styrene polymerizations [246] and copper-mediated acrylate polymerizations [257]. The C–F bond with fluorine is too strong to cleave homolytically, ruling out its use as an effective initiator. In general, any alkyl halide with activating substituents on the α-carbon (aryl, carbonyl or allyl groups) can act as an ATRP initiator. In addition, polyhalogenated compounds (like CCl_4 or $CHCl_3$) and compounds with a weak R–X bond (like N–X, S–X) can also be used.

There are several requirements that are generally recognized as essential to an effective ATRP catalyst [256, 258, 259, 260]. The metal center should be able to assume at least two oxidation states, separated by one electron, like Cu(I) and Cu(II). It should also be attractive to halogens, it should possess an expandable

coordination sphere such that when oxidized it can contain the halogen, and it should have a low affinity for alkyl radicals and the hydrogen atoms on alkyl groups.

Conventional free radical polymerizations in miniemulsions benefit kinetically from the effects of radical segregation. In solution, any radical could terminate with another theoretically. However, when the radicals are segregated into isolated reaction loci (such as miniemulsion droplets or particles) termination is no longer possible. Because the total concentration of radicals is distributed throughout the particles, the probability that any two radicals will terminate bi-molecularly is greatly reduced. The ideal situation is one in which a lone radical in a particle can terminate only with a radical that enters the particle. This is known as the "zero-one" limit [121], and in this case the rate of bimolecular termination is controlled by radical entry alone. In the absence of other effects, this lowering of the incidence of bi-molecular termination events tends to increase the overall rate of polymerization while simultaneously narrowing the molecular weight distribution. However, because of the mechanism involved, the same benefit is not seen with ATRP in miniemulsion. With ATRP, the dominating rate-controlling factor is the equilibrium between the dormant and active species. Since the equilibrium heavily favors the dormant species, the lifetime of the active species is extremely short. As such, the concentrations of these active radicals are always minute [261]. Therefore, the probability that a water phase radical will enter a particle containing another radical and terminate is exceedingly low. Any kinetic benefit that might otherwise be gained from segregation is overshadowed by this low radical concentration. It should also be noted that, because of the ATRP mechanism, increases in reaction rate, whatever their origin, will come at the expense of the deactivator species. The resulting decrease in the concentration of deactivator tends to produce broader polydispersities.

4.4.2.2
Results

There are few reported instances of ATRP in miniemulsion in the current literature. Matyjaszewski [262] and co-workers employed both forward (direct) and reverse-ATRP of n-butyl methacrylate in miniemulsion stabilized with a non-ionic surfactant, polyoxyethylene(20) oleyl ether (Brij 98), and using 4,4′-di(5-nonyl)-4,4′-bipyridine (dNbpy) with either CuBr or CuBr$_2$. They looked at the effects of using both oil and water-soluble initiators (AIBN and 2,2′-azobis(2-methylpropionamidine) dihydrochloride, or V-50) with the reverse process. With AIBN, the final polydispersity was relatively narrow (~1.4) but increased with conversion. Also, the number average molecular weight began higher than predicted and exhibited some curvature. This was attributed to slow decomposition of the AIBN, causing a slow and less quantitative formation of chains. Polydispersities were slightly lower with the V-50 and the number average weight progressed linearly with conversion, although the over-

all rate was much slower than with AIBN. Additionally, the progression of M_n, though linear, was much higher than found theoretically. In this case, the initiator decomposed faster but the radicals formed tended to terminate in the aqueous phase, contributing both to the slower overall rate and the higher than predicted actual molecular weights. The authors performed direct ATRP with an oil-soluble initiator, ethyl 2-bromoisobutyrate (EB*i*B). At a lower temperature than the reverse process, 70 °C vs 90 °C, the polymerization rate of the direct process was significantly faster. The polydispersity remained relatively flat throughout the experiment, with a final value of approximately 1.3. The molecular weight evolution, though roughly linear, was higher than predicted. Additionally, a semilog plot of the conversion data revealed some curvature, indicating a larger than expected number of chain termination events. It was postulated that the cause lay in the partitioning of the Cu(II) species into the aqueous phase. Recent studies with ATRP in aqueous dispersions lend credence to this argument [263]. They observed that the polymerization rate was insensitive to the size and number of particles and controlled entirely by the atom transfer equilibrium. The researchers also studied the effect of removing the costabilizer, hexadecane, from the recipe in order to determine if the hydrophobic dNbpy ligand alone would act as a sufficient droplet stabilizer. However, it was noted that the droplet size increased dramatically in the absence of hexadecane, indicating that the osmotic pressure would be insufficient to prevent Ostwald ripening.

Li and Matyjaszewski [264], building on the earlier work mentioned here [262], conducted reverse ATRP in miniemulsions using *n*-butyl methacrylate (BMA) with a more active catalyst system and a faster initiator. The solids content was roughly double that of the previous effort, jumping from approximately 13% to over 20%. More importantly, the surfactant (Brij 98) concentration was reduced from 13.5%wt to 2.3%wt based on monomer, decreasing the likelihood of micellar nucleation. Because of their high activities in bulk and solution ATRP, complexes of hexasubstituted tris(2-aminoethyl)amine (TREN) with Cu/Br_2 were utilized as the metal activator/deactivator. The water-soluble initiator used was 2,2′-azobis[2-(2-imidazolin-2-yl)propane] dihydrochloride (VA-044). The VA-044 was chosen for its fast decomposition rate, which facilitates a well-controlled ATRP and contributes to colloidal stability. The authors looked at the effect of the ligand and noted that there was no induction period with the TREN ligand as compared to dNbpy. While linear progressions of M_n with conversion were seen, the authors found that the molecular weight was not quantitative in initiator concentration. Instead M_n tended to be much higher than that calculated based on the initiator concentration and more closely followed a trajectory calculated from the initial concentration of deactivator, Cu(II). Assuming 100% initiator efficiency, the authors explain the deviation in terms of an excess radical concentration over the concentration of Cu(II), leading to the generation and subsequent termination of some of the oligomeric chains. Since a 1:1 molar ratio of $[Cu(II)]_0/[I]_0$ was used in most of the experiments, in theory there would be two initiator radicals for every

molecule of Cu(II) deactivator very early on in the polymerization. Many of the radicals would indeed quickly terminate until their concentration reached low enough levels that bi-molecular termination was insignificant compared to deactivation and they no longer competed for Cu(II). When a 2:1 ratio of $[Cu(II)]_0/[I]_0$ was employed, marginally better control of M_n was observed and the progression still tended to follow that calculated based upon $[Cu(II)]_0$, leading the authors to conclude that higher levels of Cu(II) would be needed for polymerizations that provide better control of M_n and relatively low polydispersities. The effect of surfactant concentration was studied using several nonionic surfactants in addition to Brij 98. The principal finding was that at higher surfactant concentrations (>13 wt% based on monomer), bi-modal molecular weight distributions and bi-modal particle size distributions of the latex were observed, indicating micellar and droplet nucleation. By increasing the initiator concentration and lowering the deactivator concentration, the authors also demonstrated that the kinetics of the polymerization are controlled primarily by the atom transfer equilibrium.
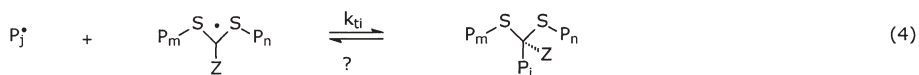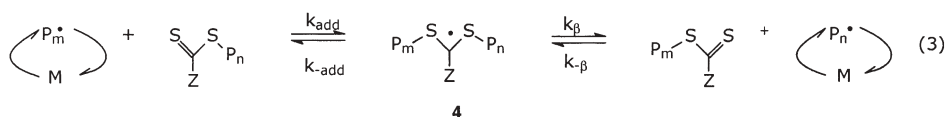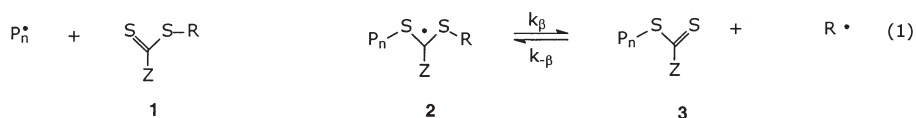
4.4.3
Reversible Addition Fragmentation Polymerization

4.4.3.1
Mechanism

The third (and also the most recently developed) controlled free radical technique discussed in this review is RAFT. In 1998 Rizzardo et al. published a novel "controlled" free-radical polymerization technique, which they designated the RAFT process [265–267] because the mechanism involves Reversible Addition-Fragmentation chain Transfer. This technique allowed the production of polymer with a narrow molecular weight distribution. In fact, this concept was not entirely new, and stemmed from the same researchers' previously published work to produce block copolymers using methacrylate macromonomers as reversible addition-fragmentation chain transfer agents in 1995 [268]. However, these macromonomers were not very effective RAFT agents. The breakthrough came with the discovery of a more reactive double bond species, S=C(Z)SR. During styrene polymerization, the propagating radicals were very reactive to the dithioesters and to a much lesser extent to the xanthates [269]. A brief description of the RAFT process is given below, and a schematic representation is given in Scheme 7.

A conventional free-radical initiator is added (contrary to some other controlled free-radical polymerization techniques) that generates radicals, which can add either to the monomer or the S=C moiety of the RAFT agent (step 1). In most cases the addition of small carbon-centered radicals to the RAFT agent is rapid and is not rate determining. Therefore, step (1) involves polymeric radical addition to **1** to form an intermediate radical species **2** that will fragment back to the original polymeric radical species or fragment to a dormant species **3**

$$P_n^\bullet \;+\; \underset{Z}{\overset{S}{\diagdown}}\!\!\diagup\!S{-}R \qquad \longrightarrow \qquad P_n{-}\underset{Z}{\overset{S}{\diagdown}}\!\!\overset{\bullet}{\diagup}\!S{-}R \quad \underset{k_{-\beta}}{\overset{k_\beta}{\rightleftharpoons}} \quad P_n{-}\underset{Z}{\overset{S}{\diagdown}}\!\!\diagup\!S \;+\; R^\bullet \qquad (1)$$

$$\mathbf{1} \qquad\qquad\qquad\qquad \mathbf{2} \qquad\qquad\qquad\qquad \mathbf{3}$$

$$R^\bullet \;+\; M \quad \xrightarrow{\;k_p^{\,1}\;} \quad P_1^\bullet \qquad\qquad\qquad\qquad\qquad\qquad\qquad\qquad\qquad (2)$$

$$\underset{M}{\overset{P_m^\bullet}{\bigcirc}} \;+\; \underset{Z}{\overset{S}{\diagdown}}\!\!\diagup\!{}^{S}\!P_n \quad \underset{k_{-add}}{\overset{k_{add}}{\rightleftharpoons}} \quad P_m{-}\underset{Z}{\overset{S}{\diagdown}}\!\!\overset{\bullet}{\diagup}\!{}^{S}\!P_n \quad \underset{k_{-\beta}}{\overset{k_\beta}{\rightleftharpoons}} \quad P_m{-}\underset{Z}{\overset{S}{\diagdown}}\!\!\diagup\!S \;+\; \underset{M}{\overset{P_n^\bullet}{\bigcirc}} \qquad (3)$$

$$\mathbf{4}$$

$$P_j^\bullet \;+\; P_m{-}\underset{Z}{\overset{S}{\diagdown}}\!\!\overset{\bullet}{\diagup}\!{}^{S}\!P_n \quad \underset{?}{\overset{k_{ti}}{\rightleftharpoons}} \quad P_m{-}\underset{\underset{P_j}{|}}{\overset{S}{\diagdown}}\!\!\overset{S}{\diagup}\!P_n \qquad\qquad (4)$$

Scheme 7 Schematic representation of the proposed RAFT mechanism. It should be noted that in these equilibria any radical can react with any dormant species or RAFT agent. (1) Addition of a propagating polymeric radical to the initial RAFT agent **1**, forming the intermediate radical **2**. The intermediate radical can either fragment into the two species it was formed from or into a dormant polymeric RAFT agent **3** and a small radical R$^\bullet$. (2) The small radical initiates polymerization, forming a polymeric radical, rather than reacting with **3** (reforming **1**). Therefore R should be a good leaving group and should have the ability to be added to the monomer. (3) Equilibrium between propagation polymeric radicals and dormant polymeric RAFT agents. (4) Intermediate radical termination

and a small radical, R$^\bullet$. R$^\bullet$ can then further propagate to form a polymeric radical (step 2 in Scheme 7), rather than adding to **3**. The dormant polymeric RAFT agent acts in a similar way to a RAFT agent, so growing polymeric radicals can also add to the dithiocarbonyl double bond of the polymeric RAFT agent, thereby forming an intermediate radical **4**. This intermediate has an equal probability of fragmenting back into its starting species or into a dormant polymeric RAFT agent and a polymeric radical, in which the dithiocarbonate moiety has been exchanged between the active and dormant polymer chains of the starting species. This equal probability of fragmenting to either side of the equilibrium is a result of the symmetry of **4**. There might be a difference in the chain length of both sides, but this will not have an effect, unless one of the two sides is extremely short. This mechanism of addition of radicals to the dithiocarbonyl double bond and fragmentation of the intermediate was shown by Moad et al. [270], who observed the intermediate radical directly by ESR.

Overall, polymer chains with a dithiocarbonate end-group are formed. If addition to the dithiocarbonyl double bond is fast compared to propagation,

and termination is suppressed by keeping the radical concentration low, all of the chains will grow in a sequential process, leading to a low polydispersity. The number of chains is determined by the amount of RAFT agent and initiator that has been consumed. Assuming termination by combination, the number of dead chains will be equal to the amount of initiator that is consumed. The number of chains with a dithiocarbonate end-group, the dormant chains, is equal to the amount of consumed RAFT agent. One should therefore keep the initiator to RAFT agent ratio low in order to obtain a high percentage of dormant chains. This criterion is especially important in the preparation of block copolymers [271–273].

In fact, the RAFT process resembles the degenerative transfer (DT) process [274]. In a polymerization in which an alkyl iodide is used as the degenerative transfer agent, the iodine atom is exchanged between a polymeric radical and a dormant chain, similar to the dithiocarbonate exchange in RAFT. However, in the case of degenerative transfer there is a direct equilibrium between the dormant and growing chains, without formation of an intermediate radical.

If reactions 1 to 3 in Scheme 7 are considered, there is no reason to assume that addition of a RAFT agent to a conventional free radical polymerization will have an effect on the polymerization rate, since the equilibrium concentration of propagating radicals will not be affected. However, it has been found that considerable retardation does take place in RAFT polymerization [275–281]. The intermediate radical was postulated to be the reason for the significant retardation of the polymerization rate. Two explanations for retardation have been put forward:

(i)   slow fragmentation of the intermediate radical [277–280]
(ii) termination of the intermediate radical (reaction 4 in Scheme 7) [275, 276, 281]

The key variable in both explanations is the fragmentation rate constant. There is a difference of six orders of magnitude between the fragmentation rate constants obtained via explanations (i) and (ii). The question of which explanation is correct has been hotly debated for over three years, but is still unresolved.

4.4.3.2
Effects of RAFT and Transfer Agents on Emulsion Polymerization Kinetics

As far back as 1948, Smith and Ewart [13] included the effects of radical desorption in emulsion polymerization kinetics, and in 1965 Romatowski et al. [282–284] showed that radicals resulting from chain transfer to monomer indeed escape from the particles.

Nomura et al. [285] and Lichti et al. [286] studied the effects of transfer agents on the kinetics of ab initio and seeded emulsion polymerization of styrene, respectively. Nomura et al. found that the polymerization rate per particle decreased with increasing amounts of carbon tetrachloride, carbon tetrabromide and primary mercaptans, and that the effects were stronger when

the transfer constant or the water-solubility was higher. Lichti et al. observed the same in seeded experiments with carbon tetrachloride and carbon tetrabromide as chain transfer agents. They were the first to actually measure the exit rate coefficient, using γ-radiolysis relaxation data. They found an increasing exit rate coefficient with increasing amounts of transfer agents and a higher exit rate coefficient when the transfer constant was higher. They also found that the entry rate coefficient increased with increasing amounts of carbon tetrabromide. Due to the counterbalancing effects of an increased exit rate and an increased entry rate the polymerization rate passed through a minimum.

Maxwell et al. [287] extended their own model for entry by taking the effect of transfer agent into account and used this model to explain the increase observed in emulsion polymerizations with monomers with a high critical chain length z and thiols of intermediate chain length. They also used this model to show that longer chain thiols are too water-insoluble to have an effect and that short chain thiols might suffer aqueous phase termination and increase the exit rate, and so they can reduce the polymerization rate instead of increasing it. No effect was expected for styrene from Maxwell's model, which was confirmed by the work of Asua et al. [288]. They found that n-dodecyl mercaptan had no effect on the polymerization rate.

The work of Monteiro et al. [289] showed that when RAFT agents are applied in emulsion, the rate of polymerization is significantly retarded. This effect is stronger when a RAFT agent with a more water-soluble leaving group is used. Exit from the particles after fragmentation was proposed to be the main reason for the observed retardation. Because of the high reactivity of the RAFT agents used, it is expected that all of the RAFT agent is consumed after a few percent conversion, and so it should no longer should have an effect. However, it was observed that the rate of polymerization decreased with increasing RAFT in interval II. Monteiro et al. claimed that this was due to transport limitation of RAFT from the monomer droplets to the particles, meaning that there is a constant flux of RAFT agent to the particles, even if all of the RAFT agent has been consumed in the particles. Therefore, not all of the chains start to grow simultaneously, resulting in broad polydispersities. However, retardation was also observed in Interval III, and this could not be ascribed to exit and transport limitations. When this work was published, intermediate radical termination [275, 276] had not yet been put forward by Monteiro et al. as a source of retardation. However, since the system might not be under zero-one conditions in Interval III due to the increased particle size, intermediate radical termination might explain these results.

Another observation Monteiro et al. made was that a red layer was observed during Interval II, consisting of low molecular weight dormant chains, swollen with monomer. At the crossover to Interval III, this red layer coalesced, forming red coagulant. The same red layer was also observed by De Brouwer et al. [290] in miniemulsions stabilized with ionic surfactants. When polymer was used as the so-called cosurfactant, this polymer was not present in the red layer, indicating that this layer was not due to droplet coalescence. Also, the use of an

oil-soluble initiator did not reduce the formation of the red layer. Using a higher radical flux (to enhance droplet nucleation) did not have an effect. Indeed, the formation of the red layer was correlated to the polymerization rate, which indicates that the product formed during the polymerization plays a crucial role in the destabilization. However, when nonionic surfactants were used, destabilization did not occur, and controlled miniemulsion polymerizations could be performed without destabilization. Later, Luo et al. suggested that the instabilities are the result of the large number of oligomers formed in the early stages of RAFT miniemulsions, causing a superswelling state [128], which could be prevented by increasing the amount of cosurfactant.

Moad et al. [291] showed that the type of RAFT agent is important. Using a very reactive RAFT agent (with a transfer constant of about 6000), similar to that used in the work of De Brouwer and Monteiro, resulted in a broad polydispersity in ab initio styrene polymerizations with ionic surfactant, which was ascribed to the fact that the RAFT agent was not uniformly dispersed in the polymerization medium. The use of less reactive RAFT agents (with transfer constants of 10–30) did not result in destabilization and the final polymer had a polydispersity close to 1.4.

Prescott et al. [292] used acetone to transport a water insoluble RAFT agent to the seed particles. The polymerization was initiated in Interval III after removing the acetone. No destabilization was observed, which according to our previous discussion might indicate that the transfer constant of the RAFT agent used was not extremely high. However, it was high enough to result in a linear increase in molecular weight, and polydispersities between 1.2 and 1.4. Although the RAFT agent is consumed at the beginning of the reaction (the molecular weight follows the theoretical linear increase), a reduction in rate is observed throughout the reaction. In these experiments, a small seed was used and the amount of monomer was such that the particle size does not increase much, which means that the system is likely to be under zero-one conditions throughout the polymerization and so intermediate radical termination cannot explain the retardation observed.

Monteiro et al. [293] also studied the effect of xanthates (RAFT agents with low transfer constants) with styrene, in ab initio styrene polymerizations. Again rate retardation was observed throughout the polymerization. This is not surprising, since the low transfer constants of these RAFT agents mean that they are present during the whole polymerization, which results in an increased exit rate throughout the reaction.

This was later confirmed by Smulders et al. [294], who experimentally determined the exit rate in similar systems using γ-relaxation experiments. The exit rate was found to increase linearly with the RAFT concentration, although the decrease in rate could not be ascribed to the increase in exit rate alone.

Summarizing, we know that RAFT can be applied in emulsion, although the mechanism for this is not yet fully understood. Highly reactive RAFT agents can lead to destabilization, although the use of nonionic surfactants seems to prevent this destabilization. Rate retardation is observed in all cases. This can

be partly ascribed to the increased exit rate, although the retardation is still observed even when all of the RAFT agent has been consumed. In that case, intermediate radical termination might explain the reduction in rate. However, even when the system is under zero-one conditions and all RAFT is consumed, retardation still occurs. This cannot be ascribed to intermediate radical termination or to exit. In fact, an explanation for this might be quite simple, as shown by Smulders [295]. Retardation with RAFT in zero-one systems in which all of the RAFT has been consumed cannot be ascribed to increased exit rate anymore, since the leaving groups of the dormant polymer chains cannot exit. Intermediate radical termination is also not a dominant mechanism, since each particle contains only one radical. However, the fact that each particle contains only one radical explains why retardation is observed in these systems. This one radical is either present as a "normal" radical, $R^\bullet$, capable of propagating and so consuming monomer, or as a "intermediate" radical, $I^\bullet$. While the radical is in the intermediate state it does not consume monomer, which in turn leads to retardation. Since the system is under zero-one conditions, the system does not reach steady state at the microscopic level (inside a particle), because a particle contains either no radical, one "normal" radical, or one "intermediate" radical. The lifetimes of $R^\bullet$ and $I^\bullet$ are given by:

$$\tau_{R^\bullet} = \frac{1}{k_{add}[dormant\ chains]} \quad \tau_{I^\bullet} = \frac{1}{2k_{-add}} \tag{19}$$

Using the rate parameters for dithiobenzoate RAFT polymerization of styrene at 70 °C, as reported by Monteiro et al. [275] ($k_{add}=4\times10^6$ dm^{3}mol^{-1}s^{-1}, $k_{-add}=1\times10^5$ s^{-1}), and a dormant chain concentration of 0.06 M, this results in a lifetime of 4.2×10^{-6} s for a "normal" radical, and a lifetime of 5.0×10^{-6} s for an intermediate radical. This means that the fraction of time that a radical is present as a propagating radical in this system is $4.2\times10^{-6}/(4.2\times10^{-6}+5.0\times 10^{-6})=0.46$. This also means that the polymerization rate in this example would only be 46% of the polymerization rate without RAFT. The mechanism proposed by Monteiro et al., which included intermediate radical termination, was supported by Fukuda et al. [281, 296]. However, the latter authors proposed a value of k_{dd} on the order of 10^4 s^{-1}. Following the same pathway, this value means that the polymerization rate with RAFT is only 7.7% of the rate without RAFT in a zero-one system. Since no good experimental data is currently available for zero-one emulsion systems with dithiobenzoate RAFT agents, at the moment no definitive statement can be made about which value of the fragmentation rate constant best describes a zero-one system. However, these results indicate that zero-one experiments can be a useful tool for determining this rate parameter, and they provide data useful as we attempt to pinpoint the correct value for the fragmentation rate constant (see previous section). Davis et al. fitted conversion-time data for a styrene polymerization with RAFT at 60 °C using $k_{add}=5.4\times10^5$ dm^3 mol^{-1} s^{-1} and $k_{-add}=3.3\times10^{-2}$ s^{-1}. For a zero-one system with 1 mol% RAFT, these values would lead to $t_{R^\bullet}=3.1\times10^{-5}$ s and

$t_{I^\cdot}$ =15.2 s. This means that zero-one polymerization should not proceed, because the radicals are present as intermediate radicals for more than 99.99% of time. Since we have experimental evidence that RAFT systems do proceed under zero-one conditions [292], these rate parameters seem highly unlikely, although it should be noted that Prescott et al. used a RAFT agent with a less stable intermediate. Zero-one experiments with dithiobenzoate RAFT agents might be the key to closing the "six-orders-of-magnitude-gap" for the fragmentation rate constant.

4.4.3.3
Application of RAFT in Miniemulsion

As with nitroxide-mediated polymerizations and ATRP, and with RAFT, miniemulsion systems are often preferred over conventional emulsion systems, although not as exclusively as with NMCRP and ATRP. In this section we will discuss some applications of RAFT in miniemulsions.

In 2000, Moad et al. reported the synthesis of controlled polystyrene using RAFT in miniemulsion [291]. Using phenyl ethyl dithiobenzoate in a SDS/cetyl alcohol stabilized system at 70 °C, 25% conversion was obtained in four hours, while a control experiment without RAFT reached 82% conversion in one hour. Molecular weight increased with conversion and the polydispersity went down to 1.18. No problems with stability were reported. On the other hand, De Brouwer et al. [290] and Tsavalas et al. [296] were unable to obtain stable latexes using dithiobenzoate RAFT agent in either anionic- or cationic-stabilized miniemulsions. They reported the formation of a red organic layer on top of the miniemulsion as soon as the polymerization started. This layer consisted of low molecular weight polymer and monomer. Luo et al. later ascribed the observed phenomena to a superswelling state, caused by the large number of oligomers formed at the beginning of the polymerization [128]. However, when nonionic surfactants like Igepal 890 and Brij 98 were used by Brouwer et al. [290], they could perform stable RAFT miniemulsion polymerizations. Miniemulsion polymerizations of EHMA, STY, MMA, BMA, and MA all resulted in stable latexes with polydispersities below 1.4, and sometimes as low as 1.1, at very high conversions. When the miniemulsions formed were used as seed latexes in either batch or semi-batch polymerization with a second monomer, block copolymers with a low polydispersity and a high level of block purity were obtained.

Butté et al. [261] were able to perform miniemulsion polymerizations stabilized with SDS and hexadecane using dithiobenzoate and "pyrrole" RAFT agents. In most cases oligomerized RAFT agents were used, but "monomeric" RAFT agents were also applied successfully. Although they used basically the same systems, Butté et al. did not observe the red layer formation reported earlier by De Brouwer and Tsavalas. Linear molecular weight growth and relatively narrow polydispersities were reported, although they were broader than for bulk polymerizations. This was ascribed to the presence of dead chains in the oligomers and differences in miniemulsion droplet sizes, leading to dif-

ferences in monomer-to-RAFT ratios. Smaller particles have a larger surface/volume ratio and are therefore preferentially entered by z-mers, leading to monomer consumption in these particles which is replaced by monomer from the larger particles.

Butté found that the polymerization rate decreased with RAFT. This was supposed to be the result of an increasing exit rate. However, even when oligomeric RAFT agents were used, which should not lead to an increased exit rate, a decrease in rate was observed, which was ascribed to the presence of "monomeric" RAFT agent in the oligomer mixture. Finally, Butté reported the synthesis of block copolymers in miniemulsion by adding styrene to a fully polymerized MMA miniemulsion and by adding BA to a 63% polymerized styrene miniemulsion. In both cases it was shown that block copolymer was formed, although polydispersities were relatively high.

In order to prevent the formation of the red layer observed by De Brouwer and Tsavalas, Vosloo et al. performed SDS-stabilized miniemulsion polymerizations of styrene using pre-formed dithiobenzoate-end-capped styrene oligomers, formed in bulk [297]. Two types of cosurfactant (hexadecane and cetyl alcohol) and two oligomers with different molecular weights were used. Red layer formation was not observed in any of the miniemulsion polymerizations, and the results were better – lower polydispersities, and molecular weights that were closer to the theoretical values – when hexadecane and the lower molecular weight oligomers were used.

Lansalot et al. studied the influence of the structure of the RAFT agent on styrene miniemulsion polymerization [298]. The use of 1-phenylethyl phenyldithioacetate (PEPDTA) was compared to cumyl dithiobenzoate (CDB) and 1-phenylethyl dithiobenzoate (PEDB). It was shown that PEPDTA did not show retardation in bulk experiments, while CDB and PEDB show a large decrease in rate with increasing RAFT concentration. This was ascribed to the less stable PEPDTA macroRAFT radical. When the same RAFT agents were used in styrene miniemulsion polymerizations, stabilized by SDS/hexadecane, again the PEPDTA showed much higher polymerization rates than CDB and PEDB. However, in contrast to the bulk experiments with PEPDTA, a decrease in rate with an increase in RAFT was observed in the miniemulsion. This was ascribed to the exiting of radicals formed after addition and the fragmentation of the initial RAFT agent. This was confirmed by miniemulsion polymerization experiments performed using oligomerized PEPDTA, where the leaving radical cannot exit to the aqueous phase. In that case, using the same concentration as in the experiment with "monomeric" PEPDTA, the polymerization rate dramatically increased to almost the same polymerization rate as without RAFT.

4.4.4
Colloidal Stability

After being frustrated by poor colloidal stability (phase separation or coagulation) in controlled macroemulsion polymerization (NMP, ATRP, RAFT), re-

searchers turned to living miniemulsion polymerization [299–304]. It was expected that the colloidal stability should be improved in living miniemulsion polymerization on the premise that molecular weight controlling agents (RAFT agent, nitroxide, and ATRP catalyst) do not need to be transferred from the monomer reservoir to the polymerization loci. However, this strategy only gave limited success. Problems included loss of colloidal stability, large particle size, broad particle size distributions, and irreproducible particle sizes were observed [221, 222, 226, 296, 305–307]. It is evident the stabilization of colloids during living polymerization is more difficult than during regular miniemulsion polymerization. The stability of latex seems to be sensitive to the recipe. Georges and co-workers [222, 307] reported that, for the styrene miniemulsion polymerization of TEMPO-mediated living polymerization, when the surfactant concentration was reduced from 1.4%wt to 0.7%wt but the HD was kept constant at 3 wt%, the system could be made stable. In an effort to commercialize nitroxide-mediated miniemulsion polymerization, Georges [226] proposed a modified miniemulsion SFRP process in which TEMPO-terminated polystyrene oligomers were used to initiate the polymerization with 10 wt% HD and 6.7 wt% sodium dodecylbenzenesulfonate (surfactant), yielding polymers that have a high degree of livingness and stable latex. Charleux [223] found that about 5 wt% hexadecane is needed for ST miniemulsion SFRP to get stable latex, but with n-butyl acrylate, the proportion of HD must be decreased to less than 1 wt%. For butyl acrylate SFRP in miniemulsion, it has been reported that the particle size is not reproducible [226]. The El-Aasser group reported successful miniemulsion polymerization that employed nitroxides with controlled molecular growth and good miniemulsion stability [221]. It is interesting to note that the level of costabilizer was more than 5%wt, far more than the typical 2%wt. Even so, El-Aasser's particle size is much larger than the non-living counterpart, and the particle size distribution is much broader. In the next paper of the El-Aasser group [308], TEMPO-terminated oligomers of polystyrene were prepared via bulk polymerization of styrene, and they were used as initiator in miniemulsion polymerization. The stable latexes were obtained with 3 wt% HD and smaller particles. The Matyjaszewski group [309] studied ATRP-controlled free radical miniemulsion polymerization and found that using either anionic (SLS) or cationic (dodecyltrimethylamomonium bromide) surfactant led to instability. It was argued that the catalyst may interfere with SLS, while no reason was given for the instability of dodecyltrimethylamomonium bromide. The final particle size was more than 1 μm in the normal ATRP polymerization of butyl methacrylate, and more than 250 nm in reverse ATRP. It has been reported that the use of nonionic polymeric surfactant improved the stability. Also, the longer the PEO segment in the surfactant, the better the stability. In the case of Tween 20, a portion of the monomer phase separated, forming small pools in the reaction mixture, but these would dissipate as the polymerization progressed, and there was no coagulation of polymer at higher conversion. In another ATRP paper by Matyjaszewski et al. [262], dNbpy, nonionic Brij 98, hexadecane, and the water-soluble azo com-

pound 2,2′-azobis (2-methylpropinonamide) dihydrocholoride (VA-50), were used as ligand, surfactant, costabilizer, and initiator, respectively. The resulting latexes showed improved stability. It is worth noting that a large amount of surfactant (5.0%wt, 13.5%wt based on monomer) and HD (1/10 [v/v monomer]) was used but particle sizes are large too (around 300 nm). In the most recent paper by the same group [264], it was reported that the amount of Brij 98 and HD can be reduced to 2.3%wt and 3.6%wt, respectively, by replacing VA-50 by the more reactive VA-44, and replacing dNbpy by hydrophobic hexa-substituted TREN with high catalytic activity, which gives polymerization with good colloidal stability and particle sizes of 200–250 nm. De Brouwer et al. [296, 305] reported stability problems in controlled free radical miniemulsion polymerization using RAFT. It was reported that when an ionic surfactant (either cationic or anionic) was used, a monomer bulk phase constituting up to 35% of the total organic material in the system could be observed at low monomer conversion. The phenomenon can be seen with various different monomers, different initiator systems, and different costabilizers. Sanderson [310] also reported these instability issues at less than 5 wt% SDS. De Brouwer et al. [305] found that when nonionic surfactant is used, the polymerization is well controlled in terms of molecular weight, and the colloidal stability is good. However, both Butté et al. [261] and Lansalot et al. [298] did not report any instability issues in RAFT miniemulsion polymerization. In Butté's work, 3.3%wt HD and 1.67%wt SDS was employed. The miniemulsion were prepared by a three-step approach: after mechanical preemulsification for 10 minutes and sonication for 20 minutes, the mixture was passed into a microfluidizer ten times. No colloidal characteristics were reported. In Lansalot's work, 2%wt hexadecane, 1%wt PST, and 0.01 mol/L water SLS were used. The miniemulsion was prepared by ultrasonication for a period of 7 minutes at 35% amplitude, 30–35 W power, in a Branson 450 sonicator. In Lansalot's work, although stable latex was obtained, the particle size was much bigger than the corresponding non-living system (except when oligomeric RAFT agent was used), and particle size distribution was broad. This seems to indicate that miniemulsification procedure plays some role in obtaining stable latex. To avoid colloidal instability, Sanderson [310, 311] successfully developed two approaches based on the predictions of Luo's theory [128]:

a. Form RAFT-endcapped oligomers in bulk, dissolve the RAFT agent into the monomer, then disperse the monomer into water under shear with surfactant and costabilizer, and recommence polymerization.
b. Use high surfactant concentrations (10%wt with respect to monomer), and high costabilizer (*n*-HD) concentration (>4%wt with respect to monomer).

From the above summary of experimental investigations into living miniemulsion polymerization, we can see that controlled miniemulsion polymerization (SFRP, ATRP, and RAFT) is less colloidal-stable during polymerization than its non-living counterpart. Colloidal instability leads to phase separation in the worst cases. In improved cases, the latex that results from the controlled mini-
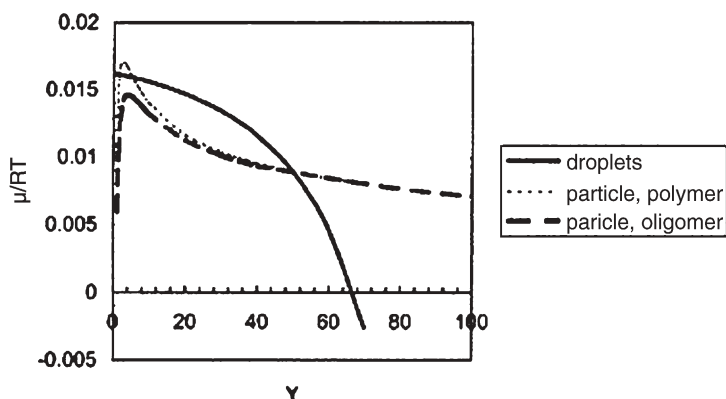
emulsion polymerization has much bigger particle size and much broader particle size distribution than that obtained using regular miniemulsion polymerization. One can also see that colloidal instability is very sensitive to the polymerization recipe. Monomer, surfactant, dormant agent, and levels of surfactant and costabilizer all have large influences on the stability. High levels of surfactant and costabilizer, and use of a nonionic surfactant and an oligomeric control agent all proved to aid stability, although larger particle sizes and broader particle size distributions were still seen. On the other hand, the literature indicates that instability is a general problem in controlled free radical miniemulsion polymerization, regardless of the living control mechanism, monomer, surfactant system (except for polymeric surfactant), or initiator system. It seems reasonable to assume that the instability is caused by the "living" nature of the systems. In a controlled free radical polymerization system, the kinetics of polymer chain formation is totally different from that for classical free radical polymerization. In classical free radical polymerization, a polymer chain is fully polymerized in about 1 s. At the very beginning of polymerization, a few polymer chains of high molecular weight are formed. During polymerization, monomer is consumed to form more and more large polymer chains. However, in controlled free radical polymerization, a large number of oligomers are formed at the beginning of polymerization. During polymerization, the oligomers gradually grow into large polymers. The feature common to all of the controlled free radical systems is the presence of large concentrations of oligomers early in the polymerization. In miniemulsion polymerization, polymerization occurs in the particles (around 100 nm in size). Ugelstad et al. [40] showed that oligomers are very efficient swelling agents, and hence the existence of oligomers may dramatically modify the state of the miniemulsion. A theoretical model has been developed by Luo et al. [128] to simulate the swelling of oligomers formed in the controlled miniemulsion polymerization.

The chemical potential of monomer droplets is determined by [128]

$$\mu_d = RT \left(\ln \varphi_{d1} + \left(1 - \frac{1}{m_2} \right) \varphi_{d2} + \varphi_{d2}^2 \, \chi_{12} + \frac{2 \bar{V}_1}{\gamma \, r_d} \, RT \right) \tag{20}$$

Before the start of polymerization, the monomer chemical potentials in all droplets can be assumed to equal because the monomer has at least limited solubility in the aqueous phase. However, once a monomer droplet is initiated, a part of the monomer will polymerize into oligomers, and the droplet is converted into a particle. The particle chemical potential is described by [312]

$$\mu_d = RT \left(\ln \varphi_{d1} + \left(1 - \frac{1}{m_2} \right) \varphi_{d2} + \left(1 - \frac{1}{m_3} \right) \varphi_{p3} + \varphi_{p2}^2 \, \chi_{12} + \varphi_{p3}^2 \, \chi_{13} \right.$$
$$\left. + \varphi_{p2} \, \varphi_{p3} \left(\chi_{12} + \chi_{13} - \frac{\chi_{13}}{m_2} \right) + \frac{2 \bar{V}_1}{\gamma \, r_d} \, RT \right) \tag{21}$$

Fig. 21 Variation in the droplet chemical potential (top) and particle chemical potential (bottom) during particle swelling (from [170])

The monomer chemical potential in the particles is lower than that in the droplets, so that the monomer in the droplets will diffuse across the aqueous phase and into the particles, leading to changes in the monomer chemical potentials of the the particles and droplets. The change in the monomer chemical potential is illustrated in Fig. 21, where Y is defined as the swelling capacity: the ratio of the weight of a swollen particle to its weight before it is swollen.

As shown in Fig. 21, the particles swell with monomer diffusion (increase in Y). During swelling, the monomer chemical potential in the particles first rapidly increases and then decreases gradually down to zero with more and more monomer swelling. On the other hand, the droplets shrink and the co-stabilizer is concentrated since it cannot (by definition) diffuse out with the monomer. The monomer chemical potential decreases monotonically. During the process of monomer diffusion, if the monomer chemical potential in the droplets is equal to that of the particles, equilibrium is established and monomer diffusion ceases. In Fig. 21, the formation of high MW polymer is shown for contrast. Three intersections of the droplet and particle chemical potential curves can be seen. Two of these occur at low Y and the third at a much higher Y. As is often the case with three equilibrium points, the middle point is unstable. When the system arrives at the first intersection during swelling (lowest Y), monomer transfer stops and the system reaches an equilibrium state that is called the *normal swelling state*. In this case, the other two equilibrium points will never be reached. However, in the case of controlled polymerization, the formation of oligomers rather than high molecular weight polymer leads to a lower mixing free energy so that the monomer in the particles has a lower chemical potential. If the effect is large enough so that the chemical potential of the droplets remains higher than that of the particles at the peak of the particle chemical potential curve, the system will move to the right-most equilibrium point. This will be denoted as the *super-swelling state*. In this case, a large amount of monomer will transfer from the droplets to the particles.

Super-swelling may be the cause of the stability problems encountered in controlled miniemulsion polymerization. As the super-swelling equilibrium point is approached, a large amount of monomer would transfer from a large number of droplets to a small number of particles, which would cause the monomer droplets to shrink and the particles to swell. This would broaden the particle size distribution, or even destroy the miniemulsion. In the worst case, the super-swelling would lead to a very large size difference between the droplets and particles. The particles may be swollen to around 1 μm, a critical size where the system becomes shear-sensitive and buoyant forces dominate. Because shear is low in a miniemulsion polymerization reactor, the particles would rapidly approach a breaking-coagulating dynamically balanced particle size, as in suspension polymerization. In this case, particle size could be more than 10 μm, or they may even form a bulk phase, depending on the shear field. Alternatively, it is possible to destroy the miniemulsion using so-called hetero-coagulation (small particles/droplets coagulating onto large ones) when the size difference becomes large. The hypothesis that super-swelling causes the instability is also supported by two other papers on controlled free radical miniemulsion polymerization that used a degenerative transfer agent (C6F13I) to control molecular weight. It was reported that the final latex morphology was well controlled. C6F13I is a relatively inefficient transfer agent (C_{tr}=1.4 at 70 °C), so the degree of polymerization of the product was rather high at the beginning of polymerization. Super-swelling is less likely to occur in such a case.

Based on Luo's simulations [128], it has been found that the super-swelling state is rather sensitive to recipe variations. Simply increasing the costabilizer level and/or using a nonionic polymeric surfactant would probably eliminate super-swelling, and hence, the instability. More recently, Sanderson [310] reported that two strategies could successfully form stable latex from RAFT miniemulsion polymerization:

a. Replace common RAFT by RAFT-endcapped oligomers
b. Use high levels of SDS and HD

The fact that these two quite different approaches are both successful can largely be reconciled using Luo's theory. Replacing common RAFT by RAFT-endcapped oligomers can avoid the super-swelling because the dangerous stage of oligomer formation is avoided. Using oligomers of a molecular weight controlling agent has also proved very helpful with SFRP in miniemulsion [226, 232]. High levels of SDS would lead to low interfacial tension, which helps to suppress the super-swelling, and high HD levels would also suppress the super-swelling. The super-swelling could also explain the instability or broad particle size distribution in most cases, as discussed in the literature [128].

Super-swelling was postulated as a cause of instability in controlled free radical miniemulsion polymerization. Asua [312] thought that the interfacial tension used in the simulations was too high and the droplet size was too small. However, it is turned out that the question about droplet size is due to a misunderstanding. It is well accepted that a well-performed miniemulsion has
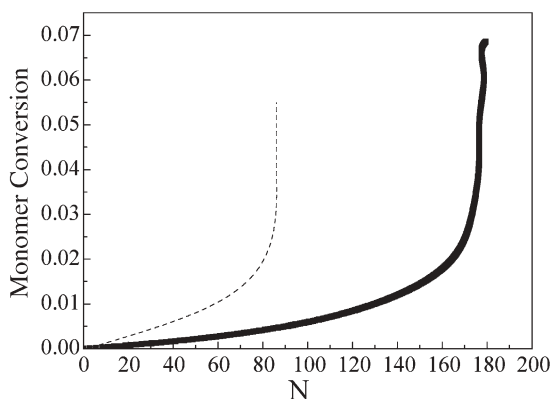
Fig. 22 Plot of monomer conversion versus the number of input free radicals in a droplet (dotted: D=50 nm; solid: D=100 nm) (from [170])

increased interfacial tension. Actually, the interfacial tension used in the simulations was cited from Landfester's work on miniemulsions [313]. Another controversy is about the view of the nucleation process in controlled free radical miniemulsion polymerization. In Luo's work [312], it was found that superswelling happens only in the presence of a small fraction of particles with rather high conversion (10%); the majority of droplets have zero conversion. It is difficult to understand what would lead to such scenarios. However, Luo's simulations [179] showed that the nucleation process of RAFT miniemulsion polymerization could be very different to that of regular miniemulsion polymerization. As shown in Fig. 22, the simulations suggest that, by introducing a highly reactive RAFT agent, a large number of free radicals (N_c) need to be captured by a droplet before rapid polymerization in the droplet can take place, which is totally different from the situation in regular miniemulsion polymerization. More interestingly, it was found that droplet size had a significant influence on N_c. In Fig. 23, droplets larger than 150 nm (about 8.24% of all droplets) have been nucleated. Interestingly, monomer conversion for droplets less than 130 nm in size (unnucleated) is less than 2.5%, while conversion for droplets larger than 150 nm in size (nucleated particles) is much higher, depending the radical flux. The nucleation process for ATRP or SFRP in miniemulsion has not been reported yet, though it is very important. However, Charleux [215] has theoretically studied the segregation effect of the emulsion for SFRP. The results showed that segregation is only effective for particles far smaller than 130 nm (for example 50 nm). The polymerization rate in miniemulsion, in most cases, is similar to that in homogeneous polymerization because the droplet size miniemulsion polymerization usually is around 100 nm. However, in reality, droplet size is polydispersed, so we cannot exclude the existence of very small droplets, where the segregation is effective. In such a case, it is possible that a minor fraction of the very small particles has a much higher polymerization rate than the majority of particles with larger particle
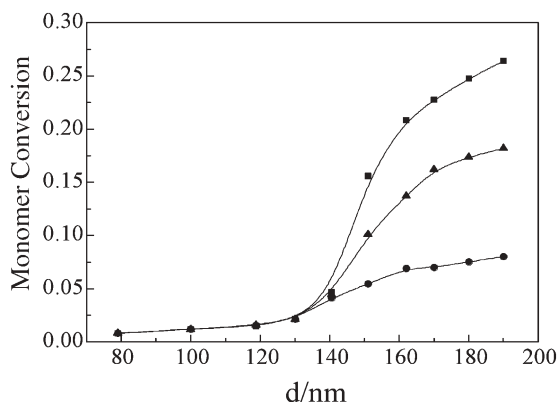
Fig. 23 The monomer conversion in particles with different initial droplet sizes at various average free radical fluxes (average of ten runs, in s^{-1}). Filled squares: 0.02; filled triangles: 0.05; filled circles: 0.1 (from [107])

sizes where segregation is not effective. The same argument is suitable for ATRP in miniemulsion. Additionally, it is well-known that it takes some time for SFRP and ATRP to set up the propagation/dormant equilibrium. It is likely that the time required to build up the equilibrium is droplet-size dependent. In such cases, the scenarios above might also occur. In fact, it has been reported that the reverse ATRP in miniemulsion has a higher colloidal stability than the direct ATRP in miniemulsion [264].

The above argument suggests that the initial droplet size distribution may play an important role in super-swelling or colloidal instability. This indicates that one should monitor the emulsification procedure for controlled free radical emulsion polymerization closely.

4.5
Other Applications and Future Directions

Recently, many new reactions have been carried out in miniemulsions. Most of these are polymerizations, but a number of nonpolymerization reactions have been proposed. This section will survey these applications, and close with some speculation on the future of miniemulsions.

4.5.1
Anionic/Cationic Polymerization in Miniemulsions

Maitre et al. [314] carried out anionic polymerization of phenyl glycidyl ether (PGE) in miniemulsion using didodecyldimethylamonium hydroxide as an *inisurf* (combination initiator and surfactant). Long chain alcohols were used as the costabilizer and stable miniemulsions were created by sonication. Monomer conversion was low, as was the degree of polymerization, which only

reached eight. The degree of polymerization was dependent on the initiator concentration, the type of alcohol, and its concentration. Comparison with bulk polymerization suggests that polymerization takes place near the droplet surface, since no high molecular weight material (expected from bulk polymerization in the droplet core) is formed. The authors postulate that initiation and propagation take place near the droplet-water interface, initiated by the inisurf. Termination with water takes place after a few propagations. However, the oligomers formed would be surface active and are thought to adsorb at the interface and increase the solubility of PGE in the locus of interfacial polymerization, enhancing subsequent propagation reactions. One might conjecture that with a hydrophobic initiator, polymerization in the droplet core might be encouraged, resulting in higher degrees of polymerization.

The same researchers [315, 316] reported the anionic ring opening polymerization of 1,3,5-tris(trifluoropropylmethyl)cyclotrisiloxane in miniemulsion using didodecyldimethylammonium bromide as the surfactant and sodium hydroxide as the initiator. Molecular weights were 2000–30,000. A two state mechanism was put forward, consisting of anionic kinetically-controlled ring opening polymerization continuing to complete conversion, followed by condensation and backbiting reactions. The delay between the two stages was long enough to allow high polymer yield.

These same researchers [317] reported the anionic polymerization of *n*-butyl cyanoacrylate in macroemulsion and miniemulsion. Dodecylbenzenesulfonic acid (DBSA) was used as the surfactant. The DBSA slows the rate of interfacial anionic polymerization through reversible termination, preventing an undesirably high degree of polymerization. Polymerization in macroemulsion resulted in a much higher degree of polymerization, perhaps due to droplet polymerization where the interface is less significant.

This same research group also reported [318] the cationic polymerization of *p*-methoxystyrene in miniemulsion. DBSA was used as both a protonic initiator and surfactant. A monomer conversion of 100% was achieved in eight hours at 60 °C. Molecular weights were low (approximately 1,000) and solids of up to 40% could be achieved with good colloidal stability. Polymerization takes place at the interface, initiated by the proton, and terminated by water. Molecular weight increased with conversion, suggesting either reversible termination or decreasing termination.

While all of these results are far from providing commercial products, they highlight the possibilities for alternative polymerization chemistries in miniemulsions.

4.5.2
Polycondensation in Miniemulsions

Barrère and Landfester [319] reported the synthesis of polyester in miniemulsions. Hydrophobic polyesters were synthesized in miniemulsion. DBSA was used as a *catsurf* (catalyst and surfactant) and HD was used as the co-

stabilizer. The pH was kept below 4 in order to prevent deprotonation of the acid monomers. Molecular weights of approximately 1000–2000 were found, with yields generally 70–80%. Both molecular weights and yields varied with monomer choice. Most interestingly, the presence of the particle-water interface did not change the polymerization-depolymerization equilibrium; the yield was the same in 100 nm particles as in very large droplets. However, the water concentration within the particle was found to be critical. Highly hydrophobic monomers reduced the monomer concentration in the particles, pushing the equilibriums toward esterification, and increasing yield. Alcohols bearing electron-donating groups were found to displace the equilibrium toward ester formation. They also report the formation of polyester-polystyrene hybrid particles using a one-pot procedure. In a separate paper [319] the same authors report one-pot polymerizations of polyurethane/acrylic hybrids. The procedures for both the polyester/polystyrene and the polyurethane/polyacrylate polymerizations were similar. First, the entire system was miniemulsified; then the polycondensation took place. After the polycondensation, a free radical initiator was added and the addition monomers were polymerized. Two molecular weight peaks were found for the polyurethane/polyacrylate system, a low one for the polyurethane, and a much higher MW peak for the polyacrylate. Hydroxybutyl acrylate, when added, was found to be a crosslinking agent, since it can undergo polycondensation and polyaddition.

4.5.3
Other Polymerizations in Miniemulsions

Extremely hydrophobic monomers do not polymerize well via macroemulsion polymerization due to their very low rates of monomer transport across the aqueous phase. Obviously, these monomers can be polymerized much more effectively in a miniemulsion system. One example of this is provided by Landfester et al. [320]. In this paper, fluoroalkyl acrylates are polymerized in a miniemulsion with low levels of a protonated surfactant. When fluorinated monomers were copolymerized with standard hydrophobic and hydrophilic monomers, either core-shell structures or statistical copolymers were formed.

A similar situation occurs with vinyl chloride (VC) for a very different reason. Vinyl chloride is very soluble in water, but polyvinyl chloride (PVC) is not soluble in its own monomer. VC does swell PVC, and for that reason, there is a driving force for VC transport across the aqueous phase in macroemulsion polymerization. This transport is aided by the fact that VS is very soluble in water. However, this is one macroemulsion system that might greatly benefit from the miniemulsion synthesis route.

Willert and Landfester [321] have polymerized amphiphilic copolymers from miniemulsion systems. The hydrophobic monomer was miniemulsified, while the hydrophilic monomer resides in the continuous phase. Polymerization was found to take place in the droplet phase, at the interface, or in the continuous phase; the quality of the product depended strongly on the primary

locus of polymerization. Inverse miniemulsions (oil as the continuous phase, with water-soluble monomer dissolved in water droplets) was also used.

Marie et al. [322] have reported the synthesis of polyaniline particles via inverse and direct miniemulsion. Inverse miniemulsons of anilinium hydrochloride were oxidized by hydrogen peroxide, resulting in highly crystalline polyaniline. Oxidation of aniline miniemulsions in water also leads to highly crystalline polyaniline. The same research group reports the use of chitosan as a surfactant for miniemulsions [338], resulting in latex particles with functional biopolymer surfaces for grafting in biological applications. Taden et al. [324] report the enzymatic polymerization of lactone to form biodegradable nanoparticles.

Claverie et al. [325] have polymerized norbornene via ROMP using a conventional emulsion polymerization route. In this case the catalyst was water-soluble. Particle nucleation was found to be primarily via homogenous nucleation, and each particle in the final latex was made up of an agglomeration of smaller particles. This is probably due to the fact that, unlike in free radical polymerization with water-soluble initiators, the catalyst never entered the polymer particle. Homogeneous nucleation can lead to a less controllable process than droplet nucleation (miniemulsion polymerization). This system would not work for less strained monomers, and so, in order to use a more active (and strongly hydrophobic) catalyst, Claverie employed a modified miniemulsion process. The hydrophobic catalyst was dissolved in toluene, and subsequently, a miniemulsion was created. Monomer was added to swell the toluene droplets. Reaction rates and monomer conversion were low, presumably because of the proximity of the catalyst to the aqueous phase due to the small droplet size.

4.5.4
Other Miniemulsion Applications

The miniemulsification technique can also be applied to nonpolymerization systems. The number of nonpolymerization applications of miniemulsions is small, but seems to be growing. Landfester [326] has reviewed the generation of nanoparticles in miniemulsions. Revelino et al. [327] has studied crystallization from direct and inverse miniemulsions. It was found that, since each droplet must be nucleated separately, the undercooling necessary to effect crystallization increases dramatically. The crystallization rate was higher in miniemulsions and proportional to droplet size. Taden et al. [328] studied the crystallization of polyethylene oxide from miniemulsions. Crystallization only occurred at large supercooling. Drying of the crystallized dispersion resulted in a highly ordered arrangement of polyethylene oxide platelets. Montenegro et al. [329] studied crystallization of alkanes from miniemulsions. Wegner et al. [330] have used polymeric nanospheres produced via miniemulsion polymerization to control nucleation and growth of inorganic crystals from aqueous media.

Vaihinger et al. [331] have molecularly imprinted polymer nanospheres as synthetic affinity receptors via miniemulsion techniques. Landfester et al. [332] have created semiconducting polymer nanospheres in aqueous dispersions via the synthetic miniemulsion technique. That is, conducting polymers were dissolved in solvent and then miniemulsified. Films produced by spin coating retained the nanosphere character until they were annealed above the glass transition temperature. In similar work, Piok et al. [333–335] formed organic light-emitting devices fabricated from semiconducting nanospheres created by the miniemulsification process. Willert et al. [336] created inorganic and metallic nanoparticles by the miniemulsification of molten salts and metals. Zu Putlitz et al. [337] created "armored latexes" and hollow inorganic shells made of clay sheets by templating cationic miniemulsions and latexes.

4.5.5
Future Directions

It would seem that miniemulsions have finally moved from being a laboratory curiosity to being a viable commercial process and a useful synthetic technique for producing interesting materials with nano-scale structure. It would appear that polymer-polymer hybrids and polymer-inorganic hybrids achieved via miniemulsion polymerization will result in new classes of water-borne materials. Other, traditionally solvent-based, polymerization chemistries may soon be carried out routinely via the miniemulsion route due to improvements in polymerization catalysts. The use of miniemulsions in ROMP has been cited above. Metallocene polymerization of ethylenic monomers has been carried out in macroemulsion. A short review and discussion of this work is given in [338]. If these water-tolerant polymerization chemistries are successful, it cannot be long before they are ported into miniemulsions. Controlled radical polymerization, particularly using RAFT chemistry, is a natural application for miniemulsion technology. Perhaps most importantly, miniemulsion techniques will be used in a variety of nonpolymerization technologies to produce nano-scale, highly structured materials.

References

1. Asua JM (2002) Prog Polym Sci 27:1283
2. Guyot A (2001) Curr Trends Polym Sci 6:47
3. Antonietti M, Landfester K (2002) Prog Polym Sci 27:689
4. Trommsdorf E, Schlidknecht E (1956) Suspension polymerization in polymer processes. Interscience, New York
5. Ugelstad J, El-Aasser MS, Vanderhoff JW (1973) J Polym Sci Pol Lett 11:503
6. Gardon JL (1970) Brit Polym J 2:1
7. Poehlein GW (1982) In: Piirma I (ed) Emulsion polymerization. Academic, New York, p 357
8. Poehlein GW (1985) ACS Sym Ser 285:131–150

9. Poehlein GW, Dougherty DJ (1976) Rubber chemistry and technology 50:601
10. Song Z (1988) PhD Thesis, Georgia Institute of Technology, Atlanta, GA
11. Ugelstad J, Hansen FK (1976) Rubber Chem Technol 49:536
12. Harkins WD (1947) J Am Chem Soc 69:1428
13. Smith WV, Ewart RH (1948) J Chem Physics 16:592
14. Alexander AE, Napper DH (1971) Prog Polym Sci 3:145
15. Blackley DC (1982) Emulsion polymerization. Academic, New York
16. Baxendale JH, Bywater S, Evans MG (1946) T Faraday Soc 42:675
17. Baxendale JH, Evans MG, Kilham JK (1946) T Faraday Soc 42:668
18. Priest WJ (1952) Phys Chem J 56:1077
19. Roe CP (1968) Ind Eng Chem 60:20
20. Fitch RM, Tsai CH (1971) In: Fitch RM (ed) Polymer colloids. Plenum, New York, p 73
21. Fitch RM, Tsai CH (1971) In: Fitch RM (ed) Polymer colloids. Plenum, New York, p 103
22. Fitch RM (1973) Brit Polym J 5:467
23. Lichti G, Gilbert RG, Napper DH (1983) J Polym Sci Pol Chem 21:269
24. Feeney PJ, Napper DH, Gilbert RG (1984) Macromolecules 17:2520
25. Maxwell IA, Morrison BR, Napper DH, Gilbert RG (1991) Macromolecules 24:1629
26. Chamberlain BJ, Napper DH, Gilbert RG (1982) J Chem Soc Farad T I 78:591
27. Ugelstad J, Kaggerud KH, Hansen FK, Berge A (1979) Makromol Chem 180:737
28. Ugelstad J, Mfutakamba HR, Mork PC, Ellingsen, Berge A, Schmidt R, Holm L, Jorgedel A, Hansen FK, Nustad K (1985) J Polym Sci Pol Sym 72:225
29. Hansen FK, Ofstad EB, Ugelstad J (1976) Theory and practice of emulsion technology. Academic, New York
30. Ugelstad J, Flagstad H, Hansen FK, Ellingsen T (1973) J Polym Sci 42:473
31. Hansen FK, Ugelstad J (1979) J Polym Sci 17:3047
32. Morton M, Kaizermann S, Altier MW (1954) J Colloid Interf Sci 9:300
33. Beuermann S, Buback M (2002) Prog Polym Sci 27:191
34. Sundberg DC, Hsieh JY, Soh SK, Baldus RF (1982) ACS Sym Ser 165:327
35. Buback M, Garcia-Rubio LH, Gilbert RG, Napper DH, Gulliot J, Hamielec AE, Hill D, O'Driscoll KF, Olaj OF, Shen J, Solomon D, Moad G, Stickler M, Tirrell M, Winnick MA (1988) J Polym Sci Pol Phys 26:293
36. Barnette DT, Schork FJ (1987) Chem Eng Prog 83:25
37. Fris N, Hamielec AE (1973) J Polym Sci Pol Chem 11 3321
38. Rawlings JB, Ray WH (1988) Polym Eng Sci 28:257
39. Ballard MJ, Gilbert RG, Napper DH, Pomery PJ, O'Sullivan PW, O'Donnell JH (1986) Macromolecules 19:1303
40. Soh SK, Sundberg DC (1982) J Polym Sci Pol Chem 20:1331
41. Ostwald WZ (1901) Z F Phys Chem 37:495
42. Fontenot K, Schork FJ (1993) Ind Eng Res 32:373
43. Chern CS, Chen TJ (1998) Colloids Surface A 138:65
44. Flory PJ (1953) Principles of polymer chemistry. Cornell Univ Press, Ithaca, NY
45. Ugelstad J, Mork PC, Kaggerud KH, Ellingsen T, Berge A (1980) Adv Colloid Interfac 13:101
46. Jansson LH, Wellons MC, Poehlein GW (1983) J Polym Sci Pol Lett 21:937
47. Higuchi WI, Misra J (1962) J Pharm Sci 51:459
48. Ugelstad J (1978) Makromol Chem 179:815
49. Fontenot K (1991) PhD Thesis, Georgia Institute of Technology, Atlanta, GA
50. Azad ARM, Fitch RM (1980) In: Polymer colloids II. Plenum, New York, p 95

51. El-Aasser MS, Lack CD, Choi YT, Min TI, Vanderhoff JW, Fowkes FM (1984) Colloids Surface 12:79
52. Ugelstad J, Kaggerud KH, Fitch RM (1980) In: Fitch RM (ed) Polymer colloids II. Plenum, New York, p 83
53. Choi YT, El-Aasser MS, Sudol ED, Vanderhoff JW (1985) J Polym Sci Pol Chem 23: 2973
54. Chamberlain BJ, Napper DH, Gilbert RG (1982) J Chem Soc Farad T 1 78:591
55. Chen CM, Gothjelpsen L, Schork FJ (1986) Polym Proc Eng 4:1
56. Delgado J, El-Aasser MS, Silebi CA, Vanderhoff JW (1986) Polym Mat Sci Eng 54:444
57. Rodriguez VS, Delgado J, Silebi CA, El-Aasser MS (1988) Polym Mat Sci Eng 58:761
58. Delgado J, El-Aasser MS, Vanderhoff JW (1986) J Polym Sci Pol Chem 24:861
59. Asua JM, Rodriguez VS, Silebi CA, El-Aasser MS (1990) Makromol Chem M Symp 35–36:59
60. Rodriguez VS, Delgado J, Silebi CA, El-Aasser MS (1989) Ind Eng Chem Res 28:65
61. Rodriguez VS, Asua JM, El-Aasser MS, Silebi CA (1991) J Polym Sci Pol Physics 29:483
62. Fontenot K, Schork FJ (1992) Polym Reaction Engineering 1:75
63. Fontenot K, Schork FJ (1993) Polym React Eng 1:289
64. Samer CJ, Schork FJ (1997) Polym React Eng 5:85
65. Ma JW, Cunningham MF, McAuley KB, Keoshkerian B, Georges MK (2003) Macromol Theor Simul 12:72
66. Ma JW, Cunningham MF, McAuley KB, Keoshkerian B, Georges M (2003) Chem Eng Sci 58:1177
67. Ma JW, Smith JA, McAuley KB, Cunningham MF, Keoshkerian B, Georges MK (2003) Chem Eng Sci 58:1163
68. Ma JW, Cunningham MF, McAuley KB, Keoshkerian B, Georges MK (2002) Macromol Theor Simul 11:953
69. Samer CJ, Schork FJ (1999) Ind Eng Res 38:1801
70. Landfester K, Bechthold N, Tiarks F, Antonietti M (1999) Macromolecules 32:2679
71. Bechthold N, Tiarks F, Willert M, Landfester K, Antonietti M (2000) Macromol Symp 151:549
72. Bradley M, Grieser F (2002) J Colloid Interf Sci 251:1
73. Wang S, Schork FJ (1994) J Appl Polym Sci 54:2157
74. Chern CS, Chen TJ (1997) Colloid Polym Sci 275:1060
75. Chern CS, Liou YC (1999) Polymer 40:3763
76. Wu XQ, Schork FJ (2001) J Appl Polym Sci 81:1691
77. Graillat C, Guyot A (2003) Macromolecules 36:6371
78. Boisson F, Uzulina I, Guyot A (2001) Macromol Rapid Comm 22:1135
79. Lack CD, El-Aasser MS, Vanderhoff JW, Fowkes FM (1985) ACS Sym Ser 272:345
80. Azad ARM, Ugelstad J, Hansen FK (1976) ACS Sym Ser 24:1
81. Hawkett BS, Napper DH, Gilbert RG (1980) J Chem Soc Farad T I 76:1323
82. Hallworth GW, Carless JE (1974) Theory and practice of emulsion technology. Academic, New York, p 305
83. Choi YT, El-Asser MS, Sudol ED, Vanderhoff JW (1985) J Appl Polym Sci 23:2973
84. Choi YT (1986) PhD Thesis, Lehigh University, Bethlehem, PA
85. Friberg SE, Neogi P (1986) Disp Sci Tech J 7:50
86. Kislalioglu S, Friberg S (1976) Theory and practice of emulsion technology. Academic, New York, p 257
87. Lack CD, El-Aasser MS, Silebi CA, Vanderhoff JW, Fowkes FM (1987) Langmuir 3:1155
88. Shah DO, Schechter RS (1977) Improved oil recovery by surfactant and polymer flooding. Academic, New York

89. El-Aasser MS, Lack CD, Choi YT, Min TI, Vanderhoff JW, Fowkes FM (1984) Colloids Surface 12:79
90. Rodriguez VS (1988) PhD Thesis, Lehigh University, Bethlehem, PA
91. Delgado J, El-Aasser MS, Vanderhoff JW (1986) J Polym Sci Pol Chem 24:861
92. Reimers JL, Skelland AHP, Schork FJ (1995) Polym React Eng 3:235
93. Ugelstad J (1980) Adv Colloid Interfac 13:101
94. Reimers JL, Schork FJ (1996) J Appl Polym Sci 60:251
95. Reimers JL, Schork FJ (1996) J Appl Polym Sci 59:1833
96. Aizpurua I, Amalvy JI, Barandiaran MJ (2000) Colloids Surface A 166:59
97. Lelu S, Novat C, Graillat C, Guyot A, Bourgeat-Lami E (2003) Polym Int 52:542
98. Wang ST, Schork FJ, Poehlein GW, Gooch JW (1996) J Appl Polym Sci 60 2069
99. Wu XQ, Schork FJ, Gooch JW (1999) J Polym Sci Pol Chem 37:4159
100. Tsavalas JG, Gooch JW, Schork FJ (2000) J Appl Polym Sci 75:916
101. Dong H, Gooch JW, Schork FJ (2000) J Appl Polym Sci 76:105
102. Reimers JL, Schork FJ (1996) Polym React Eng 4:135
103. Chern C-S, Sheu J-C (2000) J Polym Sci Pol Chem 38:3188
104. Samer CJ, Schork FJ (1999) Ind Eng Res 38:1792
105. Mouron D, Reimers J, Schork FJ (1996) J Polym Sci Pol Chem 34:1073
106. Wang S, Poehlein GW, Schork FJ (1997) J Polym Sci Pol Chem 35:595
107. Reimers JL, Schork FJ (1997) Ind Eng Resh 36:1085
108. Asua J, Alduncin J, Forcada J (1994) Macromolecules 27:2256
109. Miller CM, Blythe PJ, Sudol ED, Silebi CA, El-Aasser MS (1994) J Polym Sci Pol Chem 32:2365
110. Miller CM, Sudol ED, Silebi CA, El-Aasser MS (1995) Macromolecules 28:2754
111. Miller CM, Sudol ED, Silebi CA, El-Aasser MS (1995) Macromolecules 28:2765
112. Miller CM, Sudol ED, Silebi CA, El-Aasser MS (1995) Macromolecules 28:2772
113. Blythe PJ, Morrison BR, Mathauer KA, Sudol ED, El-Aasser MS (1999) Macromolecules 32:6944
114. Blythe PJ, Klein A, Sudol ED, El-Aasser MS (1999) Macromolecules 32:6952
115. Blythe PJ, Klein A, Sudol ED, El-Aasser MS (1999) Macromolecules 32:4225
116. Blythe PJ, Morrison BR, Mathauer KA, Sudol ED, El-Aasser MS (2000) Langmuir 16:898
117. Ghazaly HM, Daniels ES, Dimonie VL, Klein A, El-Aasser MS (2001) J Appl Polym Sci 81:1721
118. Luo Y, Schork FJ (2002) J Polym Sci Pol Chem 40:3200
119. Alduncin JA, Asua JM (1994) Polymer 35:3758
120. Blythe PJ, Klein A, Phillips JA, Sudol ED, El-Aasser MS (1999) J Polym Sci Pol Chem 37:4449
121. Gilbert RG (1995) Emulsion polymerization: A mechanistic approach. Academic, London
122. Kabalnov AS, Pertzov AV, Shchukin ED (1987) J Colloid Interf Sci 118:590
123. Candau F, Pabon M, Anquetil J-Y (1999) Colloid Surface A 153:47
124. Sood A, Awasthi KJ (2003) Appl Polym Sci 88:3058
125. Erdem B, Sully Y, Sudol ED, Dimonie VL, El-Aasser MS (2000) Langmuir 16:4890
126. Landfester K, Bechthold N, Föster S, Antonietti M (1999) Macromol Rapid Comm 20:81
127. Landfester K, Bechthold N, Tiarks F, Antonietti M (2000) Macromolecules 32:5222
128. Luo Y, Tsavalas JG, Schork FJ (2001) Macromolecules 34:5501
129. Melis S, Kemmere M, Meuldijk J, Storti G, Morbidelli M (2000) Chem Eng Sci 55:3101
130. Leiza JR, Sudol ED, El-Aasser MS (1997) J Appl Polym Sci 64:1797
131. Tang PL, Sudol ED, Adams M, El-Aasser MS, Asua JM (1991) J Appl Polym Sci 42: 2019

132. Sajjadi S, Jahanzad F (2003) Euro Polym J 39:785
133. Durant YG (1999) Book of Abstracts 217th ACS National Meeting (PMSE-326), Anaheim, CA, 21–25 March 1999, American Chemical Society, Washington, DC
134. Ouzineb K, Graillat C, McKenna TF (2001) DECHEMA Monographien (7th Int Workshop on Polymer Reaction Eng), Hamburg, Germany, 8–10 October 2001, 137:293
135. Barnette DT, Schork FJ (1989) Chem Eng Commun 80:113
136. Nomura M, Harada M (1981) ACS Sym Ser 165:121
137. Samer CJ, Schork FJ (1999) Ind Eng Res 38:1792
138. Aizpurua I, Barandiaran M (1999) Polymer 40:4105
139. Aizpurua I, Amalvy JI, de la Cal JC, Barandiaran MJ (2000) Polymer 42:1417
140. Fontenot K, Schork FJ (1993) J Appl Polym Sci 49:633
141. Odian G (1988) Principles of polymerization, 3rd edn. Wiley-Interscience, New York
142. Landfester K, Schork FJ, Kusuma VA (2003) CR Acad Sci 6(11–12):1337–1342
143. Landfester K, Bechthold N, Tiarks F, Antonietti M (1999) Macromolecules 32:5222
144. Reimers JL, Schork FJ (1996) J Appl Polym Sci 59:1833
145. Landfester K, Bechthold N, Tiarks F, Antonietti M (1999) Macromolecules 32:2679
146. Rodrigues JC, Schork FJ (1997) J Appl Polym Sci 66:317
147. Balic R (2000) PhD Thesis, University of Sydney, Sydney, Australia
148. Kitzmiller EL, Miller CM, Sudol ED, El-Aasser MS (1995) Macromol Symp 92:157
149. Mayo VF, Lewis FM (1944) J Am Chem Soc 66:1594
150. Schuller H (1986) In: Reichert K, Geisler W (eds) Polymer reaction engineering. Hüthig and Wepf, Heidelberg, Germany, p 137
151. Guillot J (1986) In: Reichert K, Geisler W (eds) Polymer reaction engineering. Hüthig and Wepf, Heidelberg, Germany, p 147
152. Wu XQ, Schork FJ (2000) Ind Eng Chem Res 39:2855
153. Delgado J, El-Aasser MS, Silebi CA, Vanderhoff JW (1987) Polym Mat Sci Eng 57:976
154. Delgado J, El-Aasser MS, Silebi CA, Vanderhoff JW, Guillot J (1987) In: El-Aasser MS, Fitch RM (eds) NATO ASI Ser E: Appl Sci 138:79
155. Delgado J, El-Aasser MS, Silebi CA, Vanderhoff JW (1988) Makromol Chem M Symp 20/21:545
156. Delgado J, El-Aaser MS, Silebi CA, Vanderhoff JW (1989) J Polym Sci Pol Chem 27:193
157. Delgado J, El-Aasser MS, Silebi CA, Vanderhoff JW (1990) J Polym Sci Pol Chem 28:777
158. Unzue MJ, Asua JM (1993) J Appl Polym Sci 49:81
159. Wu XQ, Hong XM, Schork FJ (2002) J Appl Polym Sci 85:2219
160. Caruso F, Caruso RA, Mohwald H (1998) Science 282:1111
161. Caruso F (2001) Adv Mater 13:11
162. Numo-Donlunas S, Rhoton AI, Corona-Galvan S, Puig JE, Kaler JE (1993) Polym Bull 30:207
163. Antonova LF, Leplyanin GV, Zayev YY, Rafikov SR (1978) Polym Sci USSR 20:778
164. Turner SR, Weiss RA, Lundberg RD (1985) J Polym Sci Pol Chem 37:535
165. Kim JH, Chainey M, El Aasser MS, Vanderhoff JW (1992) J Polym Sci Pol Chem 30:535
166. Emelie B, Pichot D, Guillot J (1988) Makromol Chem 189:1879
167. Shoaf GL, Poehlein GW (1992) Polym React Eng 9:1
168. Charmot D, D'Allest JF, Dobler F (1996) Polymer 37:5237
169. Ganachaud F, Sauzedde F, Elaissari A, Pichot C (1997) J Appl Polym Sci 65:2315
170. Luo YW, Schork FJ (2001) J Polym Sci Pol Chem 39:2696
171. Kim JH, Chainey M, El Aasser MS, Vanderhoff JW (1990) J Polym Sci Pol Chem 28:3188

172. Gilbert RG, Anstey JF, Subramaniam N, Monteiro MJ (1999) ACS Polym Prepr Div Polym Chem 40:102
173. Blackley DC (1975) Emulsion polymerization. Wiley, New York, p 244
174. Dong H, Gooch JW, Poehlein GW, Wang ST, Wu X, Schork FJ (2001) ACS Sym Ser 766:8–17
175. Nabuurs T, Baijards RA, German AL (1996) Prog Org Coat 27:163
176. Van Hamersveld EMS, van Es GS, Cuperus FP (1999) Colloids Surface A 153:285
177. Van Hamersveld EMS, Van Es GS, German AL, Cuperus FP, Weissenborn P, Hellgren AC (1999) Prog Org Coat 35:235
178. Tsavalas JG, Luo Y, Hudda L, Schork FJ (2003) Polym React Eng 11:277
179. Tsavalas JG, Luo Y, Schork FJ (2003) J Appl Polym Sci 87:1825
180. Tsavalas JG, Schork FJ, Landfester K (2003) J Coating Technol (in press)
181. Shoaf GL, Stockl RR (2003) Polym React Eng 11:319
182. Li, Daniels ES, Dimonie VL, Sudol ED, El-Aasser MS (2001) Polym Mat Sci Eng 85:258
183. Wang C, Chu F, Graillat C, Guyot A (2003) Polym React Eng 11:541
184. Barrere M, Landfester K (2003) Macromolecules 36:5119
185. El-Aasser MS, Li M, Jeong P, Daniels ES, Dimonie VL, Sudol ED (2001) DECHEMA Monographien (7th Int Workshop on Polymer Reaction Engineering), Hamburg, Germany, 8–10 October 2001, 137:1
186. Jeong P, Dimonie VL, Daniels ES, El-Aasser MS (2002) ACS Sym Ser 801:357
187. Kawahara H, Goto T, Okamoto Y, Kage H, Ogura H, Matsuno Y (2002) Kagaku Kogaku Ronbun 28:175
188. Landfester K, Dimonie VL, El-Aasser MS (1998) DECHEMA Monographien 134 (6th Int Workshop on Polymer Reaction Engineering 1998), Berlin, 5–7 October 1998, 134:469
189. Roberts JE, Marcu I, Dimonie V, Daniels E, El-Aasser MS (2003) ACS Polym Prepr Div Polym Chem 44:277
190. Marcu I, Daniels ES, Dimonie VL, Hagiopol C, Roberts JE, El-Aasser MS (2003) Macromolecules 36:328
191. El-Aasser MS, Vanderhoff JW, Poehlein GW (1977) Coating Plastic Prepr 37:92
192. El-Aasser MS, Hoffman JD, Manson JA, Vanderhoff JW (1980) Org Coating Plast Chem 43:136
193. Vanderhoff JW, El-Aasser MS, Hoffman JD (1978) US Patent 4070323
194. Noh MH, Jang LW, Lee DC (1999) J Appl Polym Sci 74:179
195. Noh MH, Lee DC (1999) J Appl Polym Sci 74:2811
196. Garcés JM, Moll DJ, Bicerano J, Fibinger R, McLeod DG (2000) Adv Mater 12:1835
197. Van Herk AM, German AL (1999) Microsph Microcaps Lipos 1:457
198. Erdem B, Sudol ED, Dimonie VL, El-Aasser MS (2000) J Polym Sci Pol Chem 38:4419
199. Erdem B, Sudol ED, Dimonie VL, El-Aasser MS (2000) J Polym Sci Pol Chem 38:4431
200. Erdem B, Sudol ED, Dimonie VL, El-Aasser MS (2000) J Polym Sci Pol Chem 38:4441
201. Tiarks F, Landfester K, Antonietti M (2001) Langmuir 17:5775
202. Antonietti M, Landfester K (2002) Chem Ing Tech 74:543
203. Landfester K, Montenegro R, Scherf U, Guntner R, Asawapirom U, Patil S, Neher D, Kietzke T (2002) Adv Mater 14:651
204. Ramirez LP, Landfester K (2003) Macromol Chem Phys 204:22
205. Solomon DH, Rizzardo E, Cacioli P (1985) Eur Pat Appl EP 135280
206. Georges MK, Moffat KA, Veregin RPN, Kazmaier PM, Hamer GK (1993) Polym Mater Sci Eng 69:305
207. Fischer H (1997) Macromolecules 30:5666
208. Gridnev AA (1997) Macromolecules 30:7651

209. Moad G, Solomon DH (1995) The chemistry of free radical polymerization, 1st edn. Elsevier, Amsterdam
210. Fukuda T, Terauchi T, Goto A, Ohno K, Tsujii Y, Miyamoto T, Kobatake S, Yamada B (1996) Macromolecules 29:6393
211. Fukuda T (2002) Handbook of radical polymerization. Wiley, New York, Ch 9
212. Qiu J, Charleux B, Matyjaszewski K (2001) Prog Polym Sci 26:2083
213. Butte A, Storti G, Morbidelli M (1998) In: Reicher KH, Moritz HU (eds) 6th Int Workshop on Polymer Reaction Engineering. DECHEMA Monographien, Berlin, 5–7 October 1998, 134:497
214. Butte A, Storti G, Morbidelli M (2000) Macromolecules 33:3485
215. Charleux B (2000) Macromolecules 33:5358
216. Pan G, Sudol ED, Dimonie VL, El-Aasser MS (2002) Macromolecules 35:6915
217. Lansalot M, Farcet C, Charleux B, Vairon J-P, Pirri R, Tordo P (2000) ACS Sym Ser 768:138
218. Prodpan T, Dimonie VL, Sudol ED, El-Aasser M (1999) Polym Mater Sci Eng 80:534
219. MacLeod PJ, Keoshkerian B, Odell P, Georges MK (1999) Polym Mater Sci Eng 80:539
220. Lansalot M, Charleux B, Vairon J-P, Pirri R, Tordo P (1999) ACS Polym Prepr 40:317
221. Prodpan T, Dimonie VL, Sudol ED, El-Aasser M (2000) Macromol Symp 155:1
222. MacLeod PJ, Barber R, Odell P, Keoshkerian B, Georges MK (2000) Macromol Symp 155:31
223. Farcet C, Lansalot M, Charleux B, Pirri R, Vairon JP (2000) Macromolecules 33:8559
224. Pan G, Sudol ED, Dimonie VL, El-Aasser MS (2001) Macromolecules 34:481
225. Keoshkerian B, MacLeod PJ, Georges MK (2001) Macromolecules 34:3594
226. Farcet C, Charleux B, Pirri R (2001) Macromolecules 34:3823
227. Cunningham MF (2002) Prog Polym Sci 27:1039
228. Tortosa K, Smith JA, Cunningham MF (2001) Macromol Rapid Comm 22:957
229. Farcet C, Belleney J, Charleux B, Pirri R (2002) Macromolecules 35:4912
230. Farcet C, Charleux B, Pirri R (2002) Macromol Symp 182:249
231. Keoshkerian B, Szkurham AR, Georges MK (2001) Macromolecules 34:6531
232. Cunningham MF, Tortosa K, Lin M, Keoshkerian B, Georges MK (2002) J Polym Sci Pol Chem 40:2828
233. Cunningham MF, Xie M, McAuley KB, Keoshkerian B, Georges MK (2002) Macromolecules 35:59
234. Ma JW, Cunningham MF, McAuley KB, Keoshkerian B, Georges MK (2002) Macromol Theor Simul 11:953
235. Ma JW, Cunningham MF, McAuley KB, Keoshkerian B, Georges MK (2003) Macromol Theor Simul 12:72
236. Matyjaszewski K, Wang J (1995) J Am Chem Soc 117:5614
237. Matyjaszewski K, Wang J (1995) Macromolecules 28:7901
238. Matyjaszewski K, Xia J, Patten T, Abernathy T (1996) Science 272:866
239. Sawamoto M, Kamigaito M, Higashimura T, Kato M (1995) Macromolecules 28:1721
240. Sawamoto M, Kamigaito M, Ando T, Kato M (1996) Macromolecules 29:1070
241. Sawamoto M, Kamigaito M, Kotani Y, Kato M (1996) Macromolecules 29:6979
242. Uegaki H, Kotani Y, Kamigato M, Sawamoto M (1998) Macromolecules 31:6756
243. Moineau G, Minet M, Dubois P, Teyssié P, Sennenger T, Jérôme R (1999) Macromolecules 32:27
244. Lecomte P, Drapier I, Dubois P, Teyssié P, Jérôme R (1997) Macromolecules 30:7631
245. Brandts JAM, van de Geijn P, van Faassen EE, Boersma J, van Koten G (1999) J Organomet Chem 584:246
246. Kotani Y, Kamigaito M, Sawamoto M (1999) Macromolecules 32:2420

247. Percec V, Barboiu B, Neumann A (1996) Macromolecules 29:3665
248. Patten TE, Matyjazsweski K (1998) Adv Mater 10:901
249. Matyjaszewski K (1999) Chem Eur J 5:3095
250. Pan CY, Lou XD (2000) Macromol Chem Phys 201:1115
251. Chen XP, Padias AB, Hall HK (2001) Macromolecules 34:3514
252. Matyjaszewski K, Wei M, Xia J, Gaynor S (1998) Macromol Chem Phys 199:2289
253. Hamasaki S, Kamigaito M, Sawamoto M (2002) Macromolecules 35:2934
254. Hamasaki S, Sawauchi C, Kamigaito M, Sawamoto M (2002) J Polym Sci Pol Chem 40:617
255. Fischer H (1999) J Polym Sci Pol Chem 37:1885
256. Sawamoto M, Kamigaito M (2000) Macromol Symp 161:11
257. Davis K, O'Malley J, Paik H, Matyjaszewski K (1997) ACS Polym Prepr 38:687
258. Matyjaszweski K, Xia J (2001) Chem Rev 101:2921
259. Takhashi H, Ando T, Kamigaito M, Sawamoto M (1999) Macromolecules 32:3820
260. Matyjaszewski K (1996) Macromol Symp 111:47
261. Butté A, Storti G, Morbidelli M (2001) Macromolecules 34:5885
262. Matyjaszewski K, Qiu J, Tsarevsky NV, Charleux B (2000) J Polym Sci Pol Chem 38:4724
263. Zhang B, Zhang ZB, Xan XL, Hu CP, Ying SK (2002) Chinese J Polym Sci 20:445
264. Li M, Matyjaszewski K (2003) Macromolecules 36:6028
265. Chiefari J, Chong YK, Ercole F, Krstina J, Jeffery J, Le TPT, Mayadunne RTA, Meijs GF, Moad CL, Moad G, Rizzardo E, Thang SH (1998) Macromolecules 31:5559
266. Le TP, Moad G, Rizzardo E, Thang SH (1998) PCT Int Appl, p 88
267. Rizzardo E, Thang SH, Moad G (1999) PCT Int Appl, p 40
268. Krstina J, Moad G, Rizzardo E, Winzor CL, Berge CT, Fryd M (1995) Macromolecules 28:5381
269. Corpart P, Charmot D, Biadatti T, Zard S, Michelet D (1998) PCT Int Appl, p 70
270. Hawthorne DG, Moad G, Rizzardo E, Thang SH (1999) Macromolecules 32:5457
271. Chong YK, Le TPT, Moad G, Rizzardo E, Thang SH (1999) Macromolecules 32:2071
272. De Brouwer H, Schellekens MAJ, Klumperman B, Monteiro MJ, German A (2000) J Polym Sci Pol Chem 38:3596
273. Monteiro MJ, Sjoberg M, Van der Vlist J, Gottgens CM (2000) J Polym Sci Pol Chem 38:4206
274. Matyjaszewski K, Gaynor S, Wang JS (1995) Macromolecules 28:2093
275. Monteiro MJ, De Brouwer H (2001) Macromolecules 34:349
276. Kwak Y, Goto A, Tsujii Y, Murata Y, Komatsu K, Fukuda T (2002) Macromolecules 35:3026
277. Barner-Kowollik C, Quinn JF, Morsley DR, Davis TP (2001) J Polym Sci Pol Chem 39:1353
278. Barner-Kowollik C, Quinn JF, Nguyen TLU, Heuts JPA, Davis TP (2001) Macromolecules 34:7849
279. Barner-Kowollik C, Vana P, Quinn JF, Davis TPJ (2002) J Polym Sci Pol Chem 40:1058
280. Barner-Kowollik C, Coote ML, Davis TP, Radom L, Vana P (2003) J Polym Sci Pol Chem 41:2828
281. Wang AR, Zhu S, Kwak Y, Goto A, Fukuda T, Monteiro MJ (2003) J Polym Sci Pol Chem 41:2833
282. Jovanovic S, Romatowski J, Schulz GV (1965) Makromol Chem 85:187
283. Schulz GV, Romatowski J (1965) Makromol Chem 85:195
284. Romatowski J, Schulz GV (1965) Makromol Chem 85:227
285. Nomura M, Minamino Y, Fujita K, Harada M (1982) J Polym Sci Pol Chem 20:1261

286. Lichti G, Sangster DF, Whang BCY, Napper DH, Gilbert RG (1982) J Chem Soc Farad T 1 78:2129
287. Maxwell IA, Morrison BR, Napper DH, Gilbert RG (1992) Makromol Chem 193:303
288. Mendoza J, De La Cal JC, Asua JM (2000) J Polym Sci Pol Chem 38:4490
289. Monteiro MJ, Hodgson M, De Brouwer HJ (2000) Polym Sci Pol Chem 38:3864
290. de Brouwer H, Tsavalas JG, Schork FJ, Monteiro MJ (2000) Macromolecules 33:9239
291. Moad G, Chiefari J, Chong YK, Krstina J, Mayadunne RTA, Postma A, Rizzardo E, Thang SH (2000) Polym Int 49:993
292. Prescott SW, Ballard MJ, Rizzardo E, Gilbert RG (2002) Macromolecules 35:5417
293. Monteiro MJ, de Barbeyrac J (2001) Macromolecules 34:4416
294. Smulders WW, Gilbert RG, Monteiro MJ (2003) Macromolecules 36:4309
295. Smulders WW (2002) PhD Thesis, Technische Universiteit Eindhoven, The Netherlands
296. Tsavalas JG, Schork FJ, de Brouwer H, Monteiro MJ (2001) Macromolecules 34:3938
297. Vosloo JJ, De Wet-Roos D, Tonge MP, Sanderson RD (2002) Macromolecules 35:4894
298. Lansalot M, Davis TP, Heuts JPA (2002) Macromolecules 35:7582
299. Uzulina I, Kanagasbapathy S, Claverie J (2000) Macromol Symp 150:33
300. Monteiro MJ, Hodgson M, de Brouwer H (2000) J Polym Sci Pol Chem 38:3864
301. Bon SAF, Bosveld M, Klumperman B, German AL (1997) Macromolecules 30:324
302. Marestin C, Noel C, Claverie J (1998) Macromolecules 31:4041
303. Lansalot M, Farcet C, Charleux B, Vairon JP, Pirri R, Tordo O (2000) ACS Sym Ser 768:138
304. Jousset S, Qiu J, Matyjaszewski K, Granel C (2001) Macromolecules 34:6641
305. De Brouwer H, Tsavalas JG, Schork FJ, Monteiro MJ (2000) Macromolecules 33:9239
306. Prodpan T, Dimonie VL, Sudol ED, El-Aasser M (1999) Polym Mater Sci Eng 80:534
307. MacLeod PJ, Keoshkerian B, Odell P, Georges MK (1999) Polym Mater Sci Eng 80:539
308. Pan GF, Sudol ED, Dimonie VL, El-Aasser MS (2002) Macromolecules 35:6915
309. Matyjaszewski K, Qui J, Shipp DA, Gaynor SG (2000) Macromol Symp 155:15
310. Tonge MP, McLeary JB, Vosloo JJ, Sanderson RD (2003) Macromol Symp 193:289
311. Vosloo JJ, Roos DW, Tonge MP, Sanderson RD (2002) Macromolecules 35:4894
312. Ausa JM (2002) Prog Polym Sci 27:1283
313. Landfester K, Bechthold N, Tiarks F, Antonietti M (1999) Macromolecules 32:5222
314. Maitre C, Ganachaud F, Ferreira O, Lutz JF, Paintoux Y, Hemery P (2000) Macromolecules 33:7730
315. Barrere M, Maitre C, Dourges MA, Hemery P (2001) Macromolecules 34:7276
316. Barrere M, Ganachaud F, Bendejacq D, Dourges MA, Maitre C, Hemery P (2001) Polymer 42:7239
317. Limouzin C, Caviggia A, Ganachaud F, Hemery P (2003) Macromolecules 36:667
318. Cauvin S, Sadoun A, Santos R, Belleney J, Ganachaud F, Hemery P (2002) Macromolecules 35:7919
319. Barrere M, Landfester K (2003) Polymer 44:2833
320. Landfester K, Rothe R, Antonietti M (2002) Macromolecules 35:1658
321. Willert M, Landfester K (2002) Macromol Chem Phys 203:825
322. Marie E, Rothe R, Antonietti M, Landfester K (2003) Macromolecules 36:3967
323. Marie E, Landfester K, Antonietti M (2002) Biomacromolecules 3:475
324. Taden A, Antonietti M, Landfester K (2003) Macromol Rapid Comm 24:512
325. Claverie JP, Viala S, Maurel V, Novat C (2001) Macromolecules 34:382
326. Landfester K (2001) Adv Mater 13:765
327. Montenegro R, Antonietti M, Mastai Y, Landfester K (2003) J Phys Chem B 107:5088
328. Taden A, Landfester K (2003) Macromolecules 36:4037

329. Montenegro R, Landfester K (2003) Langmuir 19:5996
330. Wegner G, Baum P, Muller M, Norwig J, Landfester K (2001) Macromol Symp 175: 349
331. Vaihinger D, Landfester K, Krauter I, Brunner H, Tovar GEM (2002) Macromol Chem Phys 203:1965
332. Landfester K, Montenegro R, Scherf U, Guntner R, Asawapirom U, Patil S, Neher D, Kietzke T (2002) Adv Mater 14:651
333. Piok T, Wenzl FP, Gamerith S, Gadermaier C, Patil S, Montenegro R, Kietzke T, Neher D, Scherf U, Landfester K, List EJW (2003) Mater Res Soc Symp Proc 738:245
334. Piok T, Romaner L, Gadermaier C, Wenzl FP, Patil S, Montenegro R, Landfester K, Lanzani G, Cerullo G, Scherf U, List EJW (2003) Synthetic Met 139:609
335. Piok T, Gamerith S, Gadermaier C, Plank H, Wenzl FP, Patil S, Montenegro R, Kietzke T, Neher D, Scherf U, Landfester K, List EJW (2003) Adv Mater 15:800
336. Willert M, Rothe R, Landfester K, Antonietti M (2001) Chem Mater 13:4681
337. zu Putlitz B, Landfester K, Fischer H, Antonietti M (2001) Adv Mater 13:500
338. Manders B, Sciandrone L, Hauck G, Kristen M (2001) Angew Chem Int Edit 40:4006